Institute of Paper Science and Technology

STATUS REPORTS

To The

SURFACE AND COLLOID SCIENCE

PROJECT ADVISORY COMMITTEE

April 5, 1991
Institute of Paper Science and Technology
Atlanta, GA

IPST

Atlanta, Georgia

INSTITUTE OF PAPER SCIENCE AND TECHNOLOGY

Antitrust Notice

Guidelines for Meetings

Neither the Institute of Paper Science and Technology nor any committee or activity of the Institute shall be used or include discussions for the purpose of bringing about or attempting to bring about any understanding or agreement, written or oral, formal or informal, expressed or implied, among competitors with regard to prices, terms or conditions of sale, distribution, volume of production, or allocation of territories, customers, or suppliers.

No IPST activity shall involve exchange or collection and dissemination among competitors of any information regarding prices, pricing methods, costs or production, sales, marketing, or distribution.

Neither IPST nor any committee thereof shall make any effort to bring about the standardization of any product for the purpose of or with the effect of preventing the manufacture or sale of any product not conforming to a specified standard.

The Institute does not become involved in any product standards or endorsements. IPST policy as a tax exempt educational institution expressly precludes the establishment of product standards or the endorsement of any product or process and general provisions incorporated in IPST research contracts so stated.

Rev. 10/90

NOTICE & DISCLAIMER

The Institute of Paper Science and Technology (IPST) has provided a high standard of professional service and has put forth its best efforts within the time and funds available for this project. The information and conclusions are advisory and are intended only for internal use by any company who may receive this report. Each company must decide for itself the best approach to solving any problems it may have and how, or whether, this reported information should be considered in its approach.

IPST does not recommend particular products, procedures, materials, or service. These are included only in the interest of completeness within a laboratory context and budgetary constraint. Actual products, procedures, materials, and services used may differ and are peculiar to the operations of each company.

In no event shall IPST or its employees and agents have any obligation or liability for damages including, but not limited to, consequential damages arising out of or in connection with any company's use of or inability to use the reported information. IPST provides no warranty or guaranty of results.

STATUS REPORTS

To The

SURFACE AND COLLOID SCIENCE

PROJECT ADVISORY COMMITTEE

April 5, 1991
Institute of Paper Science and Technology
Atlanta, GA

March 14, 1991

TO: MEMBERS OF THE SURFACE AND COLLOID SCIENCE PROJECT ADVISORY COMMITTEE

Enclosed is the status report covering the work to be presented at our April 5 meeting. Also attached is an agenda for the meeting.

We are looking forward to discussing our work with your and to hear your comments and suggestions. Please let me know whether you will be in Atlanta in time for dinner on Thursday, April 4. If you will be, I hope you will join us for an informal dinner, so we can all get to know each other better.

If you have any questions, please call me at (404) 853-9720.

Sincerely,

Robert A. Stratton

Enclosure

RAS/at

Institute of Paper Science and Technology, Inc.

75 14th Street, N.W.
tlanta, GA 30318

Formerly The Institute of Paper Chemistry
Appleton, Wisconsin

Telephone 404-853-9500
FAX # 404-853-9510

TABLE OF CONTENTS

SURFACE AND COLLOID SCIENCE
PROJECT ADVISORY COMMITTEE MEETING

April 5, 1991
Wyndham Hotel
Atlanta, Georgia

AGENDA

8:00	Coffee and Rolls	Woodruff Room
8:15	Welcome; Introductions, Antitrust Statement	Stratton/Lavery
8:30	Opening Remarks	Yeske
8:45	Project Reviews	
	Project 3526--Internal Strength Enhancement	Stratton
9:30	Thesis Student Research	Chris Luettgen
9:55	Coffee Break	
10:10	Project 3646--Fundamentals of Paper Surface Wettability	Etzler
10:50	Project 3681--Utilization of Recycled Fiber	Stratton/Ellis
12:00	Lunch	
1:00	Committee Discussions	Crescent Room
5:00	Adjournment	

SURFACE AND COLLOID SCIENCE
PROJECT ADVISORY COMMITTEE

IPST LIAISON: BOB STRATTON

Mr. Hugh P. Lavery (*Chairman*)
Research Associate
Union Camp Corporation
Post Office Box 3301
Princeton, NJ 08543-3301
(606) 896-1200 Ext 233

Dr. Michael Juang
Senior Research Chemist
Boise Cascade Corporation
4435 North Channel Avenue
Portland, OR 97217-0000
(503) 285-3811
(503) 285-7467 FAX

Mr. Giancarlo A. Cavagna
Research Associate
Westvaco Corporation
11101 Johns Hopkins Road
Laurel, MD 20723
(301) 497-1347
(301) 497-1309 FAX

Mr. Joseph M. Fernandez
Research Engineer
Potlatch Corporation
Fiber R & D East End
Cloquet, MN 55720
(218) 879-2374
(218) 879-2375 FAX

Dr. Kevin T. Hodgson
Research Scientist
Weyerhaeuser Paper Company
WTC 2E19
Tacoma, WA 98477
(206) 924-6249
(206) 924-4207 FAX

Mr. Philip N. Liberato
Process Engineer
Chesapeake Corporation
19th & Main Streets
West Point, VA 23181-0311
(804) 843-5000
(804) 843-5757 FAX

Dr. David H. Hollenberg
Research Fellow
James River Corporation
1915 Marathon Avenue
Neenah, WI 54956-4067
(414) 729-8187
(414) 729-8161 FAX

Dr. Al Pocius
Division Scientist
3 M Company
Adhesive Technology Center
Building 236-GA-03
St. Paul, MN 55144
(612) 736-0287

Mr. Mark J. Smith
Research Specialist
Mead Corporation
Eighth & Hickory Streets
Chillicothe, OH 45601-0000
(614) 772-3503
(614) 772-3595

INTERNAL STRENGTH ENHANCEMENT

STATUS REPORT

FOR

PROJECT 3526

TO THE

SURFACE AND COLLOID SCIENCE

PROJECT ADVISORY COMMITTEE

April 5, 1991
Institute of Paper Science and Technology
Atlanta, Georgia

Project Title: INTERNAL STRENGTH ENHANCEMENT
Project Code: NHANC
Project Number: 3526
Project Staff: R. Stratton
FY 90-91 Budget: $60,000

PROJECT OBJECTIVE: To improve internal strength and moisture tolerance in paper and paperboard. The short term goals are to establish those fundamental parameters affecting inter-fiber and intra-fiber bounding in conventional and ultra high yield pulps and to control these parameters, if possible, by chemical or mechanical treatments.

PROGRAM AREAS: End Use Performance, Reduced Operating Costs.

RATIONALE: Major limitations of paper and board for many uses are low internal bond strength and poor moisture tolerance. Improved internal strength and enhanced moisture resistance would allow a number of present grades to be produced using less fiber and would also allow new end uses to be developed.

At present, commercial papers do not attain strength levels that realize the full potential of the wood fibers. Most paper mechanical properties are markedly degraded with increasing moisture content. We need to better understand the nature of fiber properties and fiber-to-fiber bonding and changes in them with increasing moisture content, if we are eventually to improve the moisture tolerance of paper.

GOALS FOR 1990-1991:

1. Prepare woodgrain reports on the single fiber and handsheet studies on strength enhancement.

2. Determine the relationship between different measures of fiber/fiber bonding:

   - z-direction tensile strength
   - z-toughness
   - in-plane longitudinal modulus
   - out-of-plane longitudinal modulus
   - zx shear strength

3. Achieve substantial dry and moist strength enhancement through the use of novel chemical additives.

ACCOMPLISHMENTS TO DATE:

1. Developed the delamination tester as a sensitive measure of the toughness of fiber/fiber bonds.

2. Showed that Tensile Energy Adsorption (TEA) is a unique function of tensile strength independent of pulp yield and treatment with strength aids.

3. Showed that STFI compressive strength can be increased by the use of strength aids to a limited extent. Factors other than bond strength curtail further increases. STFI is directly correlated with the tensile strength independent of pulp yield and strength aid addition.

4. Showed that specific z-toughness, a measure of the inherent bondability of a pulp, is independent of pulp yield but is strongly increased when strength aids are present.

5. Showed that fines increase both tensile strength and Z-toughness. Fines in a system treated with a strength aid are much more effective in enhancing Z-toughness than in the untreated case.

6. Analyzed the damage produced during failure of individual fiber-fiber bonds and showed that both fibers of the pair sustained similar damage. The damage of a population of fibers is normally distributed. A correlation between breaking load and damage was found for individual bond pairs. For both chemical and mechanical pulps use of strength aid increases the damage produced by bond failure. Observed damage due to "skirt" effect recently reported by Nanko and Ohsawa.

7. Prepared woodgrain report on the work on single fiber bond strength.

RELATED STUDENT RESEARCH:

M.T. Goulet, Ph.D. -1989; C.E. Miller, Ph.D. - 1989; D.L. Horstmann, M.S. -1989; M.H. Lang, M.S. - 1990; M.W. Sachs, M.S. - 1989;

Michael Friese, Ph.D. Thesis, "An Experimental Study of Adsorbed Polymer Configurations Using FTIR-CIR Spectroscopy" (in progress).

Todd Braga, M.S. Project, "The Effects of Supercalendering on the Bonding in Paper" (in progress).

Christopher Luettgen, Ph.D. Thesis, "An Investigation of the Role of Mixing Conditions during Polymeric Retention Aid Addition on the Adsorption Homogeneity" (in progress).

Matthew Lang, Ph.D. Thesis, "The Kinetics of Polyelectrolyte Adsorption onto an Oppositely-Charged Surface" (in progress).

Michael Cresswell, M.S. Project, "Interactions of the Wet Strength Resin Melamine-Formaldehyde with Cellulose Surfaces"(in progress).

GOALS FOR
APRIL 1991-OCTOBER 1991:

1. Complete woodgrain report on handsheet study of strength.
2. Measure the stress-strain properties of paper in the Z direction.

SUMMARY

Single Fiber Bonds

The objective of this project is to better understand how the properties of the pulp and of chemical additives influence fiber-fiber bonding in a sheet of paper. Paper consists of layers of fibers bonded to each other at many sites (Figure 1). In the first part of this project we focused on a single bond between two fibers (Figure 2). We used sensitive instruments to measure the bonded area between the fibers and the breaking load of the bond in shear. A scanning electron microscope (SEM) was then used to observe the surfaces of the formerly bonded fibers to determine where the fracture had occurred.

Individual fiber bonds were prepared by crossing two wet fibers at right angles and drying at 105°C under pressure. The now bonded fibers were then mounted on a mylar tab (Figure 3) for testing. Due to the variability of pulp fibers, a great many bonds must be tested to obtain a valid average bond strength. The results for an earlywood loblolly pine kraft pulp are shown in Figure 4 on a probability plot. We find the bond strength to have a log normal distribution. Such a distribution is also found for the tensile strength of individual fibers (1).

Many applications of paper and board are under conditions of elevated relative humidity and it is well known that the mechanical properties are very sensitive to moisture content. Other workers have shown that both the modulus and the tensile strength of individual fibers decrease with increasing moisture content. Since sheet strength is controlled by both fiber strength and bond strength, the dependence of the latter on relative humidity was of interest. The results are shown in Figure 5 along with changes in properties of sheets made from the same fibers. There is a parallel behavior between bond strength and sheet strength.

The quality with respect to the inherent strength of the stock reaching the headbox can be expected to decrease in the near future. This is a result of increasing proportions of hardwood, filler, and secondary fiber being used. There is also a trend toward lower basis weights to reduce costs. To maintain or enhance strength under these conditions will require the use of polymeric strength aids. It is thought that these materials act to improve interfiber bonding, although an early study (2) did not find an effect at dry (50% RH)

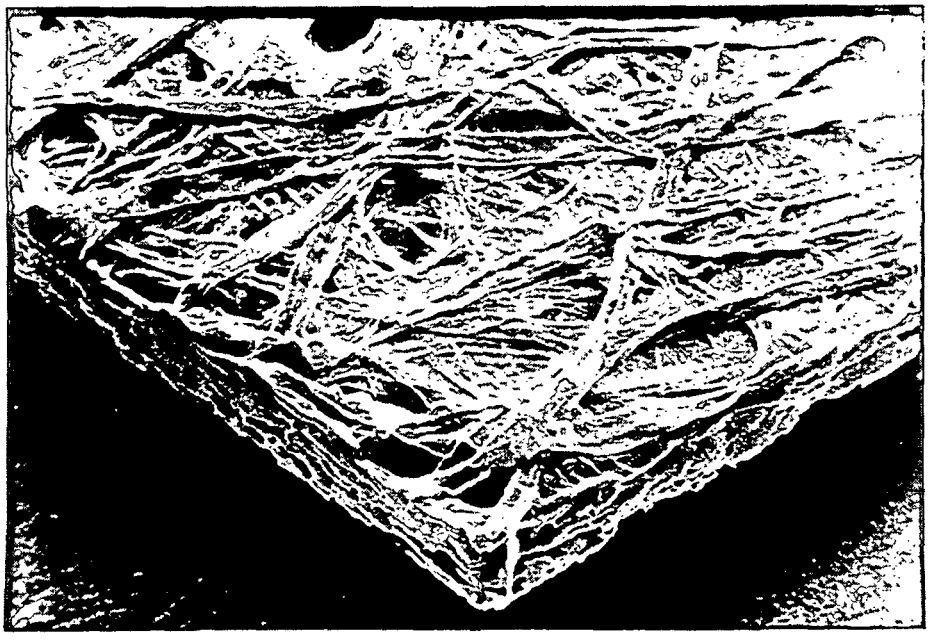

Figure 1. Scanning electron micrograph of sheet corner.

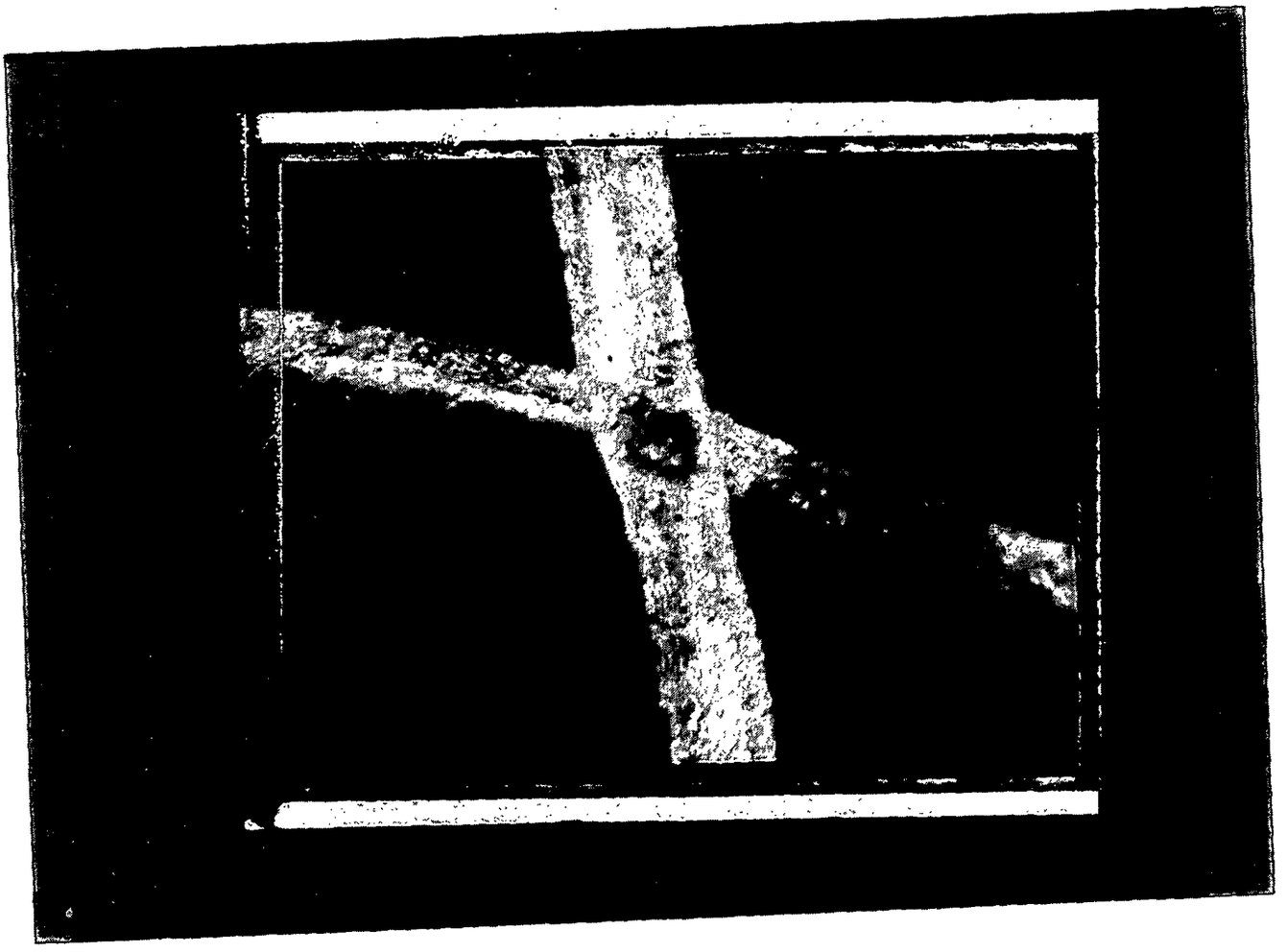

Figure 2. Scanning electron micrograph of single fiber-fiber bond. Dark region is bonded area.

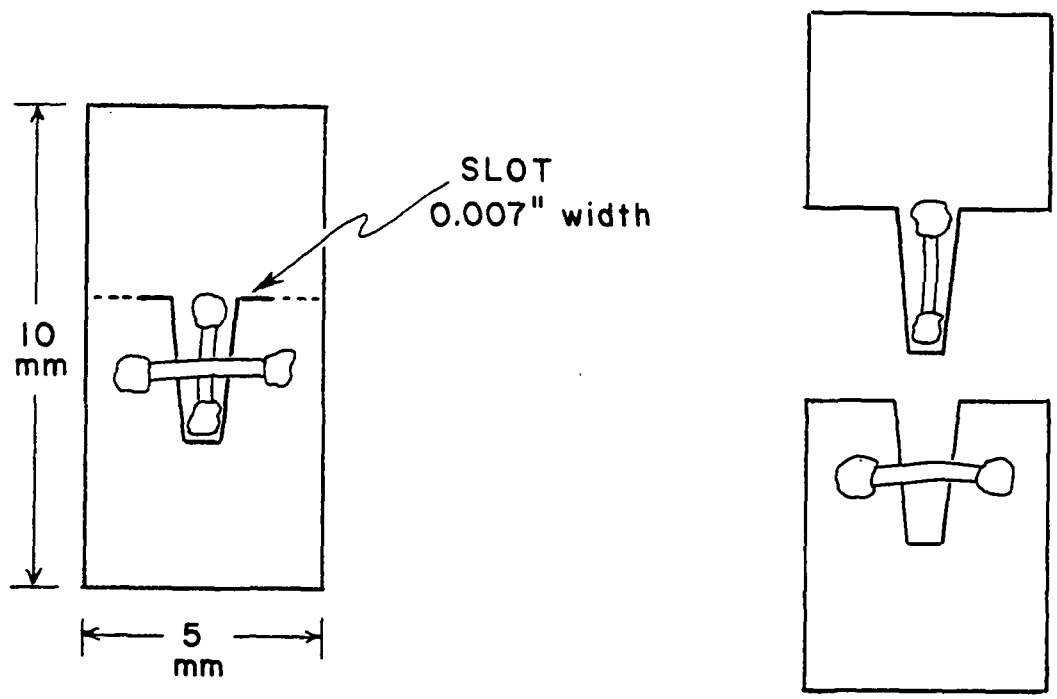

Figure 3. Mylar tab for holding bonded fibers: a) before fracture; b) after fracture.

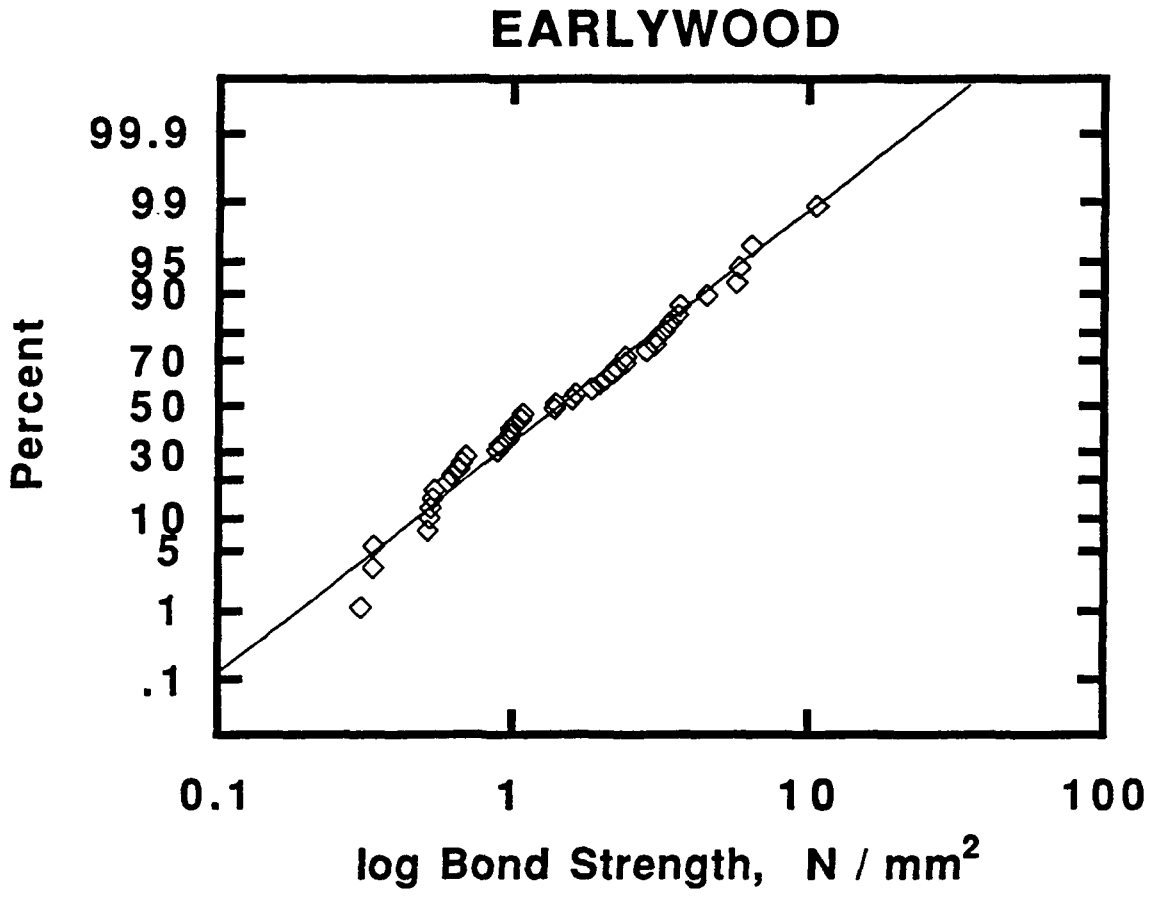

Figure 4. Probability plot of bond strengths showing log normal distribution.

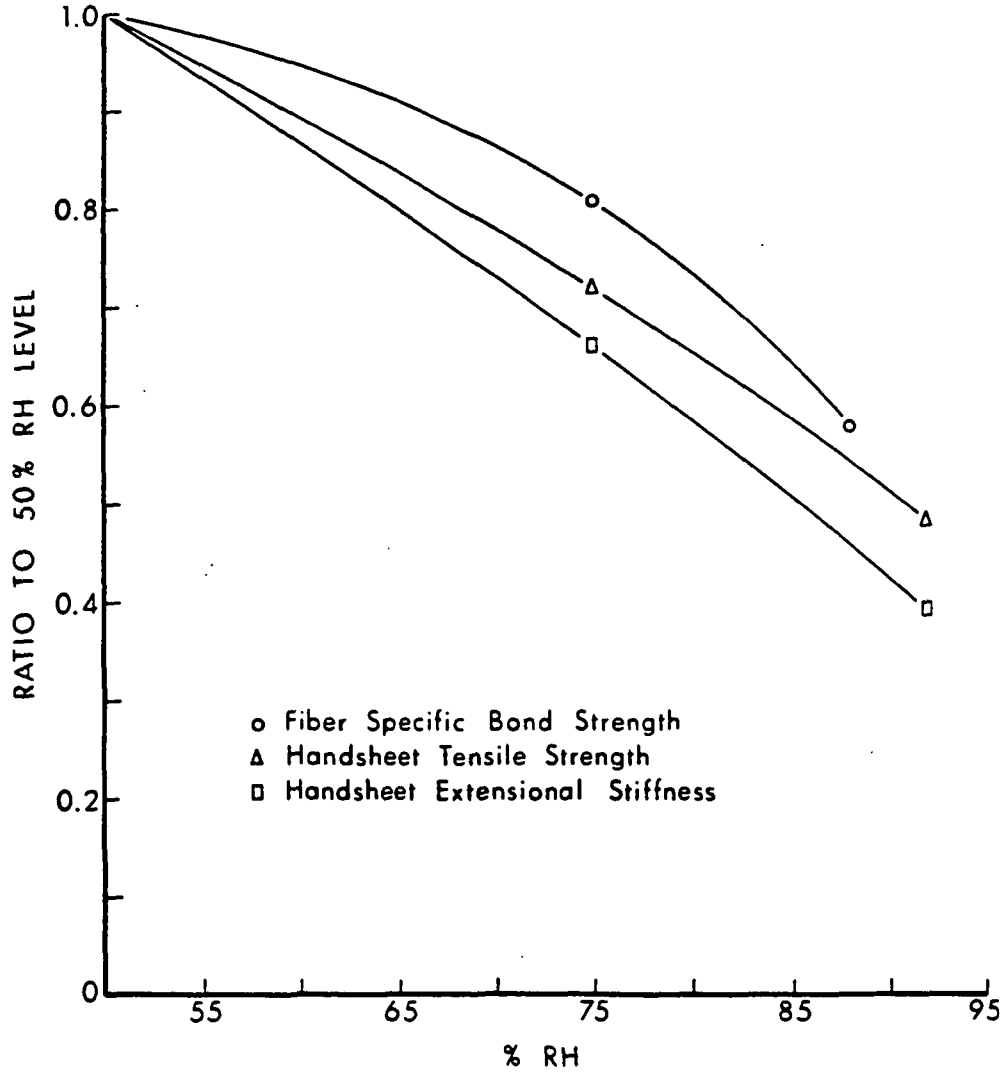

Figure 5. Change of sheet and fiber properties with relative humidity normalized to the values at 50% R. H.

conditions. We investigated two systems, each consisting of a cationic and an anionic polymer. These were added sequentially to the (wet) fibers before bonding as might be done at the wet end of the paper machine. The systems were chosen to provide the possibility of interacting with the fibers through formation of either covalent plus ionic bonds or of ionic bonds only. In the first system the stronger covalent bonds would provide most of the strength enhancement with the ionic groups being present mainly to ensure good retention on the fibers. In the second system the ionic bonds must perform both functions. These two systems were compared to untreated fibers which normally interact with each other through the formation of hydrogen bonds. The results are presented in Table I. The strength aids do not change the area per fiber bond, but do increase the breaking load and bond strength by about a factor of two. Surprisingly, the system with ionic bonds only is as good as that which forms covalent bonds. The latter, of course, also provides wet strength, but if this quality is not needed, the ionic only material would be satisfactory. Furthermore, the lack of covalent bonds should permit ready repulpability, an advantage for paper meant to be recycled.

The SEM observations provided us a great deal of information concerning how and where bonds fail. Two extremes are shown in Figures 6 and 7. The former was found most frequently with unrefined fibers untreated with strength aids, the latter with refined, treated fibers. However, a variety of degrees of damage was found. Six fibers chosen as archetypes are shown in Figure 8 and were given a ranking from 1 to 6 to indicate an (subjective) increasing severity of damage. All the other formerly bonded surfaces were then compared with these six and given a damage ranking. In addition, the presence or absence of substantial amounts of fibrillated or sheets of wall material along the edges of the fiber was noted. This material, found only with refined pulps, appeared to be independent of the amount of damage in the central portion of the bond.

Because the geometry of the loading experiment is nonsymmetrical (that is, the load is applied axially to one fiber and transversely to the other), it was of interest to determine the effect of this geometry on the damage produced during bond failure. Figure 9 shows the average damage ranking in the C (cross) direction for eleven different pulps plotted against the ranking for the T (axial) fiber. The individual values are averages of about forty fibers. There is no systematic dependence of damage on the experimental geometry.

TABLE 1. EFFECT OF BOND TYPE (REFINED PULP)

BOND TYPE	LOAD, g	AREA, microns^2	BOND STRENGTH, N/mm^2
H	0.73	2070	3.5
COVALENT	1.44	2130	7.5
IONIC	1.51	2040	9.3

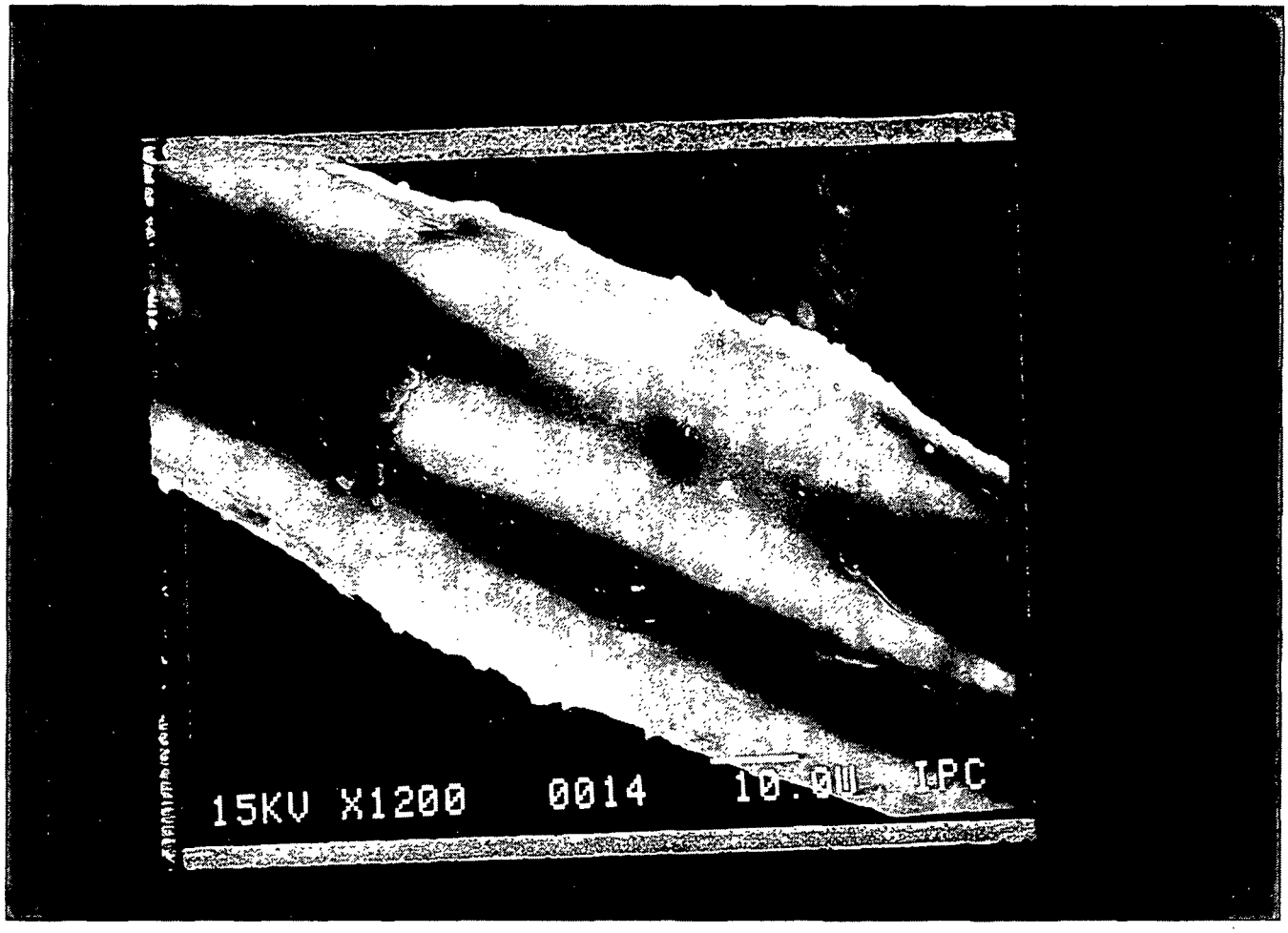

Figure 6. SEM of formerly bonded fibers with little surface damage.

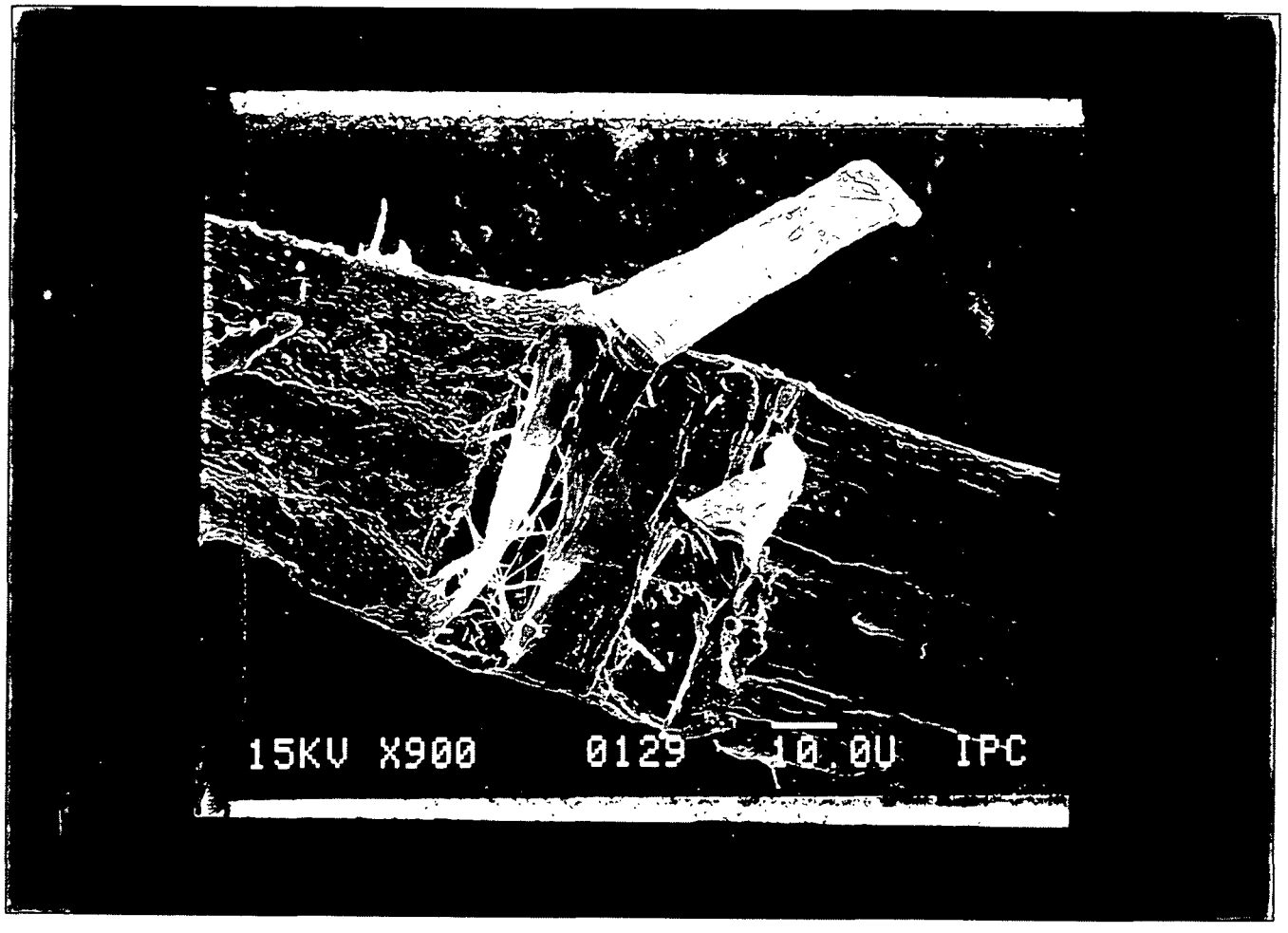

Figure 7. SEM of formerly bonded fibers with much surface damage.

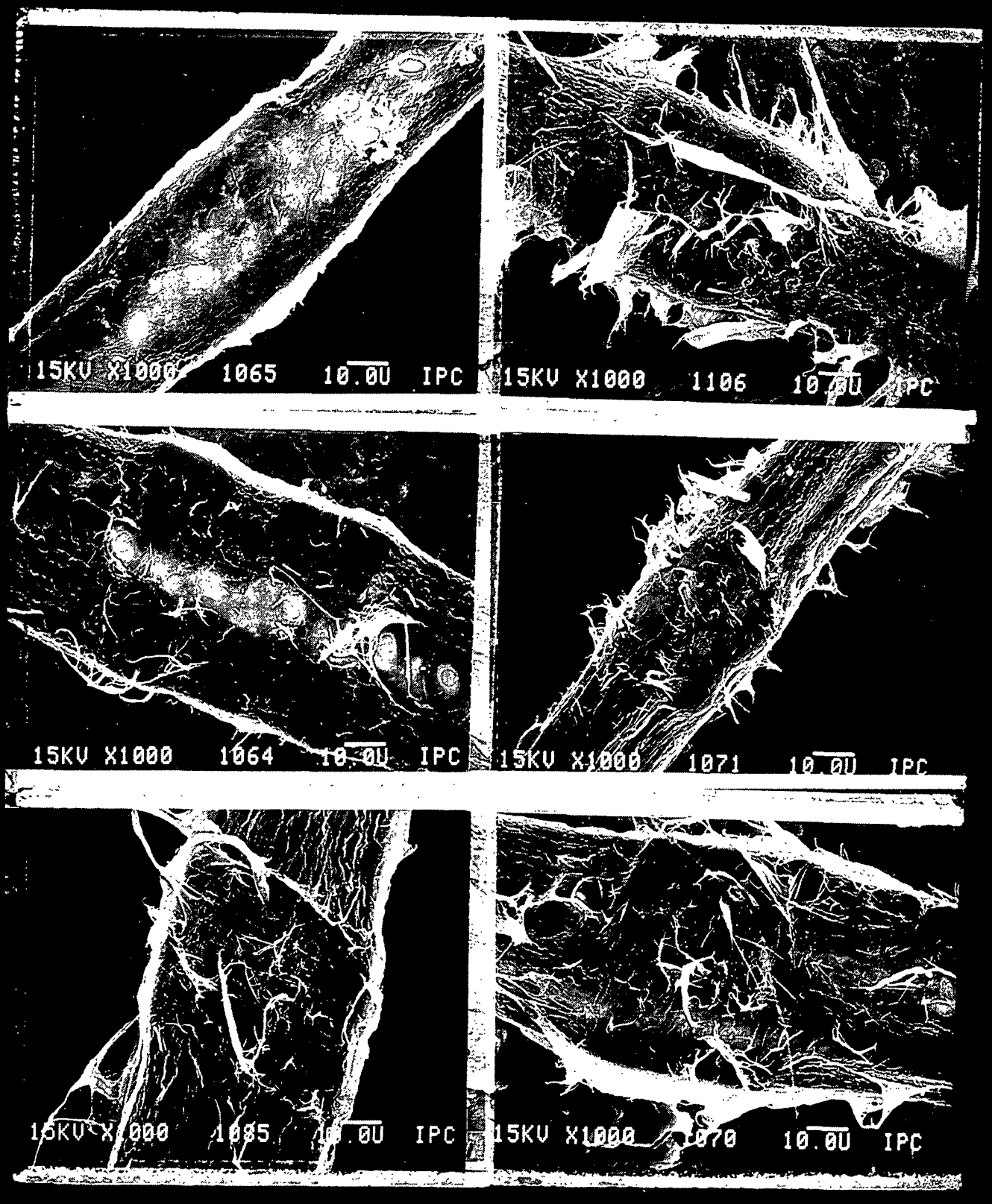

Figure 8. Archetypes of fiber damage increasing from 1 to 6.

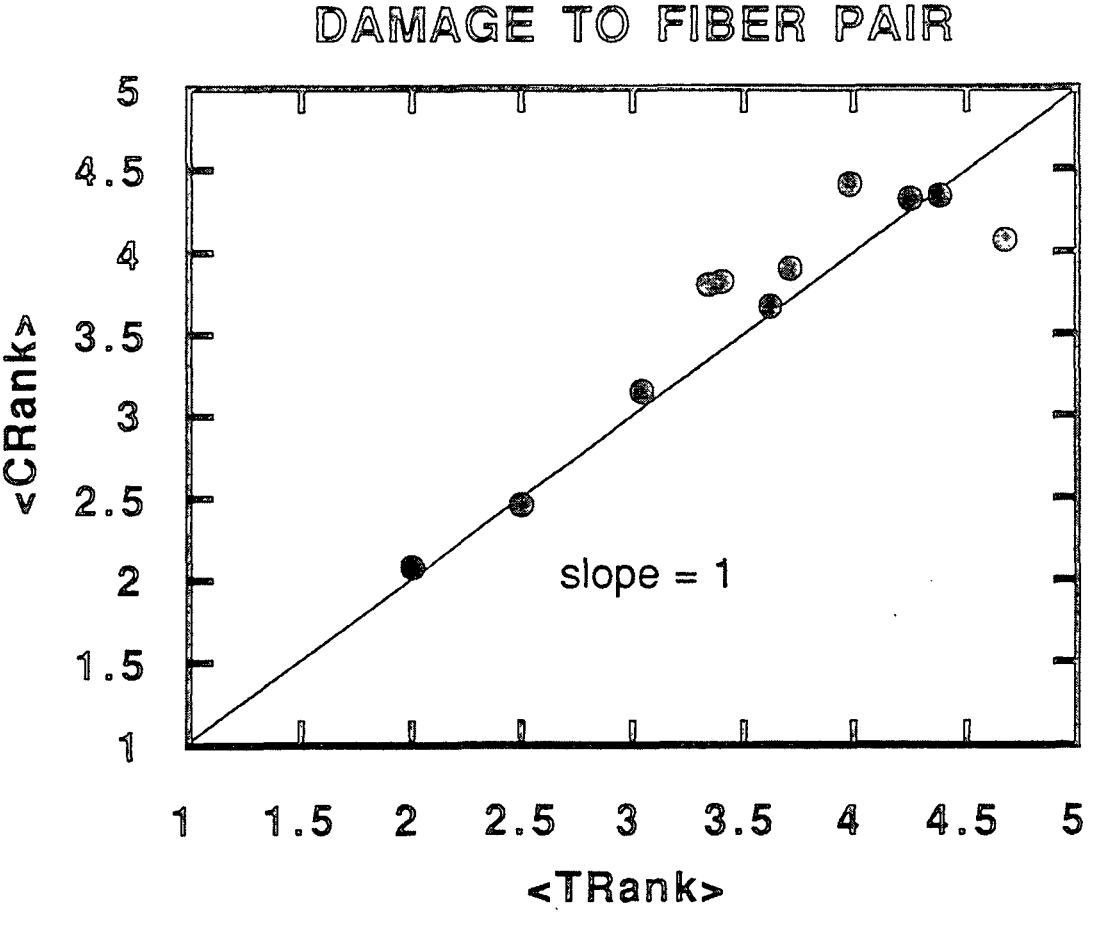

Figure 9. Comparison of the average fiber damage for the axial (T) and cross (C) fibers for 11 pulps.

There was, however, usually a wide variety of degrees of damage for a given pulp. The results for one pulp are shown in Figure 10 where the rankings for the mates of individual fiber pairs have been summed. The severity of damage is seen to be normally distributed on this subjective ranking scale.

It would be expected that greater amounts of damage would be correlated with larger bond strengths and there is some evidence that this is so. In Figure 11 the average bond strength for a given level of damage is plotted against that damage ranking for two pulps, a refined, untreated pulp (A5) and the same pulp treated with the "ionic only" strength aid (ADS). The error bars indicate the standard error of the bond strength at each ranking. The tips of the arrows indicate the overall average bond strength and damage ranking for each pulp. Obviously, the strength aid increases both the bond strength and the severity of damage to the fibers.

As mentioned above some of the formerly bonded fibers possessed additional fibrillated or wall material along their edges. As it happens, all of the fibers chosen as archetypes for the damage ranking (Figure 8) were of this type while those shown in Figures 6 and 7 were not. The two types were assigned ratings of 0 (material absent) or 1 (material present) without regard of the amount of material. At the time we were puzzled by these fragments whose presence seemed independent of the amount of damage in the central regions of the bond. We now believe that they are a result of and further evidence for the "skirt" effect recently found by Nanko and Ohsawa (3). This phenomenon is shown in Figures 12 and 13 taken from their paper. The skirt is formed by the adhesion of the S1 layer, which has swollen and separated from the S2 layer of the same fiber, to the surface of the mating fiber. Nanko and Ohsawa found this separation in both refined and unrefined fibers and suggested it occurred in the latter as a result of the pressing operation. We only found type 1 behavior for refined pulps - significantly, we did not find it for unrefined, earlywood fibers treated with a strength aid which showed large amounts of damage in the central regions of the bond. Apparently, for this pulp S1-S2 separation did not occur. The different species of pulp, Japanese beech and loblolly pine, may account for the presence or absence of S1 - S2 separation for unrefined pulp.

Nanko and Ohsawa suggest that the presence of the skirts is important for increasing the strength of fiber-fiber bonds. More important than the additional bond area that the skirts provide is their role in distributing the stress at the periphery of the bond. The stress

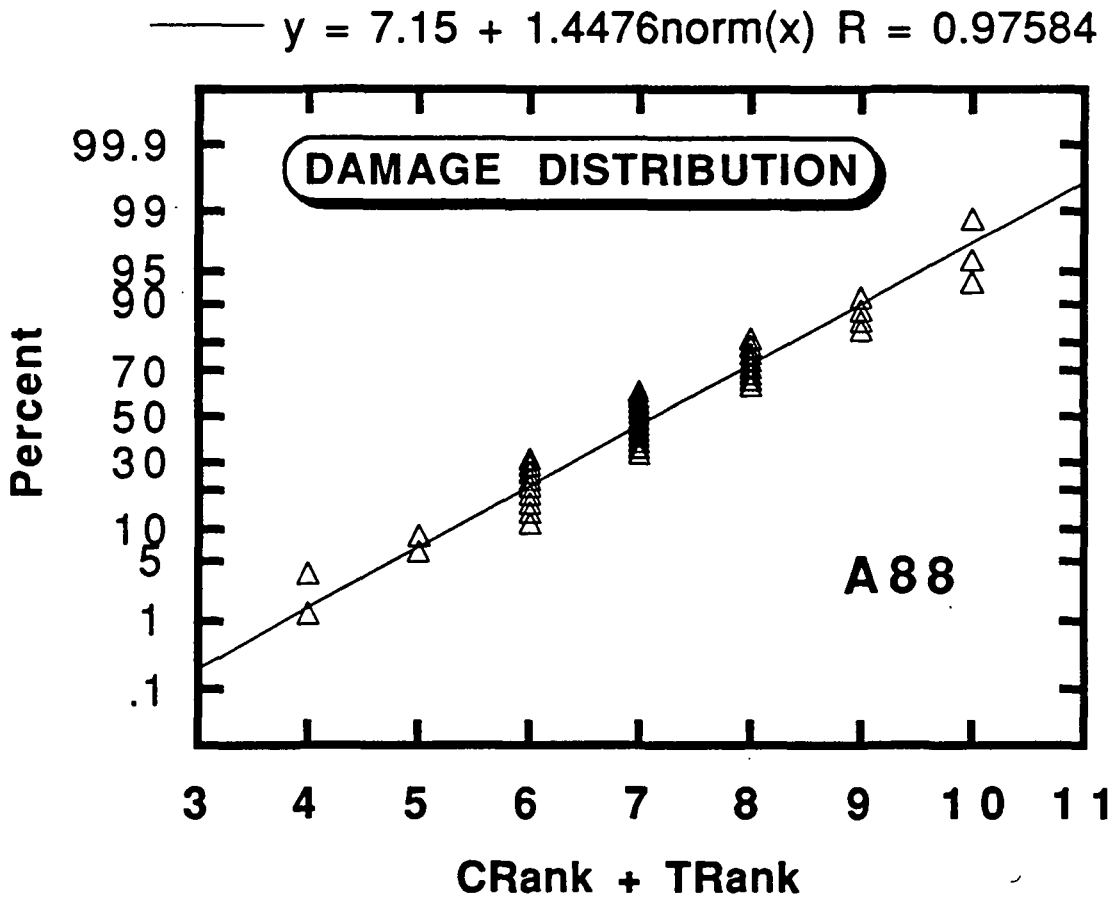

Figure 10. Probability plot of damage to individual bonds from a single pulp showing normal distribution.

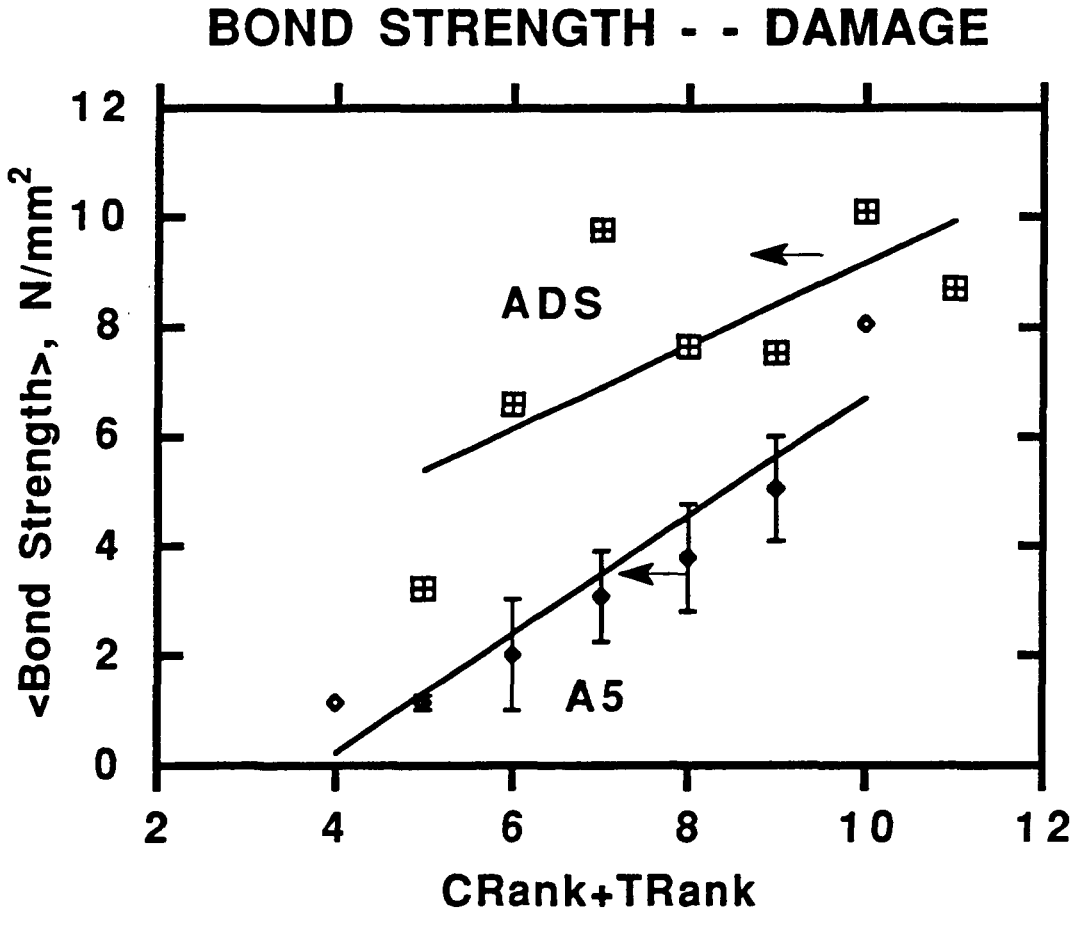

Figure 11. Average bond strength for bonds with a given damage plotted against the damage ranking for two pulps. Tips of arrows denote the overall average values for each pulp.

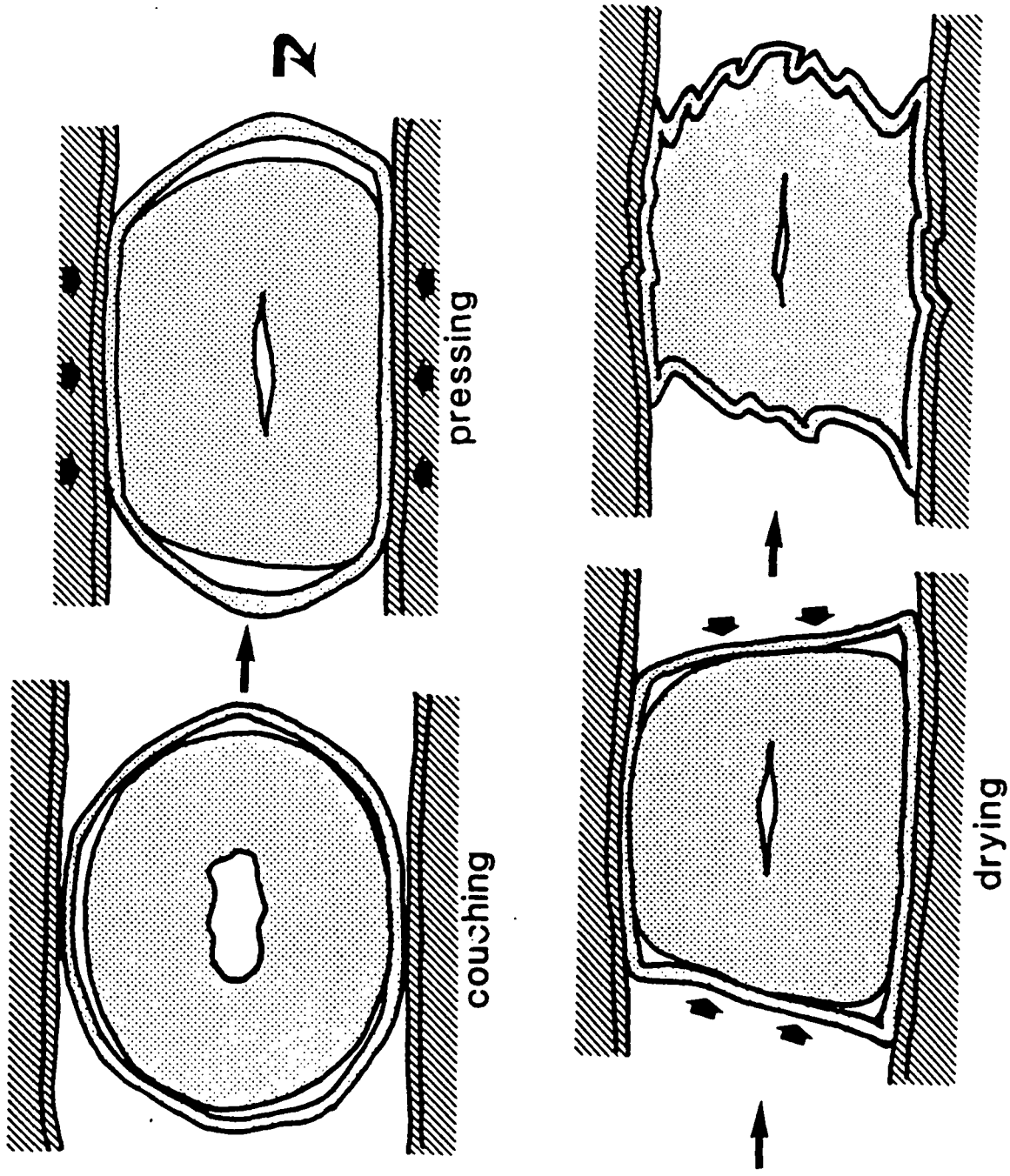

Figure 12. Schematic representation of changes in the S1 and S2 layers during sheetmaking showing skirt formation. Taken from Nanko and Ohsawa (3).

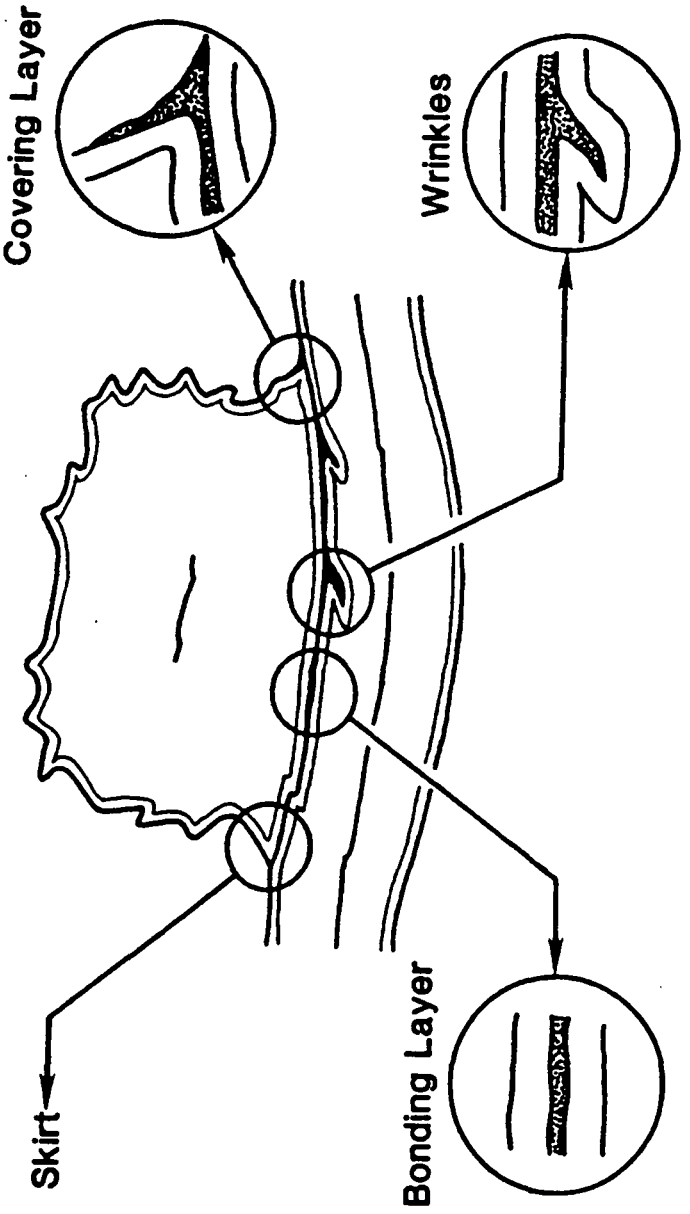

Figure 13. Schematic representation of various features in bonded fibers. Taken from Nanko and Ohsawa (3).

concentrations that are expected to be large here are reduced and are less likely to be the site of bond failure. Our data provide support for this suggestion. Bond strength is plotted in Figure 14 against the rating for the evidence of this skirt material on the mating fibers. Thus values of 0, 2, or 1 on the abscissa indicate that neither, both, or only one of the fibers showed this material. For both the untreated (A5) and treated (ADS) pulps the trend is clear: bond strength increases when the skirt material is present. The error bars show the standard error while the tips of the arrows indicate the overall average values for the bond strength and (CType + TType) value. Note that the average value for this latter parameter is approximately the same for both pulps even though the strength aid increases the bond strength substantially. Apparently, the skirt effect is little affected by additives.

The results of this study on the properties of single fiber-fiber bonds has been written up as a wood grain report and will be issued shortly.

Handsheet Studies

The study of single fiber-fiber bonds is illuminating, but very time and labor intensive. To examine the range of parameters deemed important to understanding the strength of paper would take years of effort. We sought, therefore, other means to obtain this information more rapidly. A number of methods have been suggested to evaluate the effect of bond strength on sheet strength, among them being Z-direction tensile strength, out-of-plane stiffness measurements (ultrasonic), and the delamination test of Skowronski and Bichard (4). These techniques measure respectively the strength, initial modulus, and energy to failure of the sheet in the Z-direction. In each case a portion of the parameter measured is associated with the bonds in the sheet. The exact relationships are unknown at this time. Alternatively, measurements of sheet tensile properties and fiber properties can be used with the theory of Page (5) to calculate a value for the bond strength in shear.

We have established a program to evaluate these various measures of bond strength in sheets and their dependence on pulp properties. Loblolly pine chips were kraft pulped to four different yields (Table 2) and were then refined to four different freenesses (Table 3). Portions of these were classified to remove the fines which were then retained for subsequent addition to the classified pulps in known amounts. Sheets were prepared from each of these pulps, were wet pressed at one of five different levels of pressure, and were dried under partial restraint on a steam drum. For some of the sheets wet end addition of a

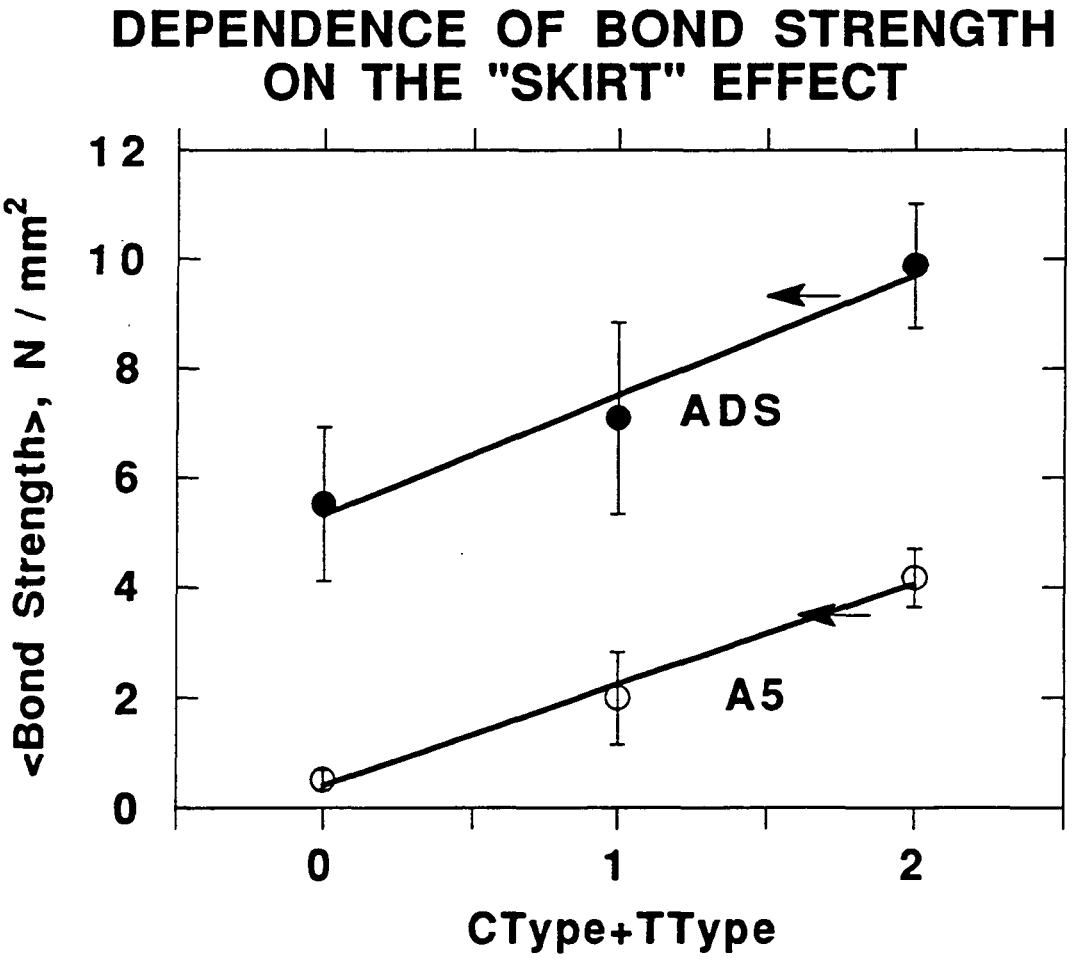

Figure 14. Average bond strength for bonds with different levels of skirt remnants following fracture. Tips of arrows denote the overall average value for each pulp.

TABLE 2. **PULP PROPERTIES**

YIELD, %	KAPPA NO.
47.5	34.7
51.2	42.2
60.4	116.0
80.7	167.0

TABLE 3. **PULPS**

YIELD, %	FREENESS, mL CSF			
47	685	600	350	200
52	740	600	340	200
60	750	600	350	200
80	780	600	340	200

strength aid was incorporated. Table 4 lists the properties measured for each of these sheets. In addition, fiber properties listed in Table 5 were measured for some of the pulps.

Because the delamination technique is relatively new, we will briefly review the concept. A sample of paper is sandwiched between two sheets of transparent tape as in Figure 15. The sandwich is then mounted on the freely - rotating wheel shown in Figure 16. The sheet is then delaminated at a constant rate with the peel angle being maintained at 90°. The load during delamination is recorded and the area under the curve (shaded area W in Figure 17) after steady-state has been attained is determined. Division of this area by the length L gives the average delamination force and division of this by the width of the sandwich gives the work (or energy) of delamination per unit area. We will call this quantity the Z-toughness.

This work is in the process of being written up in the form of a wood grain report and only a few highlights will be presented here.

Pulp fines are believed to significantly increase paper strength. Indeed, the tensile strength of a sheet made from a whole pulp is higher than that made from the same pulp from which the fines have been removed. What is the function of the fines? We compared the Z-direction tensile strength of sheets made from whole and classified pulps. The results are shown in Figure 18. Each point represents sheets made under conditions of equal pulp yield, equal refining, equal wet pressing pressure, and equal treatment (or lack thereof) of strength aid. A single curve appears to represent all the data. Perhaps more surprising is the finding that, at the upper end of the data, the classified sheets have the same Z-direction strength as do the sheets formed from whole pulps. If the fines really do contribute to the bond strength, this finding suggests that the Z-direction tensile test may not be an adequate indicator of this property for very well bonded sheets.

A direct investigation of the effect of fines is shown in Figure 19. Here the Z-toughness parameter is found to be a linear function of the amount of fines in the sheet. The effect of the strength aid was to greatly enhance the fines' contribution to the toughness. These results may indicate that Z-toughness may be a more sensitive measure of bond strength.

Strength aids can greatly influence the properties of a sheet and it is important to compare the results at constant density. The effect of chemical additive on the Z-toughness is shown

Table 4. Sheet Properties Measured

Basis weight

Caliper

IPST soft platen density

Tensile index

TEA index

Et index

STFI compressive strength index, 50% R. H.

STFI compressive strength index, 90% R. H.

Zero span tensile index

Thwing formation index

Out-of-plane longitudinal stiffness

Out-of-plane shear stiffness

In-plane longitudinal stiffness

In-plane shear stiffness

Scattering coefficient (before delamination)

Scattering coefficient (after delamination)

Z-toughness

Z-direction tensile strength

Table 5. Fiber Properties Measured

Fiber length distribution
Coarseness
Fiber width
Cell wall Thickness

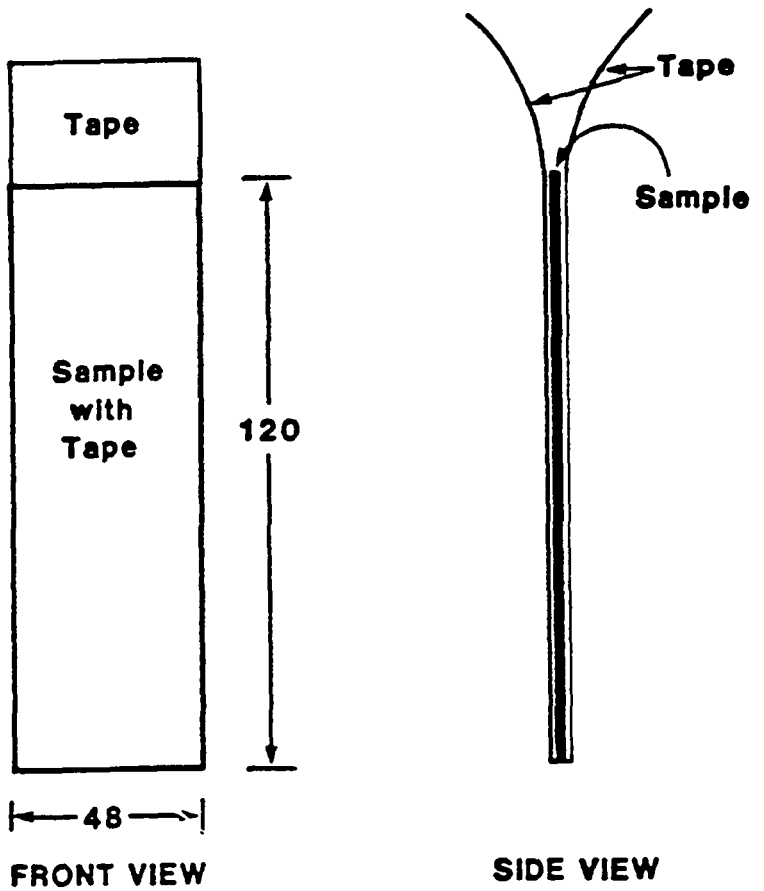

Figure 15. Schematic representation of the sandwich prepared for testing in the delamination tester.

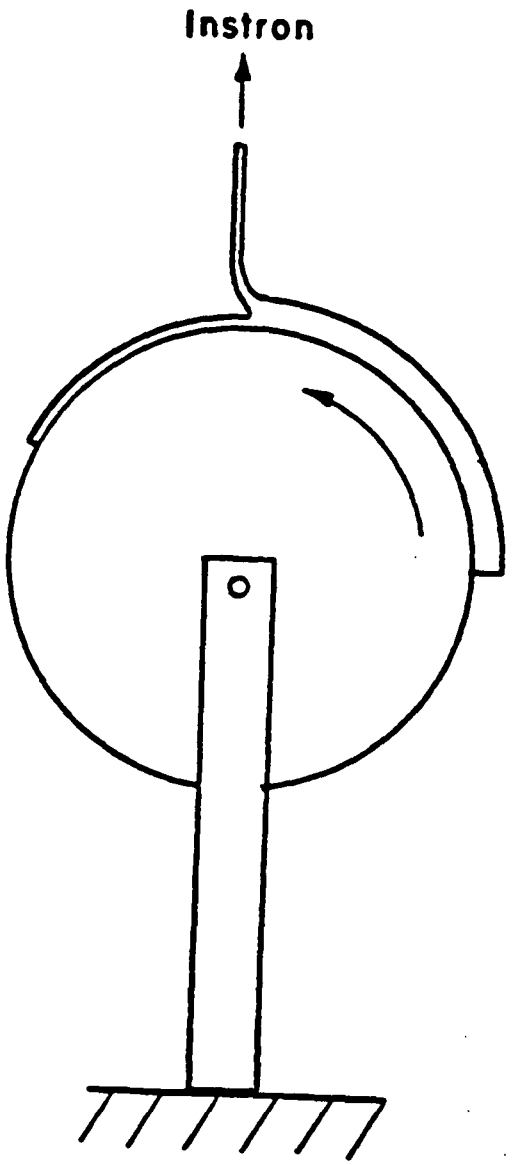

Figure 16. Schematic representation of the delamination wheel with specimen installed.

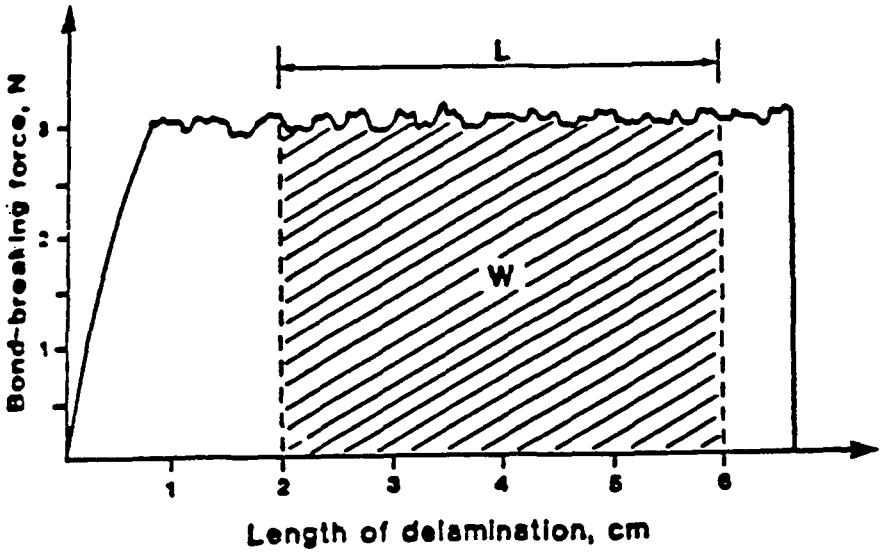

Figure 17. Sketch of load - elongation record from delamination test.

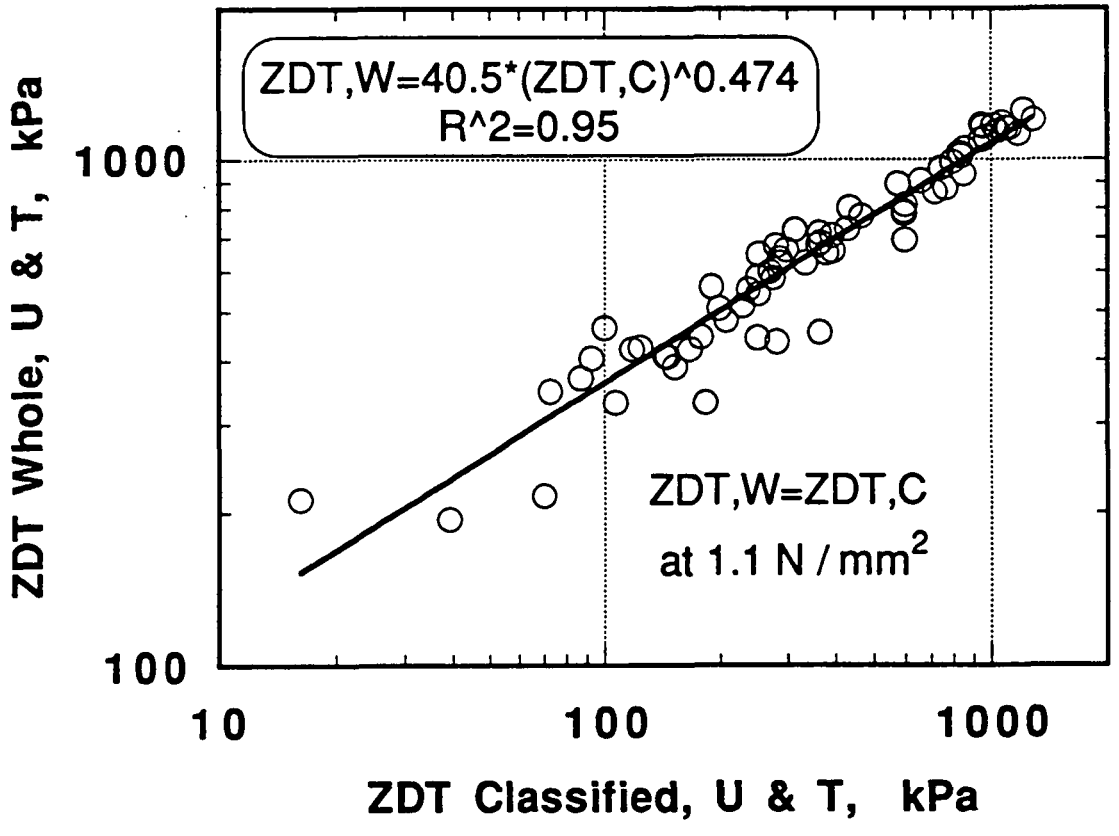

Figure 18. Doubly logarithmic plot of Z-direction tensile strength for samples identically prepared except for fines content.

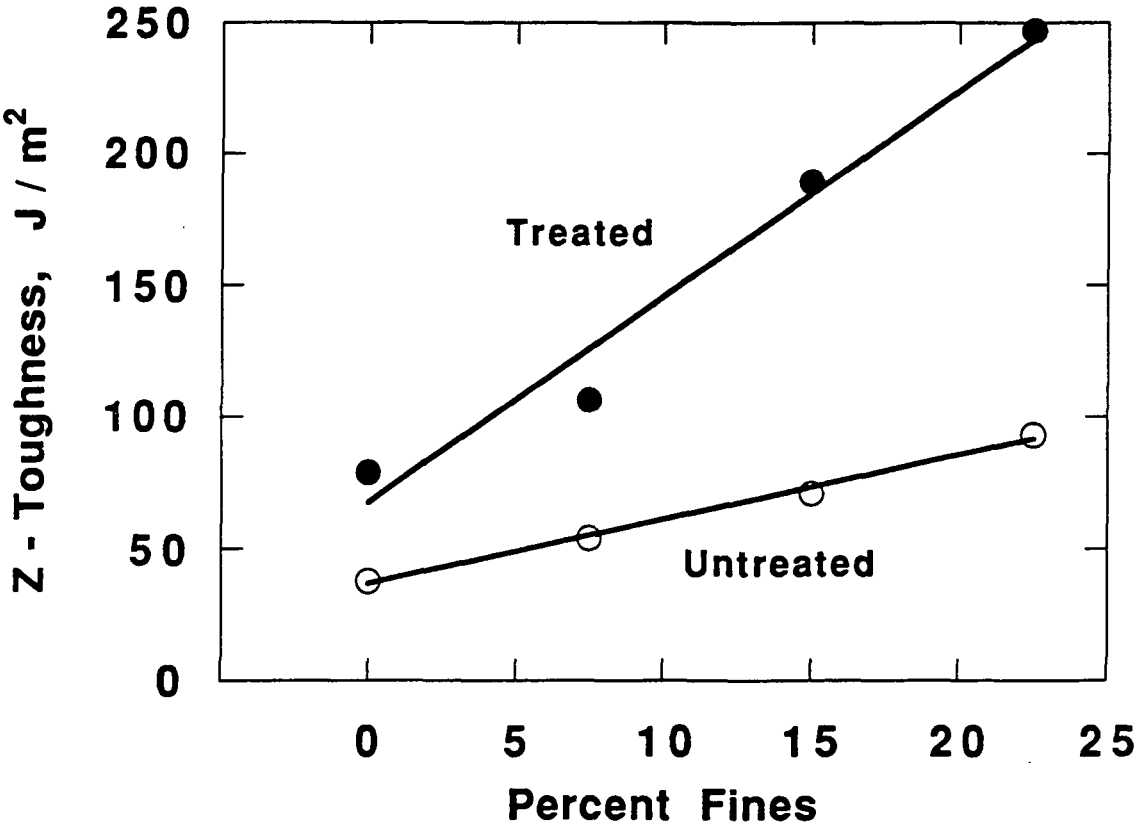

Figure 19. Dependence of Z-toughness on fines content and strength aid treatment.

in Figure 20. There is a linear increase in this property with density and a strong difference between the untreated and treated sheets. The effect of the strength aid on bond strength is obvious.

The two measures of bond strength are compared in Figure 21 for the 60% yield pulp, both whole and classified, with no strength aid added. A linear relationship exists. The finite value of the Z-toughness at zero Z-direction tensile strength may represent work being done on the sheet that is not going into bond breaking. The results for the 47% yield classified pulp with and without strength aid treatment is shown in Figure 22. Two distinct curves are found. This is perhaps not surprising since one test is measuring a strength and the other is measuring an energy (or work). It is possible that the two are affected differently by the presence of the strength aid. The detailed analysis of the rest of the data in this study may further illuminate these relationships.

Finally, having just shown the difference between strength and energy measurements (in the Z direction), we now show their common behavior in the XY plane. The tensile energy absorption (TEA), the area under the stress - strain curve, is plotted against the tensile strength, the ultimate stress on that curve in Figure 22. Data from all 229 sets were used. These included all yields, freenesses, wet pressing pressures, whole and classified pulps, and pulps treated or untreated with strength aids. A single curve is obtained. We are currently pondering the significance of this result.

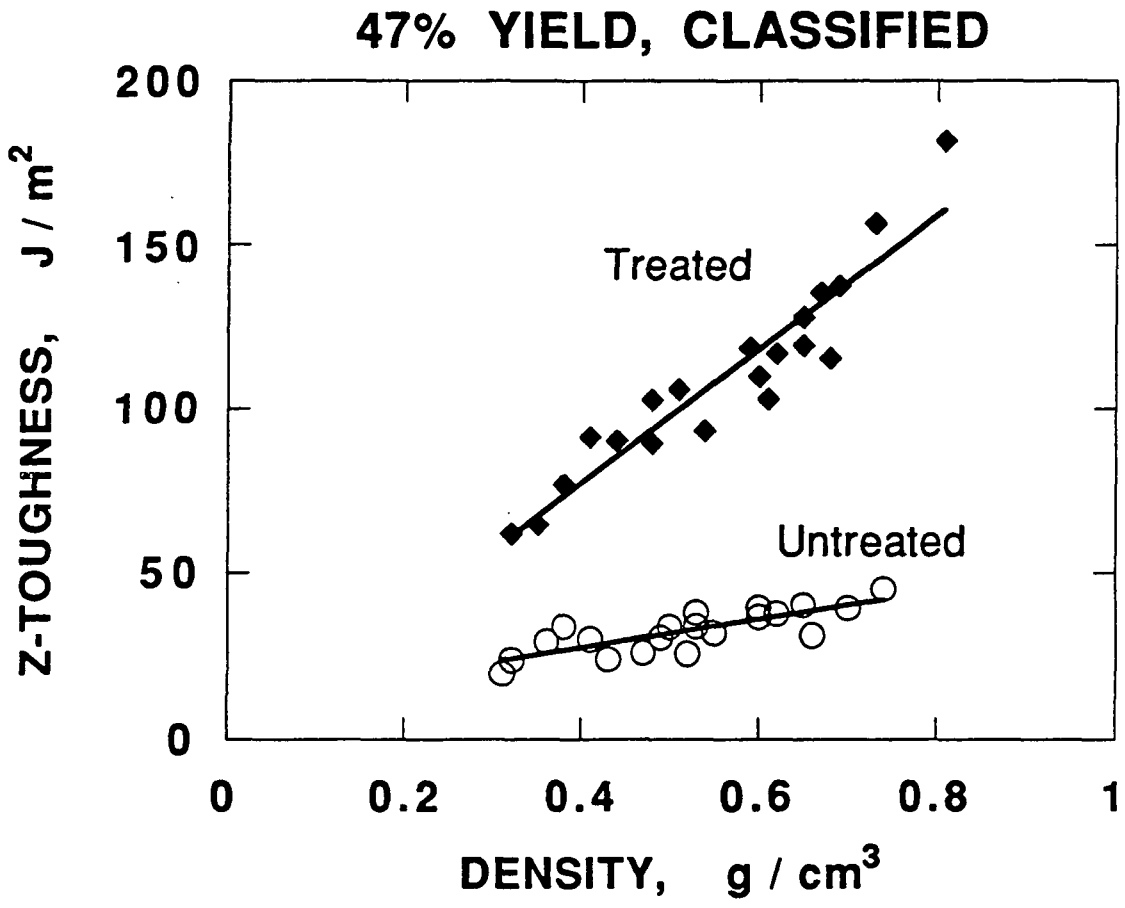

Figure 20. Dependence of Z-toughness on density and strength aid treatment for classified, 47% yield pulp.

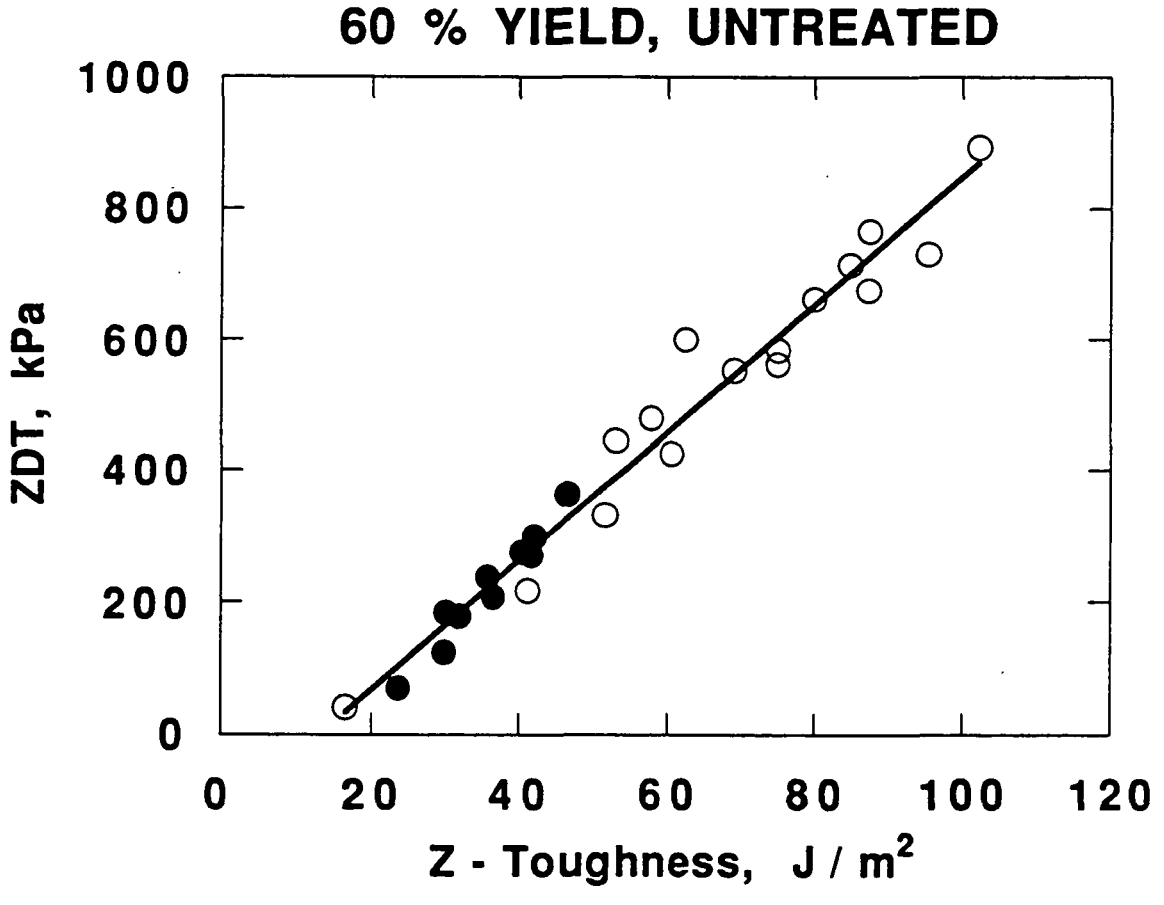

Figure 21. Comparison of Z-direction tensile strength and Z-toughness for 60% yield pulp untreated with strength aids. Open symbols, whole pulp; closed symbols, classified pulp.

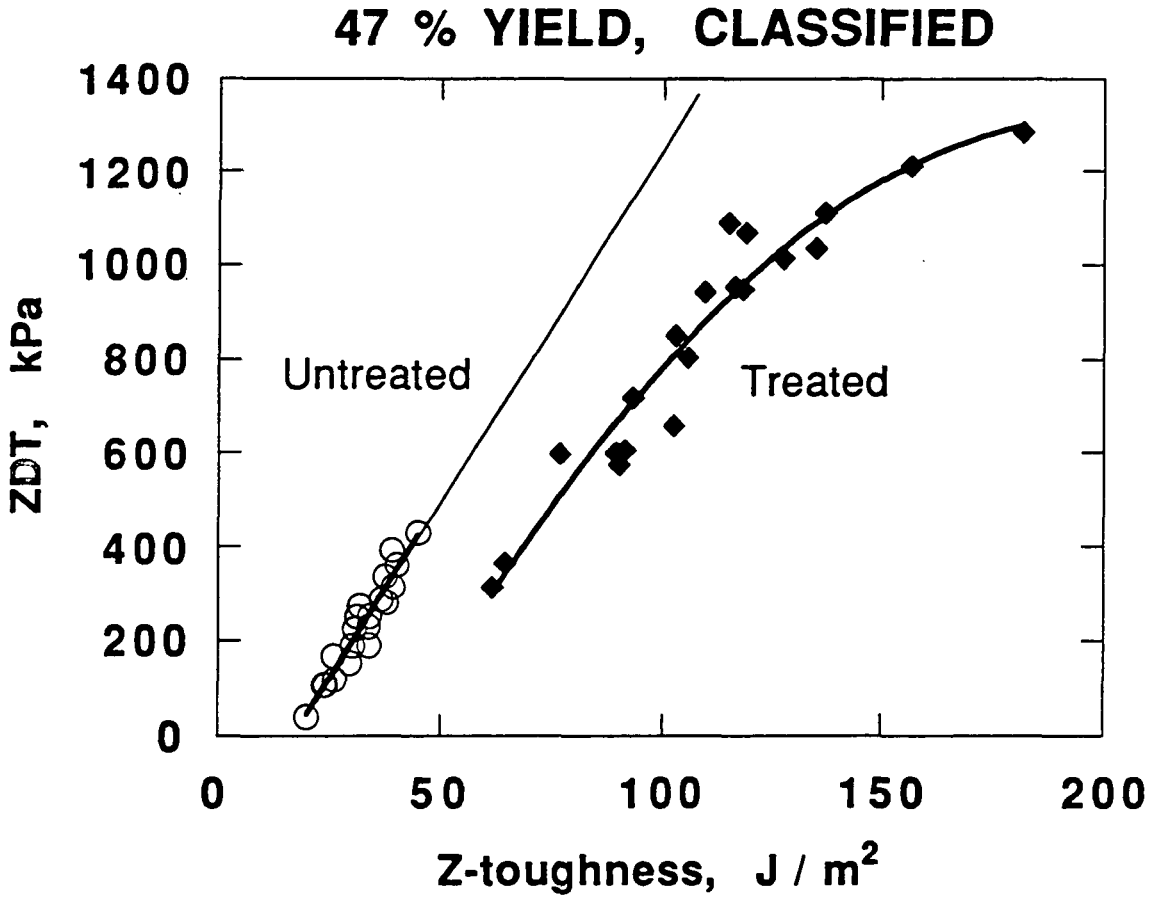

Figure 22. Comparison of Z-direction tensile strength and Z-toughness for 47% yield, classified pulp showing effect of strength aid treatment.

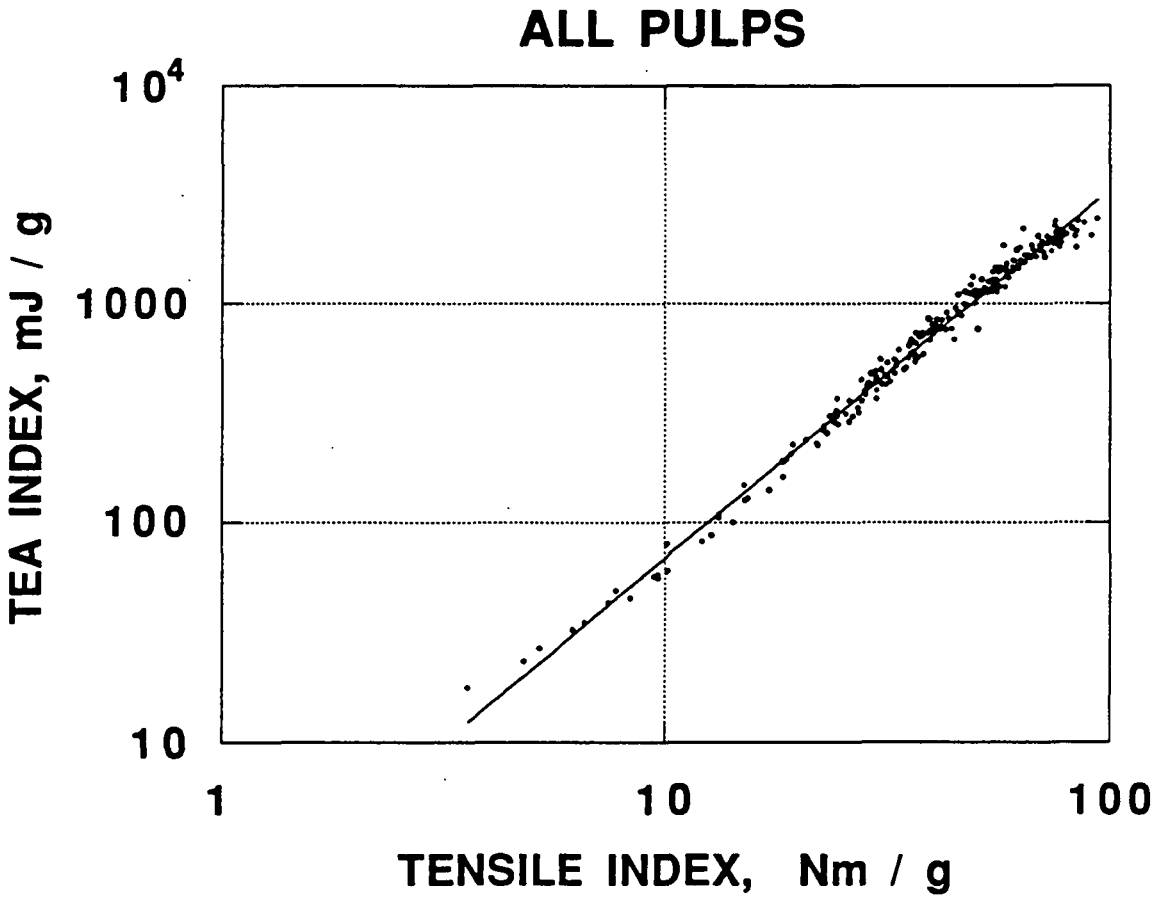

Figure 23. Doubly logarithmic plot of tensile energy absorption index against tensile index for all pulps.

Literature Cited

1. Hardacker, K. W., and Brezinski, J. P., Tappi, 56(4), 154 (1973).
2. Russel, J., Kallmes, O. J., and Mayhood, C. H., Tappi, 47(1), 22 (1964).
3. Nanko, H., and Ohsawa, J., in "Fundamentals of Papermaking", C. F. Baker, ed., Mechanical Engineering Publications Ltd., London, 1989, Vol. 2, 783.
4. Skowronski, J., and Bichard, W., J. Pulp Paper Sci., 13(5), J165 (1987).
5. Page, D. H., Tappi, 52(4), 674 (1969).

FUNDAMENTALS OF PAPER SURFACE WETTABILITY

STATUS REPORT

FOR

PROJECT 3646

TO THE

SURFACE AND COLLOID SCIENCE

PROJECT ADVISORY COMMITTEE

April 5, 1991

Institute of Paper Science and Technology
Atlanta, Georgia

Project Summary Form

Project Title: Fundamentals of Paper Surface Wettability
Project Number: 3646
Project Staff: Frank Etzler
Project Goal: Develop an understanding of the interaction of liquids and solid surfaces with particular attention to the interaction of water and cellulose and their influence on paper properties.

SUMMARY OF RESULTS SINCE MARCH 1990

Heat capacity measurements of water confined to various sizes of silica pores have been completed. The results indicate that modified water structure persists to high temperatures (at least 60°C) and that structural transitions occur in interfacial water near 15, 30, 45°C. The data collected represent the first direct thermodynamic evidence for interfacial water transitions although the existence of such transitions has been suggested by other earlier experiments. Interfacial water transitions may be important to a wide variety of phenomena including, for instance, the thermal limits of survivability of plants as well as the surface configuration and wetting characteristics of polymers including cellulose.

Statistical geometric analysis of computer simulated water has been completed. The results of our study indicate that the distribution of molecular volumes in liquid water is bimodal. This result appears to be the first microscopic support for Rontgen's hypothesis first offered in 1892 to support the density maximum in liquid water. The results also indicate that the statistical thermodynamic model for vicinal water used successfully to correlate the thermodynamic properties of such vicinal water is also correct at the molecular level.

The role of paper surface chemistry on wettability and printability of kraft linerboard has been studied. Significant variation in wettability exists across the industry spectrum. The variation in paper surface energies has been found to correlate with corresponding variations in paper surface chemistry as identified by ESCA. The surface tensions of inks typically used for flexographic printing have surface tensions high enough to be incompatible with a significant fraction of linerboards. A solution is to use inks of lower surface tension (28 dyne/cm). Such inks are easily prepared by ink companies.

A TGA accessory has been purchased for the DSC. Experiments designed to investigate the desorption of water vapor from paper samples have been designed and in part implemented. A novel method for TGA/DSC determination of the enthalpy of desorption of water from paper and other porous materials has been developed. This method will be used to study water sorption under cyclic humidity conditions. Further methods for measurement of adsorption isotherms are under development.

FUTURE WORK

1. Measurement of heat capacities of water associated with cellulosic materials with particular attention to the temperature dependence.

2. Design possible experiments to determine how the physico-chemical details of a surface influence the structure of water. Do polyhydroxyllic surfaces have special properties ?

3. Design experiments which illustrate the special role of water in colloidal forces and in fundamental papermaking processes such as polymer adsorption, flocculation, etc.

4. Continue experiments to study the effects of cyclic humidity on water vapor adsorption by paper samples.

FUNDAMENTALS OF PAPER SURFACE WETTABILITY
Project 3646

Introduction

The objective of this project is to understand the interaction of liquids with paper materials in a fundamental way. It appears important to assess the current state-of-the art and suggest future research paths. The long-term objective of the project is to achieve a fundamental understanding of the role of liquid-paper interactions in papermaking and in determining paper properties. The current work has been directed to: 1) reviewing the literature regarding the present understanding of water-cellulose interactions; 2) comparing results from model systems with that known for water-cellulose system; 3) refining Etzler's statistical thermodynamic model for vicinal water, and 4) exploring the effect of paper surface chemistry on liquid penetration (particularly as related to flexographic printing).

The Structure of Water Near Surfaces

The nature of the liquid state, at the molecular level, continues to be a forefront topic of research in physics and chemistry. Despite the efforts of a considerable number of able researchers, much regarding the nature of the liquid state remains to be learned. Fortunately, much progress has been made in the last decade; this progress suggests that considerable advances will be made in the coming years. The nature of liquids near surfaces is, at present, receiving considerable attention by both experimentalists and theoreticians. A fundamental understanding of the processes important in determining the nature interfacial (vicinal) liquids has not been achieved. Indeed, considerable ignorance of the state of vicinal liquids exists. Many fundamental experiments are necessary in order for progress to be made.

As the state of water near cellulosic surfaces is of considerable importance to paper manufacture, it is important to discuss the current understanding of water near solid surfaces. A comparison of vicinal water in model substrates and in cellulosic substrates is also of importance.

It is known that the properties of water near surfaces are modified by propinquity to solid surfaces. To date the most comprehensive studies of interfacial water properties have been made on water placed in pores of known size and geometry. It has been shown, for instance, that water in pores with a radii of 1 - 20 nm, exhibits a larger heat capacity, lower density and high viscosity. [See for instance, Etzler, F.M. Langmuir, 4, 878 (1988)]. From studies of water in clays and from density measurements of water in silica gel, it appears that water is structurally modified to distances of 3 - 6 nm. It also appears that the structural modification decays in approximately exponential manner with distance from the liquid-solid interface.

From work on a number of systems, it appears that the properties of vicinal water to a good first approximation, are independent of the physicochemical details for the surface. For example, it has been shown that the heat capacity of water near a wide variety of surfaces including cellulose is larger than the bulk. This aspect, however, deserves further attention.

The heat capacity of vicinal water appears to be a particularly useful quantity for understanding the nature of water in cellulosic systems; thus, this quantity is considered further. Stey (Ph.D. Thesis, University of Pittsburgh, 1967) has calculated the model independent distribution of single particle enthalpies for water and a number of other liquids. It was found that the enthalphy distribution for water is unusual in that the distribution is bimodal. This type of distribution contrasts with the nearly Maxwell-Boltzmann type distribution found for more simple liquids.

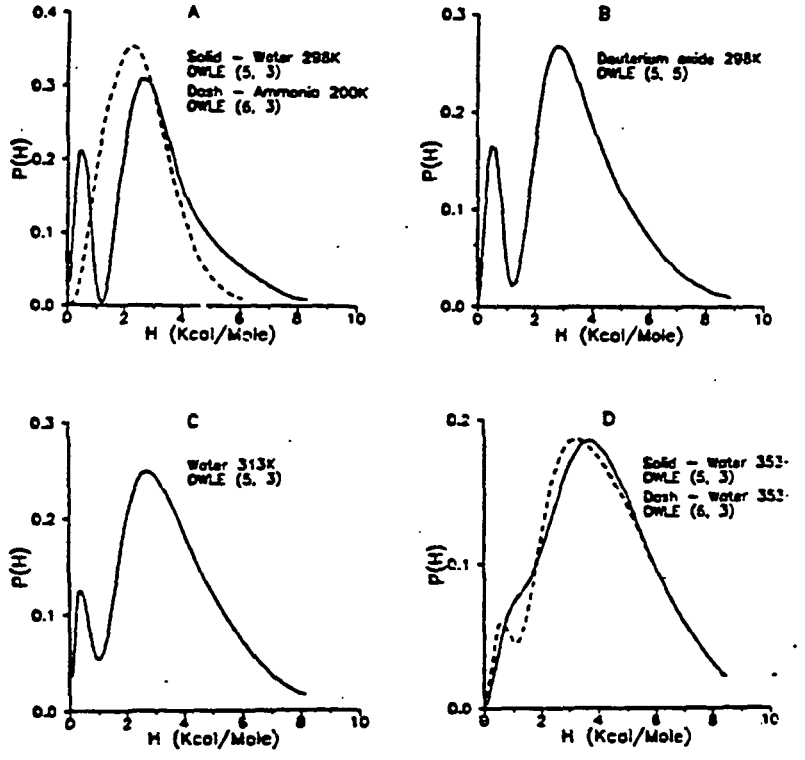

Figure 1. Stey's distribution functions. Probability, P(H), vs. enthalpy, H. (A) Water at 298 K and NH_3 at 200 K. (B) D_2O at 298 K. (C) H_2O at 313 K. (D) H_2O at 353 K.

Some of Stey's results are seen in Figure 1. It appears that the molecules represented by the low enthalpy peak in Stey's distribution are 4-hydrogen bonded water molecules while the high enthalphy peak represents molecules with 0, 1, 2, or 3 hydrogen bonds. The number of peaks in the distribution cannot be predicted from the number of hydrogen bonding states. It is generally presumed that the liquid state distributions would be nearly of the Maxwell-Boltzmann type.

The heat capacity, C_p is related to the variance, σ_h^2, of single particle enthalpies, through the well-known statistical thermodynamic relation:

$$C_p = (\sigma_h^2)/RT^2 \qquad (1)$$

For a bimodally distributed liquid the heat capacity may be considered as follows:

$$C_p = x(1)\, C_p(1) + x(2)C_p(2) + x(1)x(2)\frac{\Delta H^2}{RT^2} \qquad (2)$$

Here x(1) refers to the fraction of 4-hydrogen bonded water molecules. If it is assumed that hydrogen bonding is non-cooperative than x(1) equals the fourth power of the hydrogen bond probability between adjacent water molecules. $C_p(1)$ is taken to be the heat capacity of ice and $C_p(2)$ is estimated using a variety of experimental data, including, for instance, the activation energy of the rotational correlation time. At 298K $C_p(2)$ = 16 cal/K mole. ΔH is the mean enthalpy of transfer between the two peaks in Stey's distribution or 2.55 kcal/mole. $C_p(1)$, $C_p(2)$ and ΔH for deuterium oxide may also be estimated. At 298K approximately 6-10% of the water molecules in bulk water are 4 hydrogen bonded.

The heat capacity of water and deuterium oxide in silica pores of various diameters has been measured. The results are shown in Figure 2. A significant feature of the graph is the presence of the maxima near 7 nm pore radius. Figure 3 shows C_p as a function of x(1) as calculated from Equation 2. Significantly, Figure 3 suggests that vicinal water differs from the bulk in that hydrogen bond probability between adjacent molecules is enhanced by propinquity to solid surfaces and that the magnitude of the experimentally observed maxima may be calculated on the basis of Stey's earlier calculations. Density measurements on

water in silica pores are in agreement with the heat capacity measurements and suggest that hydrogen bond probability between adjacent water and molecules decays to the bulk value in an approximately exponential manner. Significant structuring extends 3-6 nm. The density of water in 7 nm radius silica pores is 2 - 3% lower than the bulk at 298K.

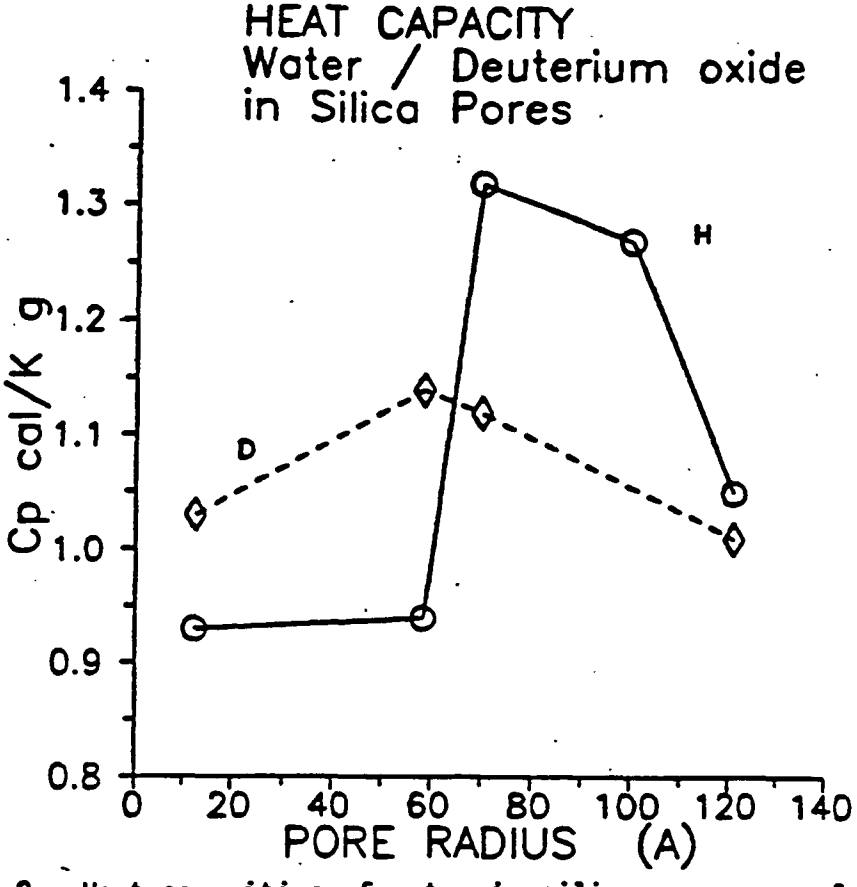

Figure 2. Heat capacities of water in silica pores as a function of pore radius at 298 K: squares H_2O; diamonds, D_2O. Radius in Angstroms (10 A = 1 nm).

Water in Cellulosic Materials

Measurement of the properties of water associated with polymeric substances is difficult as it is often impossible to separate polymer properties from water properties. Nonetheless

several attempts have been made to measure the properties of water associated with cellulosic and other polymers. Early attempts to measure the density of water in wood suggested that the water had a density much larger than bulk water (Indeed much greater than the density of Ice VIII at 25kbar!). Other measurements suggested that the expansivity of water associated with cellulosic materials is less structured than the bulk. This conclusion is in conflict with experimental evidence collected for water in clay and silica pores.

The use of thermal expansion as an indicator of vicinal water structure appears to be premature. It is not yet clear from statistical thermodynamics what the effect of enhanced hydrogen bonding between water molecules in pores would have on the magnitude of the thermal expansion coefficient. Reexamination of the apparent specific volume data for liquids associated with wood collected earlier by Weatherwax and Tarkow suggests that the high apparent density of water is due primarily to the opening of new pores (This is also an earlier conclusion of Weatherwax and Tarkow.) and that the density of water in the pores is 0.98 or 2% lower than the bulk if ethanol is treated as an unmodified pore liquid (Pore density equal to bulk density). This new result is consistent with density measurements of water and alcohols in silica pores.

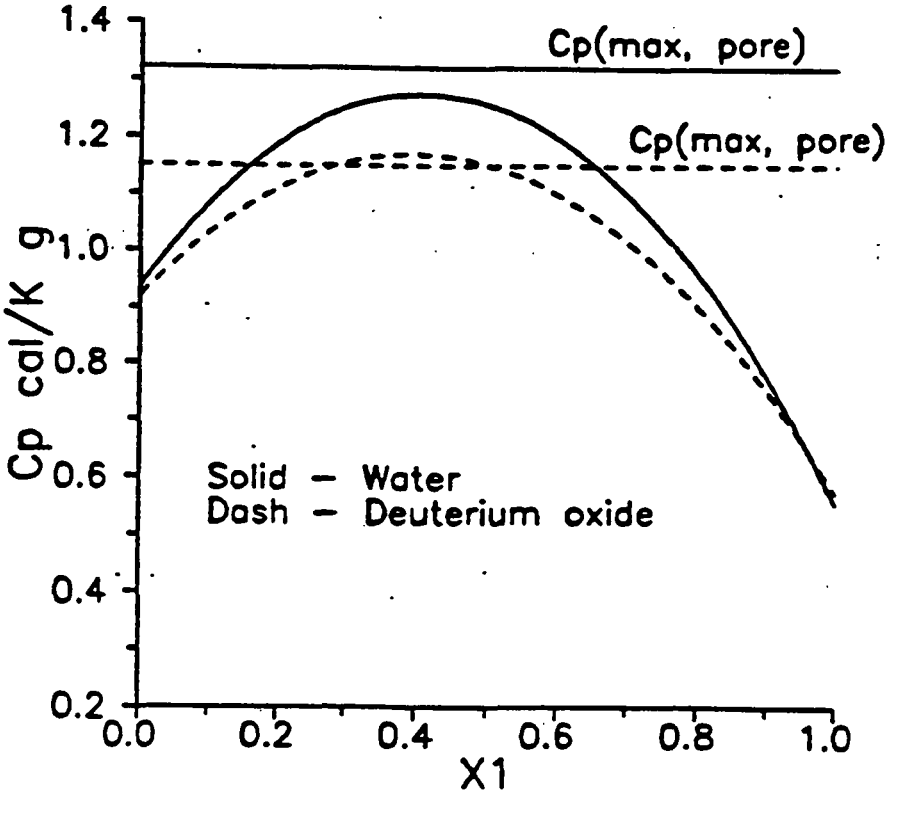

Figure 3. Hypothetical heat capacity of water and deuterium oxide as a function of x(1) at 298 K.

Figure 4 shows the apparent heat capacity of water in two kinds of wood. Figure 5 shows the apparent heat capacity of water in gelatin and starch suspensions. Both results are consistent with heat capacity measurements made in silica gel. In short, it appears that the properties of water associated with cellulosic materials and in silica gel are nearly identical and that water adjacent to either surface is more structured than the bulk.

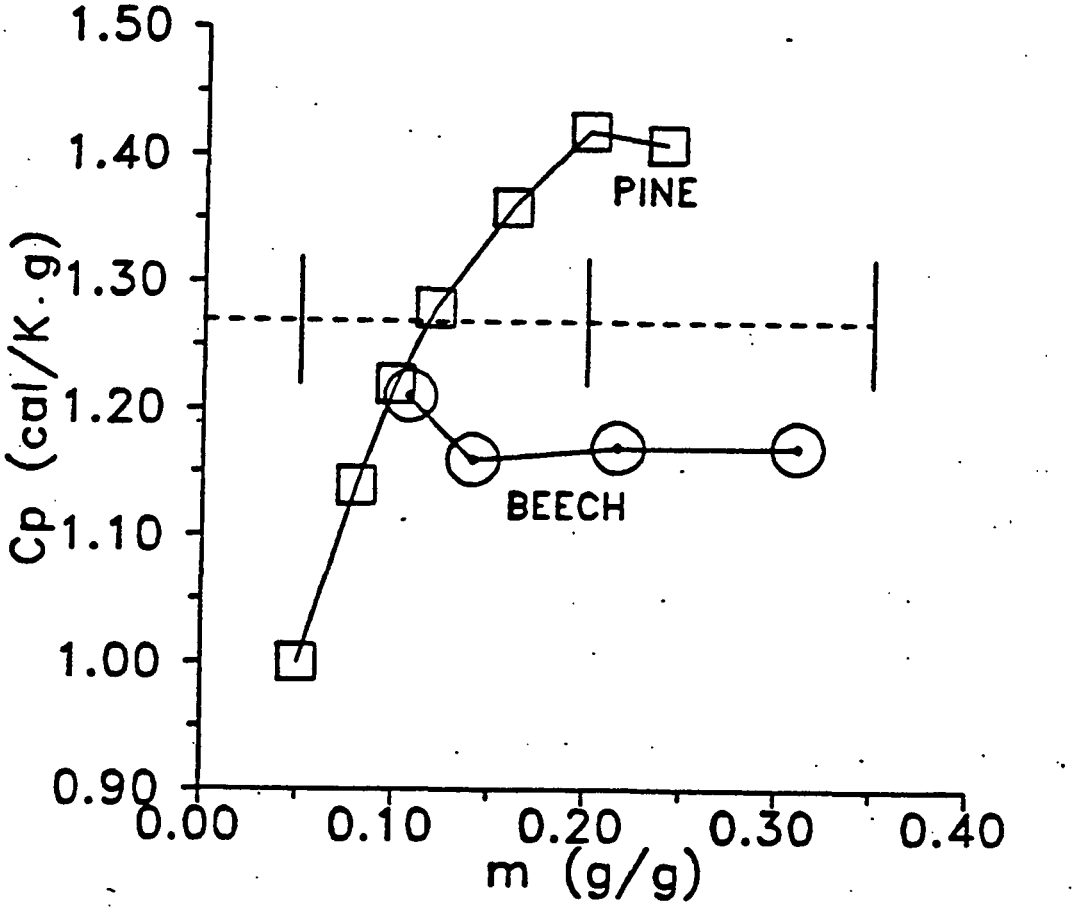

Figure 4. Apparent heat capacity of water in woods. Squares - pine; circles - beech; dashed line - maximum heat capacity as calculated from author's model.

Voronoi Polyhedra and the Structure of Vicinal Water

The results of Stey's calculations have been used successfully to correlate a number of thermodynamic properties of water near surfaces. Thus, it appears that Stey's calculated distribution can be used to make correct predictions of and correlations between macroscopic properties. Stey's calculation also makes predictions regarding the microscopic or molecular behavior of water. From thermodynamics Enthalpy, H = E + PV, where P is pressure, V is volume and E is energy. The single particle enthalpies discussed by Stey can thus be broken into two parts -- a volume part (Note: P = Constant) and an energy part. At present it is not clear whether energy or volume is the major factor in determining the form of Stey's enthalpy distribution.

It is not possible to calculate the distribution of molecular volumes in liquid via Stey's arguments without detailed knowledge of the intermolecular potential energy function. Knowledge of this function is not necessary, however, for the calculation of single particle

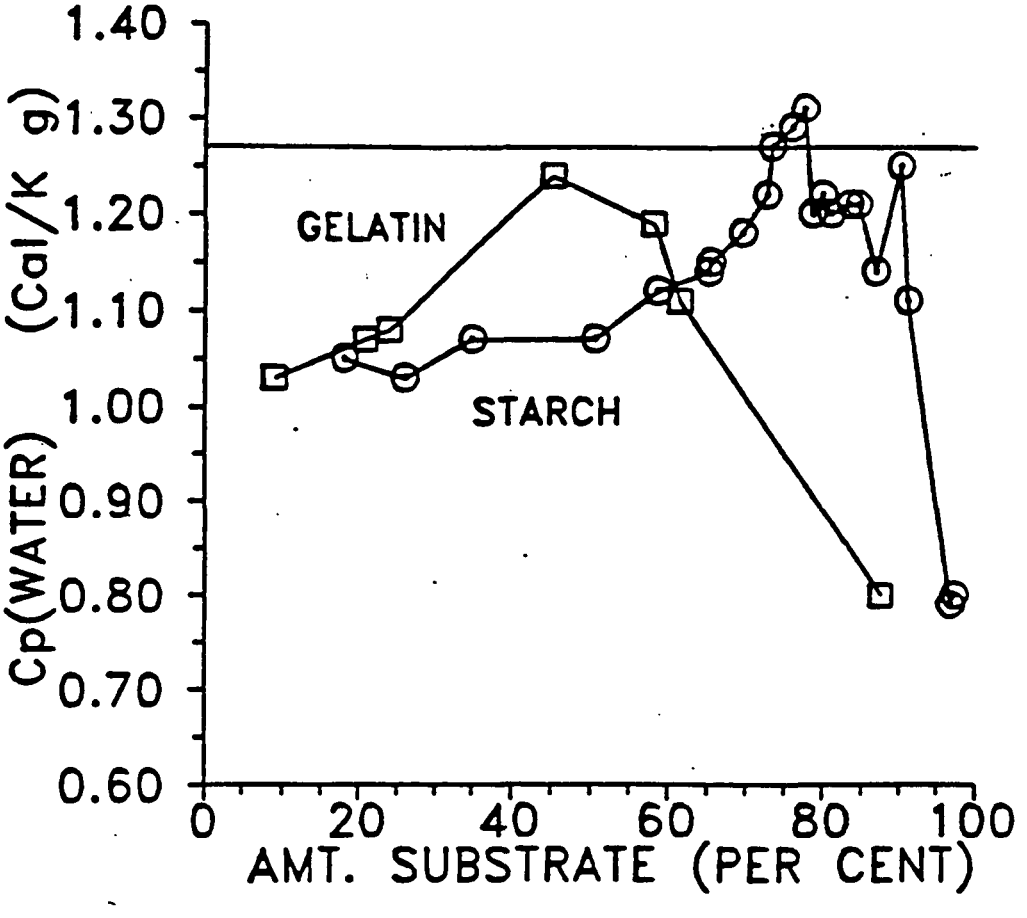

Figure 5. Apparent heat capacity of water versus per cent of substrate material in mixture. Squares - gelatin; circles - starch. Horizontal line - maximum heat capacity calculated from author's model.

enthalpies. It is possible, however, to estimate the distribution of molecular volumes from molecular dynamics calculations. The distribution of molecular volumes for liquid water is currently under investigation.

The volume of a molecule in a system can be regarded as the volume of the Voronoi polyhedra whose center is the molecular center of mass. The Voronoi polyhedra represents all points in space which are closer to a given molecular center of mass (or other reference point) than to any molecular center of mass. The temperature dependence of the isothermal compressibility for liquid water suggests that this distribution may have unusual features.

Our initial calculations concerning the properties of Voronoi polyhedra in computer-simulated water (SPC/E water) have been completed. Data on 30,000 polyhedra (3 sets of 10,000) have been collected. Figure 6 is a three-dimensional plot showing the probability of finding a polyhedron with a given number of faces and particular volume. The graph is unusual in a number of respects when compared to a simple liquid such as argon or Lennard-Jonesium. Two notable features are 1) the existence of two maxima in the distribution and 2) the high probability of 16-faced polyhedra. The abundance of 16-faced polyhedra is consistent with the existence of high-volume low energy (i.e. "ice-like") states is liquid water. The number of faces can be increased by lengthening the first neighbor distances while leaving the second neighbor distances essentially unchanged. The existence of two maxima give microscopic evidence which supports the earlier hypothesis of Roentgen and Frank suggesting simultaneous existence of "Bulky" and "Dense" regions in liquid water. The present calculation is important in that it presents the first microscopic evidence in support of Roentgen's hypothesis, first advanced nearly 100 years ago. It remains an important task to understand more clearly the interrelations between energy and volume which yield the bimodal enthalpy distribution calculated earlier by Stey.

Further analysis of the Voronoi polyhedra in SPC/E water, as seen in Figure 7 suggests that the two domains in the volume distribution are separated in energy as well as volume. A number of polyhedra types are found far more frequently in one or the other of the peaks.

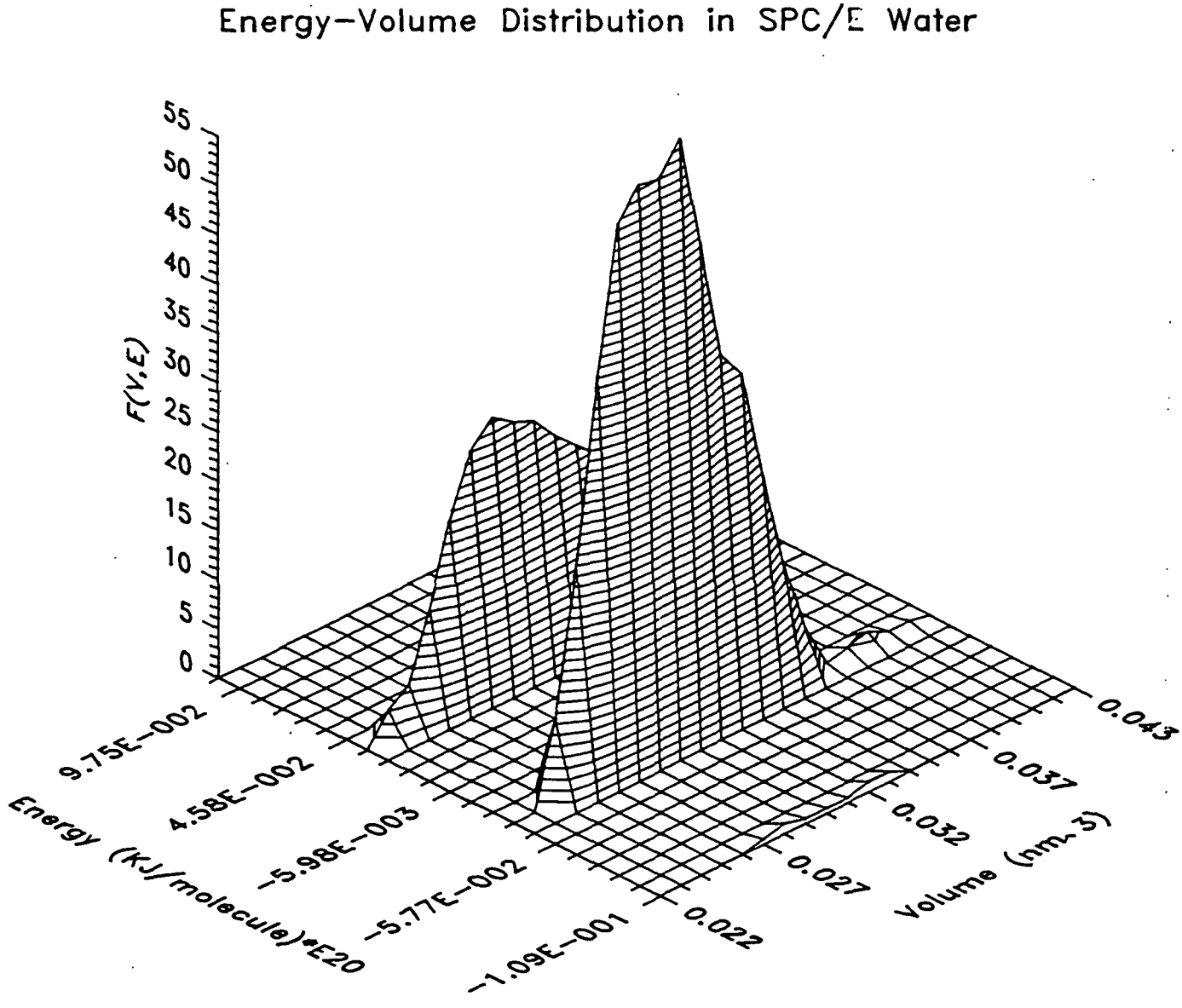
Energy–Volume Distribution in SPC/E Water
F(V,E)
55
50
45
40
35
30
25
20
15
10
5
0
9.75E-002
4.58E-002
-5.98E-003
-5.77E-002
-1.09E-001
Energy (KJ/molecule)*E20
0.022
0.027
0.032
0.037
0.043
Volume (nm-3)

Figure 7.

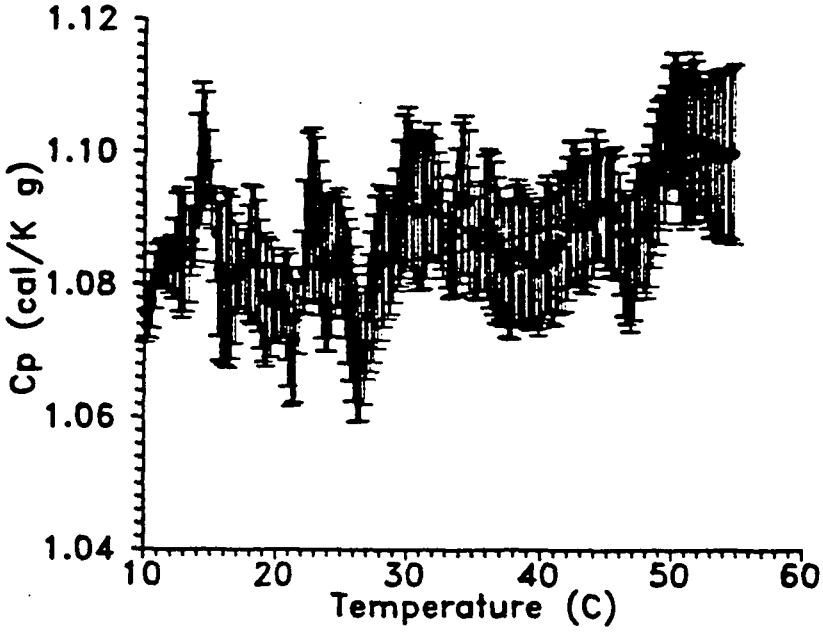

Figure 8. Heat capacity of water in 242 A diameter silica pores.

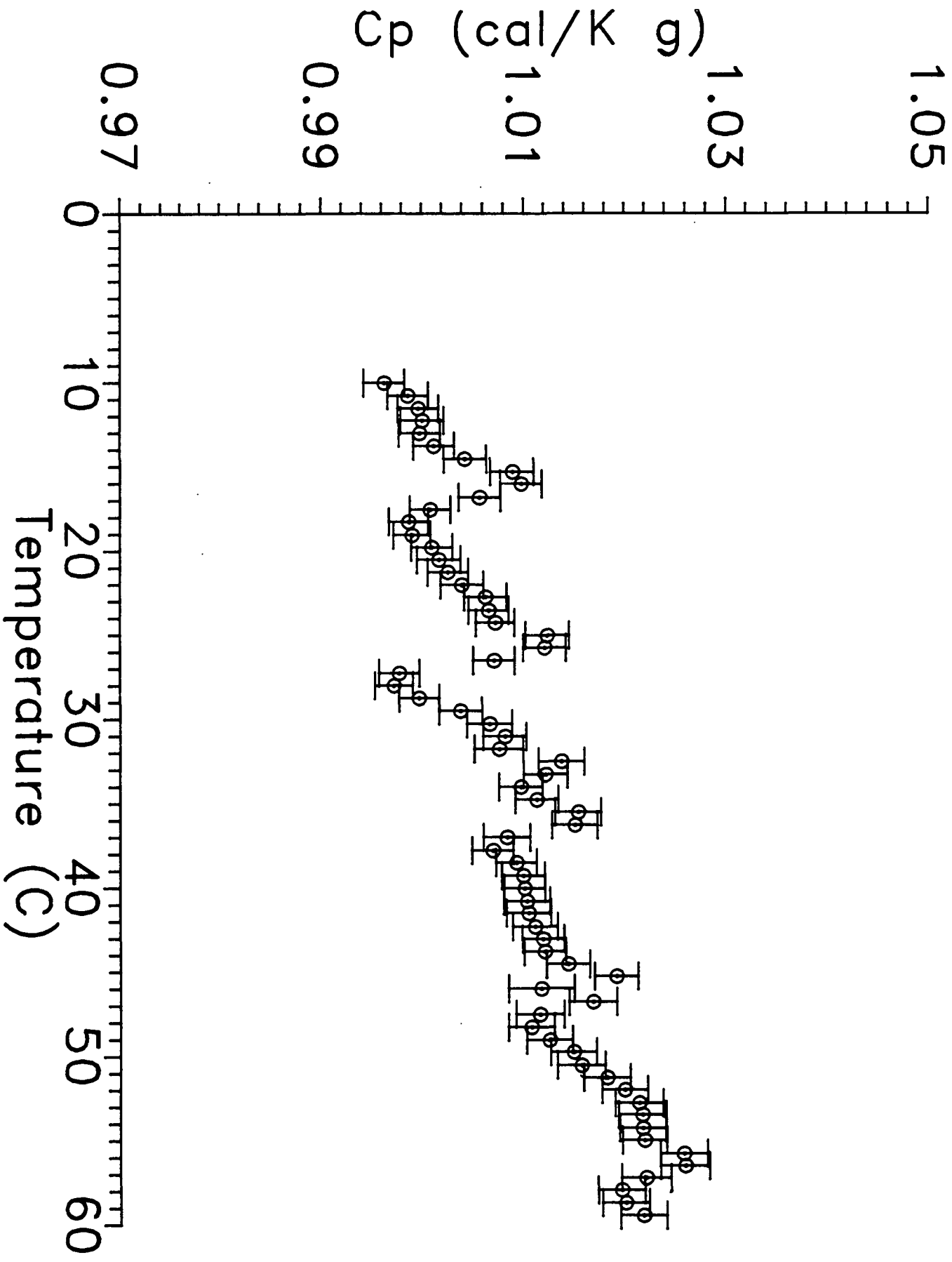

Figure 9. 40 Å

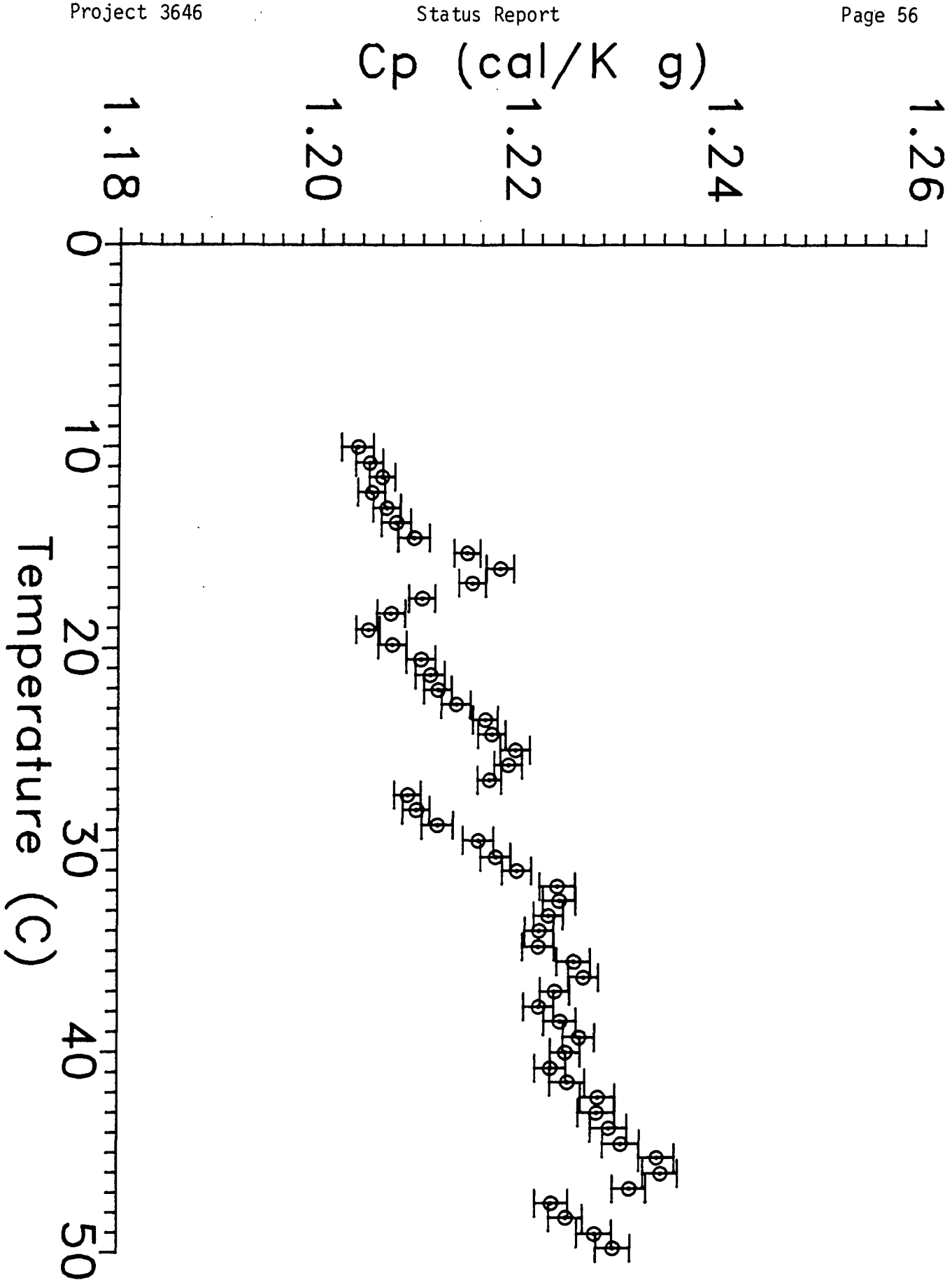

Figure 10. 140 Å

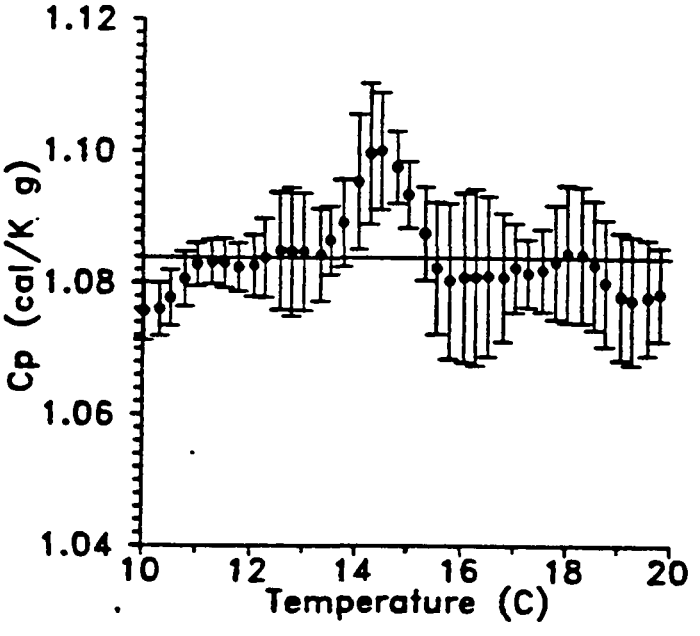

Figure 11. Detail over the temperature range from 10-20°C for water in 242 Å diameter pores.

These results suggest that the two peaks in volume distribution represent geometrically distinct domains. Methods for extracting information from the Voronoi analysis are being explored. This effort is taking us into unexplored territory.

The Temperature Dependence of the Heat Capacity of Vicinal Water

The Seteram DSC has been used to measure the heat capacity of water in 40, 140, and 242 A diameter silica pores from 10-60°C. The results of the calculations are found in Figures 8-11. The data indicate that significant structuring still occurs at rather high temperatures. Indeed ΔC_p increases slightly with temperature which suggests that bulk water structure breaks down more rapidly than vicinal water structure. Derjaguin has generally presumed that vicinal water structure breaks down by 70°C; clearly this is not the case.

More interestingly the data suggest the presence of "heat capacity spikes" near the Drost-Hansen temperatures. Drost-Hansen and later Etzler have suggested that physicological anomalies which occur near 15, 30, 45°C are the result of abrupt vicinal water structure changes. It is also known that ion selectivity by water confined to pores and that the viscosity of water between quartz plates both show unusual behavior consistent with structural transitions at the Drost-Hansen temperatures. The heat capacity spikes represent the first hard thermodynamic evidence for such vicinal water structure transitions.

The heat capacity spikes are found to be identical in all tested sizes of silica. This observation would seem to indicate that all the pore water participates in the transition.

Relation Between Interparticle Force and Vicinal Liquid Structure

The precise relation between vicinal liquid structure and interparticle force remains largely unexplored. Israelachvili et al. have, however, studied the forces between mica plates immersed in water and other liquids. This other group has discovered at least two forces not incorporated into DLVO Theory. These forces are the solvation force and the oscillatory force. The oscillatory force appear as very large oscillations in the interparticle force with a period equal to the molecular diameter near molecularity smooth surfaces.

The solvation force appears as an attractive force which is in addition to the van der Waals force incorporated into the DLVO Theory.

The solvation force is related to vicinal structuring and is typical 10-1000 times the van der Waals forces. Vicinal structure then may be responsible for the dominate attractive force between particles. [See Israelachvili et al. Macromolecules, 22, 4227 (1989)].

Kabanov et al. [Doklady Akademii Nauk SSSR, 302, 870, 1988] have discussed the temperature dependence of the adsorption rate of a polycation onto negatively charged latex particles. The temperature dependence is unusual but quite consistent with the heat capacity spikes which we have observed in silica pores. Anomalous adsorption rates were observed near 30,45 and 60°C. The data by Kabanov clearly indicate that interparticle forces involved in polymer adsorption are influenced by interfacial water structure and that flocculation theories solely based on DLVO theory are inadequate in least some respects. Polymer adsorption processes and particle flocculation are part of the papermaking process. The role of water in papermaking processes and in determining paper properties remains an under investigated area of scientific research.

Penetration of Liquids into Kraft Linerboards

The penetration of liquids into kraft linerboards has been measured. The penetration of liquids into a porous substrate is governed by the Washburn equation:

$$\frac{dh}{dt} = [r/4\eta g]\gamma_{LV} \cos\theta \qquad (3)$$

Here η is the liquid viscosity, θ is the contact angle and γ_{LV} is the liquid vapor surface tension and (dh/dt) is rate of penetration. According to the Washburn equation, if a surface is not wet (contact angle > 90°) then the rate of penetration is negative which in turn implies that the liquid will not penetrate. If surface is completely wet (contact angle = 0) then the Washburn equation becomes:

$$\frac{dh}{dt} = [r/4\eta h]\gamma_{LV} \qquad (4)$$

thus penetration is governed primarily by viscosity and not surface energetics when $\theta = 0$. Drop penetration time measurements made on a large number of kraft linerboard samples suggest that paper surface energy may play a significant role in flexographic printing. Linerboard samples which are not wet by typical inks have been found to exhibit poor print quality.

ESCA (Electron Spectroscopy for Chemical Analysis) studies of various linerboard samples have been performed. Some correlations with wettability were found. Specifically, it was found that wettability correlated either with the amount of surface hydrocarbon materials or with the amount surface silicon. The silicon content which correlates with hydrophobicity presumably results from the presence of silicone compounds.

We have also noted that bleached linerboard show Cl at the surface and are generally more hydrophillic while linerboards which show S are more hydrophobic.

It appears that ESCA may be a useful tool for understanding the nature of paper surfaces. The details of the surface chemistry of the pulp from which paper is made, undoubtedly determine the properties of the resulting paper.

Printing trials using inks of various surface tensions, indeed, show wetting leads to poor printing as evidenced by image analysis of edge sharpness and uniformity of ink coverage.

Water Vapor Sorption by Cellulosics

As part of an effort to understand the nature of paper/water interactions under cyclic humidity conditions, an effort has been made to develop calorimetric methods for the study of water vapor sorption.

To date a novel method, employing DSC/TGA (Differential Scanning Calorimetry/ Thermal Gravimetric Analysis has been made to develop calorimetric methods for the study of water vapor sorption from porous materials.

In the apparatus, A Seteram DSC/TGA, the temperature, sample mass and heat flux can be simultaneously monitored. The principal equation governing the measured heat flux, dH/dt, is:

$$dH/dt = m\ Cp\ dT/dt + Hv\ dm/dt$$

Here m is the sample mass, Cp the sample heat capacity and dT/dt the instrumental scan rate, dm/dt is the time derivative of the sample mass and Hv the heat of vaporization or desorption of the volatile component. For samples containing a reasonably large fraction of volatile component the vaporization process will overwhelmingly dominate the magnitude of dH/dt. Dryer samples require estimation of the sample heat capacity.

Measured heats of vaporization for water evaporating from silicas with known specific surfaces areas, show that the heat of vaporization becomes considerably larger than the bulk value at surface coverages of less than 4-5 monolayers.

It has been possible to measure the heat of vaporization of water from linerboard samples equilibrated at 90% RH and evaporated to dryness. These data show that the heat of desorption for water from paper is about 1.5-2.0 times the normal bulk heat of vaporization. It appears that the precise value of the heat of desorption may vary with the specific linerboard tested. The large heat of desorption indicates that all of the adsorbed water is closely associated with paper surfaces. Two factors which will influence the magnitude of the heat of desorption are the enthalpy of chemisorption in the first monolayer and the degree of surface coverage. The specific surface area of the samples and the details of the surface chemistry would be related to the enthalpy of chemisorption and the depth of coverage.

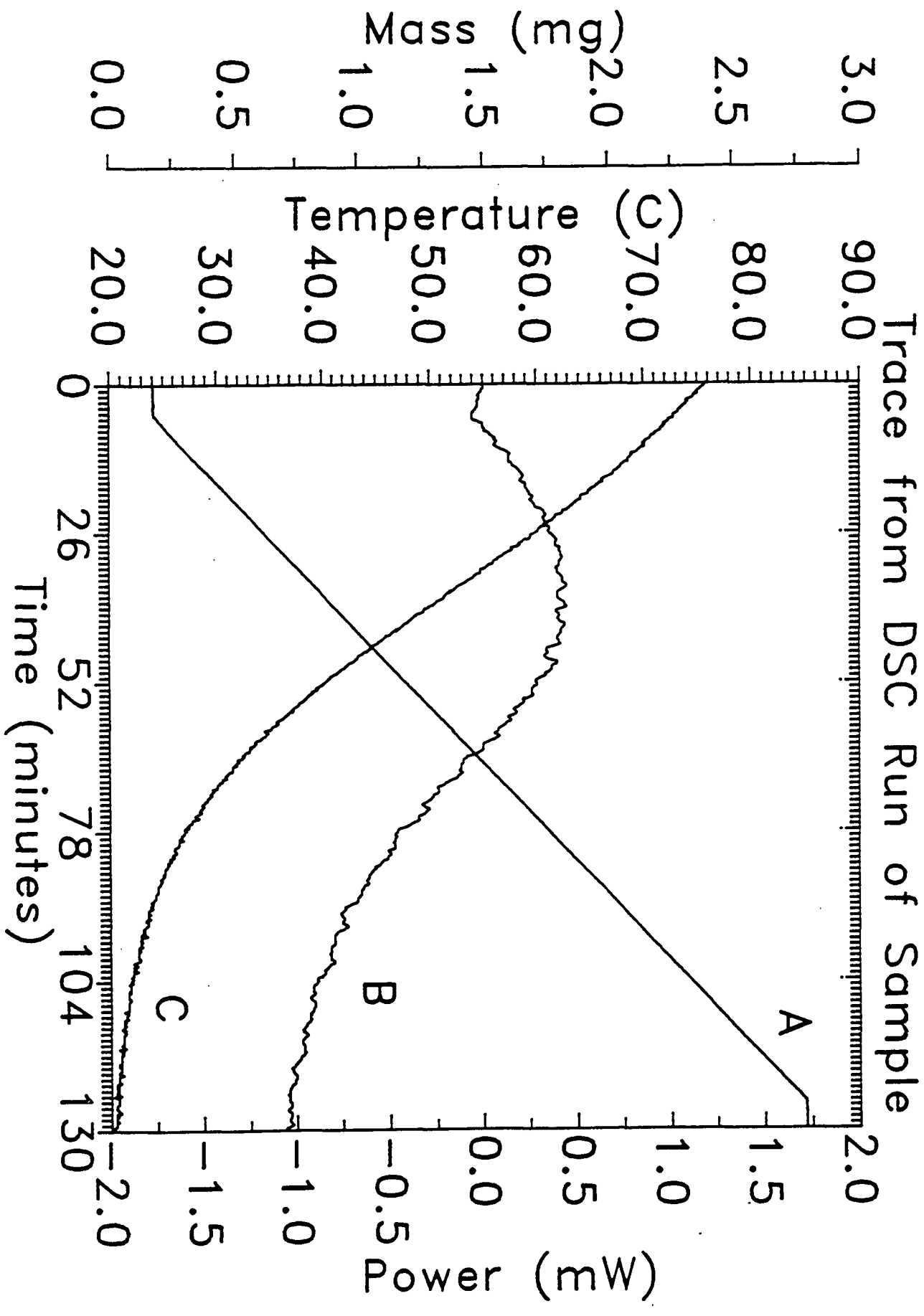

Figure 12. Output of DSC/TGA experiment. Curve A - temperature, Curve B- Power, Curve C-mass

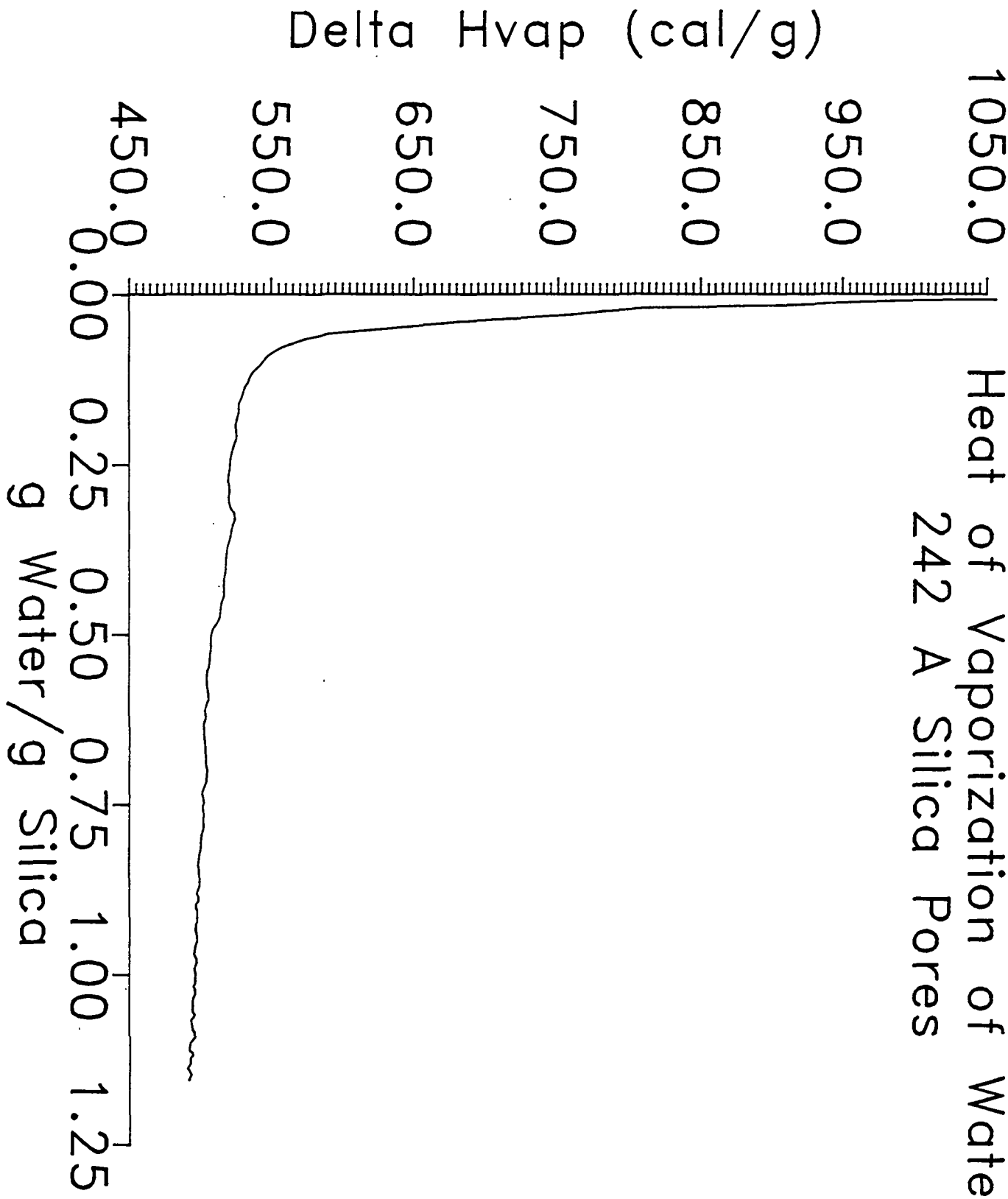

Figure 13. Heat of vaporization of water from a silica.

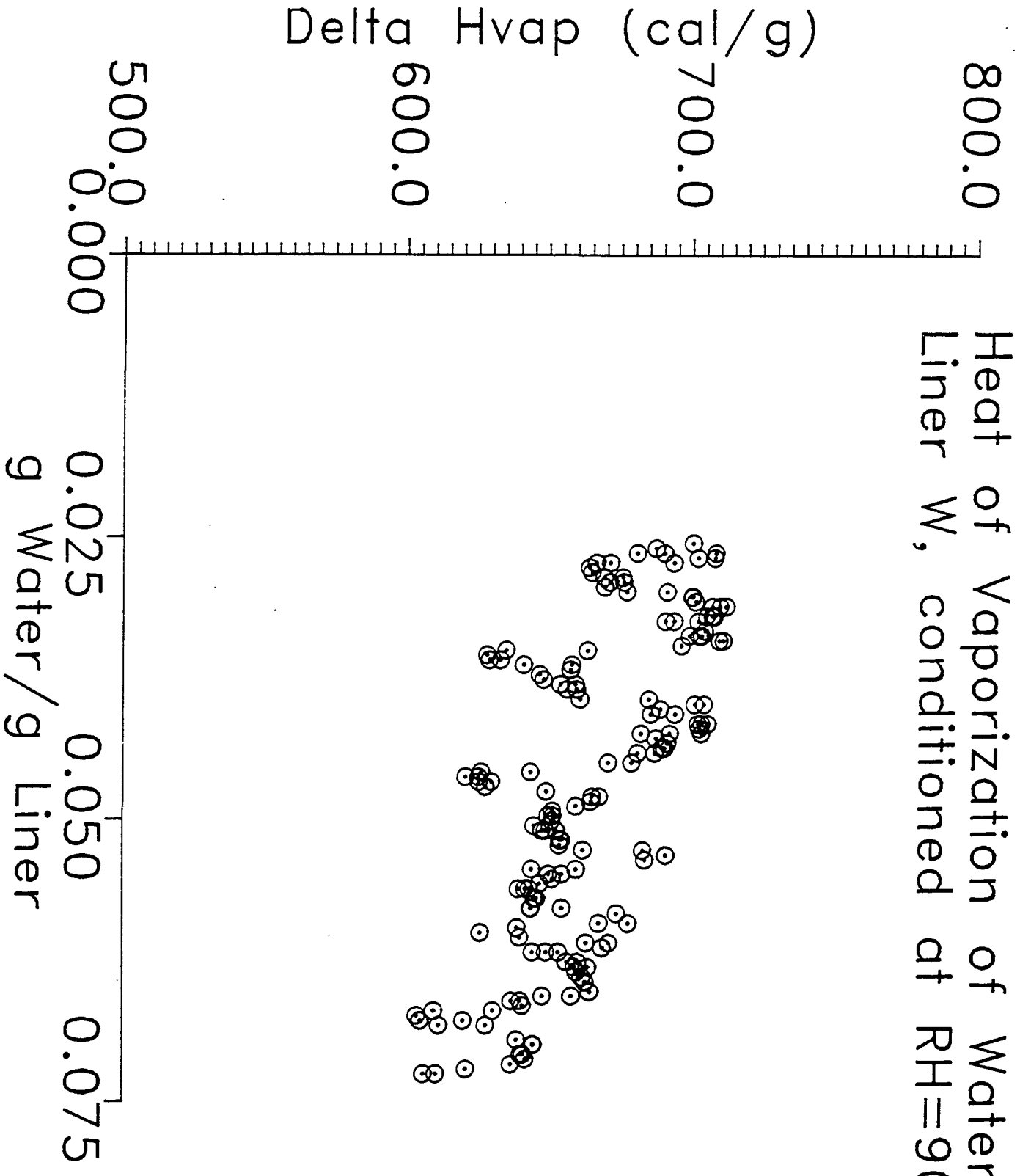

Figure 14. Heat of vaporization of water from linerboard sample (W).

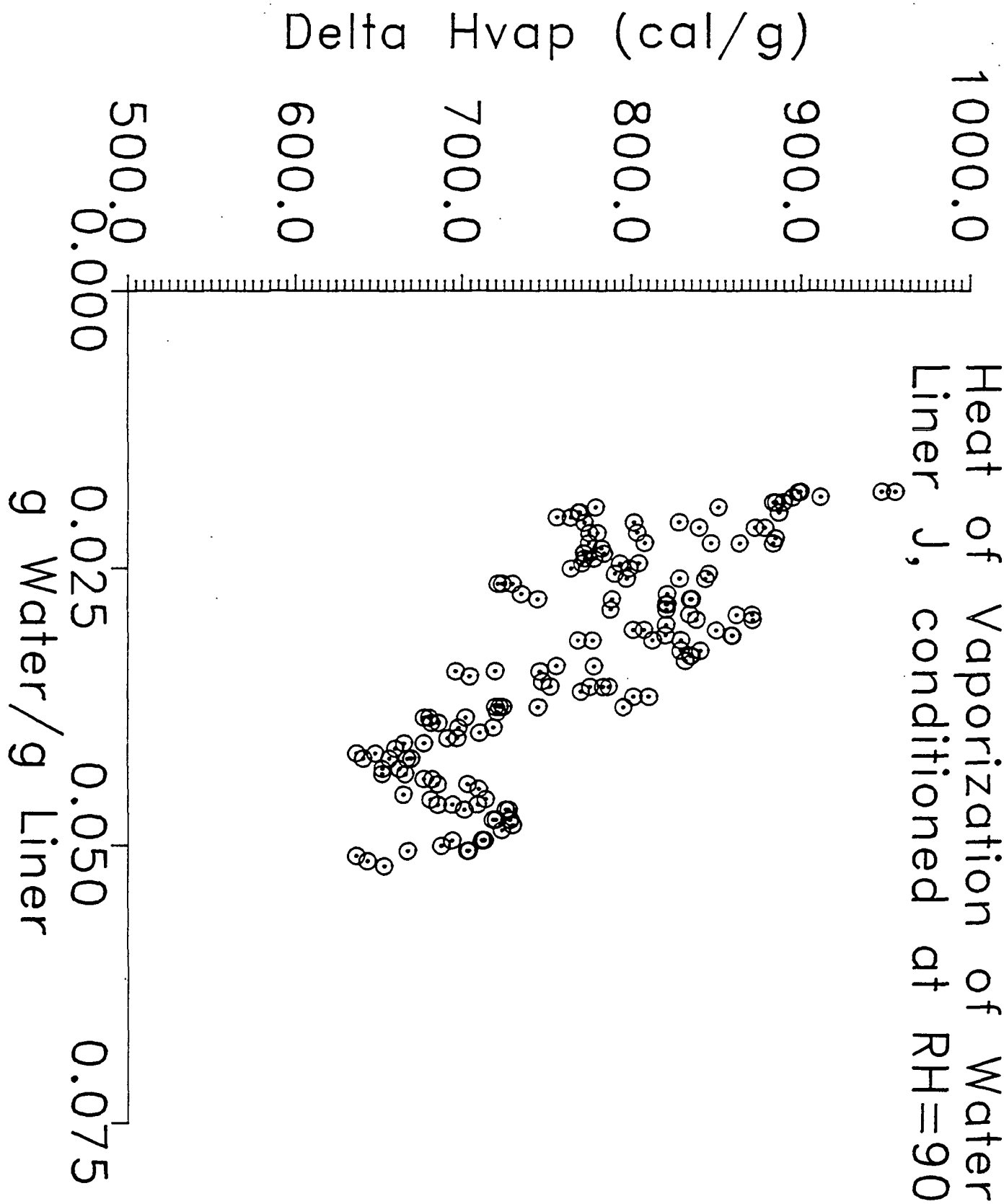

Figure 15. Heat of vaporization of water from linerboard sample (J).

FUTURE WORK

1. Measurement of heat capacities of water associated with cellulosic materials with particular attention to the temperature dependence.

2. Design possible experiments to determine how the physico-chemical details of a surface influence the structure of water. Do polyhydroxyllic surfaces have special properties ?

3. Design experiments which illustrate the special role of water in colloidal forces and in fundamental papermaking processes such as polymer adsorption, flocculation, etc.

4. Continue experiments to study the effects of cyclic humidity on water vapor adsorption by paper samples.

UTILIZATION OF RECYCLED FIBER

STATUS REPORT

FOR

PROJECT 3681

TO THE

SURFACE AND COLLOID SCIENCE

PROJECT ADVISORY COMMITTEE

April 5, 1991

Institute of Paper Science and Technology
Atlanta, Georgia

Project Title: UTILIZATION OF RECYCLED FIBERS
Project Code: RECYC
Project Number: 3681
Project Staff: R. Stratton, R. Ellis
FY 90-91 Budget: $185,000

Program Goal:

To develop the technological understanding necessary for a significant expansion in the use of recycled fiber from secondary sources. Examine the practical limitations on the expanded use of secondary fibers in various paper grades.

Program Areas:

Environmental Impact, End Use Performance

Rationale:

The paper industry may be required through legislative or regulatory action to expand its utilization of recycled fibers in papermaking grades where such utilization is not now economically practiced. Some of the secondary fiber material may include recycled grades that are now considered to be of inferior quality, such as mixed grades and newsprint. The inferior quality of these raw materials is likely to be offset by their low cost and availability.

The impact of increased use of lower quality secondary fiber on the important properties of certain product grades such as writing papers, coating stock, linerboard, and the practical limitations on the use of secondary fibers of various types in such grades, have not been systematically explored. The purposes of this study are to characterize the degradation of important properties attendant on the use of non-traditional secondary fibers in non-traditional paper grades, determine the practical limits on the use of secondary fibers in various paper grades, and to identify processing alternatives that will permit the expanded use of such fibers in various paper grades, and to identify processing alternatives that will permit the expanded use of such fibers without degradation of critical product properties.

Recent reports suggest that high oxidative treatments of secondary fibers can improve strength and related properties, apparently as a result of oxidation of contaminants.

The handsheet study to access the impact of repeated recycle on fiber and sheet properties is underway. Results for Bleached Southern Pine and Hardwood are near completion. Use of the Page equation to analyze strength data shows that the fiber-fiber bond strength of recycled fiber is equivalent to never dried fiber. Therefore, sheet strength loss is dominated by loss of bonded area. Fiber coarseness and perimeter are reduced by repeated recycle.

Goals for 1990 - 1991:

What is the impact of recycled fiber on product performance and papermaking?

a) Select a series of dominate fiber species in the U.S. waste streams and determine the following:

   1) Strength and optical characteristics
   2) Drainage characteristics
   3) Pressing characteristics

b) Modify the MAPPS System to include the effect of recycling.

Can the effect of contaminants be eliminated by using strong Oxidative treatments?

a) Determine the effect of High temperature O_2 and O_3 treatment on the typical contaminates in a waste stream.

Accomplishments to Date:

In FY 89-90, this project was initiated with a review of waste paper utilization in the United States. This review is still underway, but is scheduled for completion by June 1990.

Work carried out under Project 3428, "Removal of 'Sticky' Contaminants from Recycled Fiber," has been reexamined. A theoretical framework for flotation has been developed. Removal by flotation can be understood in terms of the surface energies of the contaminants and of the flotation medium, the important factor being the strength of attachment between the air bubble and the contaminant. A report on this work has been written.

The pilot scale flotation deinking equipment has been received and installed. Student work using it is underway.

Related Student Projects:

1. Jeffrey Faust, M.S. project, "Impact on Strength for Pressing vs. Size Starch on Linerboard and Medium Grade Papers Made from Recycled Material" (in progress).
2. Kelly Sedlachek, M.S. project, "Impact of Recycling on Printing/Writing Papers" (in progress).
3. Ronald Vollbrecht, M.S. project, "The Quantitative Effect of Dry Strength Additives on Fiber-Fiber Bond Strength" (in progress).
4. Cheryl Keller, Special Project, "Effects of Surfactants on the Deinking of Recycled Paper Container Laser-Printed Ink" (in progress).

Goals for April 1991 - October 1991:

1. Determine the important parameters for the effective flotation removal of laser-printed ink from fiber.
2. Determine the influence of collector systems on the separation of fibers and contaminants by flotation.
3. Continue the handsheet study for "Western" pulp species.
4. Begin experiments on O_2 and O_3 treatments.
5. Begin experiments on pressing and drainage.

Project Status:

FLOTATION OF STICKIES

This is a synopsis with additional theoretical interpretation of a study (1, 2) by Joseph J. Becher and Jack D. Hultman carried out under Project 3428. This project, "Removal of 'Sticky' Contaminants from Recycled Fiber," was funded by the American Paper Institute (API). The work was reported in Progress Reports One and Two dated June 18, 1980 and May 6, 1981, respectively, and was performed at the Institute of Paper Chemistry. Because of the current importance of secondary fiber utilization, and because this early work is not available in the open literature, it was deemed useful to summarize its findings. Permission has been granted by the API for this.

INTRODUCTION

Removal of contaminants from secondary fiber ("deinking") is accomplished by washing, flotation, or a combination of the two. Washing is effective for removing particles smaller than about 10-20 μm in extent (3), while flotation works best for particles in the range 10-200 (3, 4). Newsprint inks can be readily dispersed into small particles which can be removed by washing. Pulping of secondary fiber containing sticky contaminants such as hot melt or pressure sensitive adhesives typically results in the production of larger particles. Project 3428 examined the application of surface chemistry principles to the flotation of such sticky contaminants.

The process of removal of one type of solid particle from the presence of another by (froth) flotation has been used in ore beneficiation and deinking of paper for many years. Separation is dependent on their being a difference in surface free energy between the two types of solids (i.e. fiber and ink). When an air bubble attaches to a solid suspended in a liquid a contact angle θ can be defined as shown in Figure 1, i.e. the angle between the solid surface and the tangent to the air/liquid interface at the intersection with the solid surface. The angle is measured through the liquid phase.

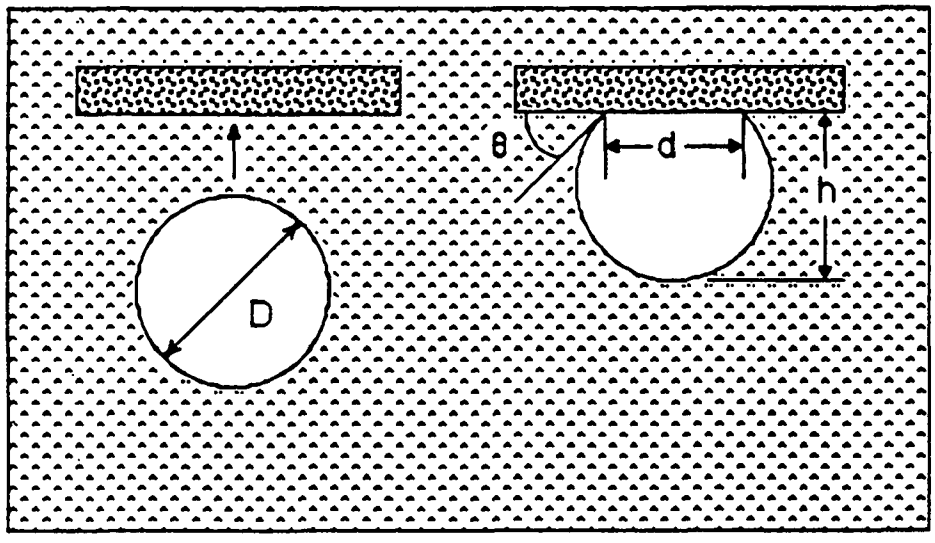

Fig 1. Schematic Representation of Bubble Attachment to a Sticky.

In order for a liquid to spread on a solid the work of adhesion W_{SL} must be greater than the work of cohesion W_{LL} of the liquid. These quantities are related to the interfacial tensions as follows

$$W_{SL} = \gamma_{SV} + \gamma_{LV} - \gamma_{SL} \quad (1)$$

$$W_{LL} = 2\gamma_{LV} \quad (2)$$

where the subscripts indicate the solid, liquid, or vapor phase. The spreading coefficient $S_{L/S}$ is given by

$$S_{L/S} = W_{SL} - W_{LL} \quad (3)$$

or, in terms of the interfacial tensions as

$$S_{L/S} = \gamma_{SV} - \gamma_{LV} - \gamma_{SL} . \quad (4)$$

A necessary condition for flotation is that the air bubble be able to displace the liquid in order to become attached. This is equivalent to requiring that the liquid not spread on the solid or $S_{L/S} < 0$. The forces created by the interfacial tensions are shown in Figure 2. A force balance (in the plane of the surface of the solid) results (5) in Young's equation

$$\gamma_{SV} = \gamma_{SL} + \gamma_{LV} \text{ Cos } \theta \quad (5)$$

When equation 5 is substituted into 4, the spreading coefficient becomes

$$S_{L/S} = \gamma_{LV} (\text{Cos } \theta - 1) \quad (6)$$

and the necessary condition for bubble attachment ($S < 0$) is Cos $\theta < 1$ or $\theta > 0$. Although necessary, this is not a sufficient condition for practical applications. In a flotation cell the air bubble/solid attachment must be able to withstand the forces

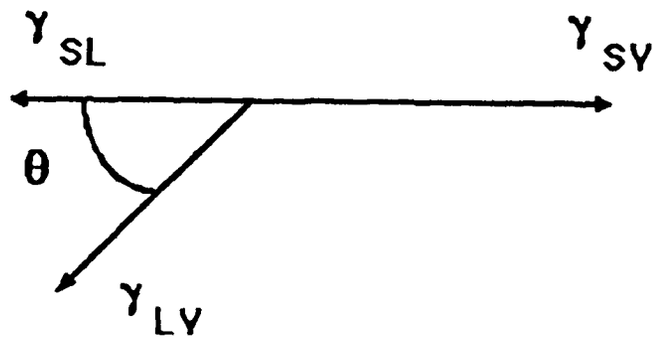

Fig 2. Balance of Surface Tensions at the Air-Liquid-Solid Interface.

caused by the differential buoyancy of the two and the shearing forces produced by the bubble ascension and the turbulent mixing.

The strength of the attachment F_a is equal to the product of the perimeter of the bubble/solid interface and the liquid surface tension.

$$F_a = \pi\, d\, \gamma_{LV} \operatorname{Sin} \theta \qquad (7)$$

Here d is the diameter of the circle formed by the attachment (see Figure 1), and the expression is multiplied by Sin θ to produce the component of the surface tension perpendicular to the solid surface.

This can be rewritten in terms of the preattached bubble diameter D and the ratio d/D as

$$F_a = \pi\, D\, (d/D)\, \gamma_{LV} \operatorname{Sin} \theta \qquad (8)$$

Assuming that the volume of the bubble does not change upon attachment and that the attached bubble has the shape of a spherical segment, we can express the equality of the two volumes as

$$V = (\pi/6)\, D^3 = (\pi/24)\, h\, (4h^2 + 3d^2) \qquad (9)$$

where h is the height as defined in Figure 1. By expressing h in terms of d and the contact angle θ, equation 9 can be rearranged to

$$d/D = 2 \operatorname{Sin} \theta / \left[(1 + \operatorname{Cos} \theta)^3 + 3(1 + \operatorname{Cos} \theta) \operatorname{Sin}^2 \theta \right]^{1/3} \qquad (10)$$

This function is shown in Figure 3 where the almost linear dependence of d on contact angle for a given bubble size is seen. (Strong positive curvature occurs at still higher angles, but the latter are of no practical importance.) Over the more limited range $0 < \theta < 65^o$ found experimentally in the present work equation 10 can are closely approximated by

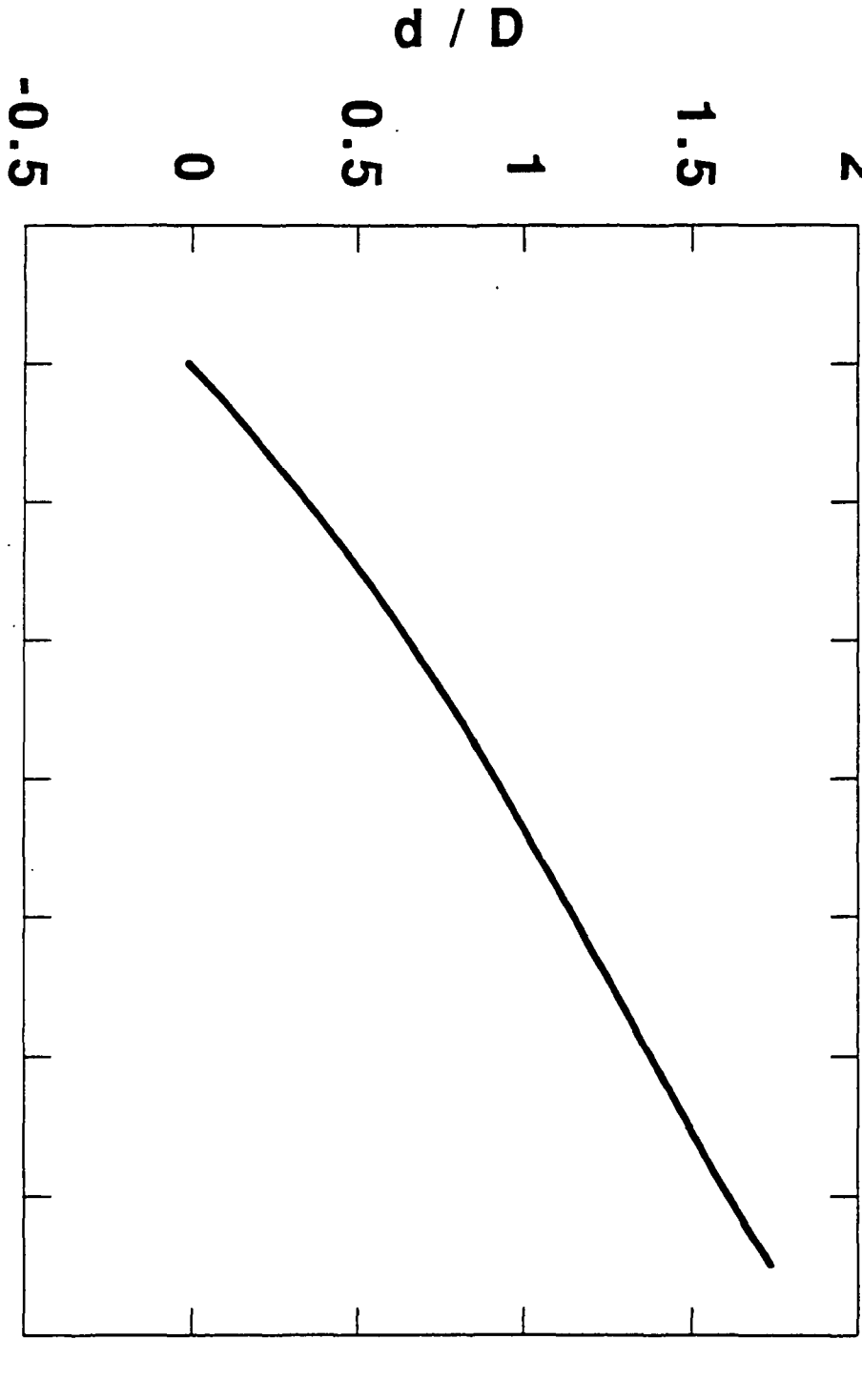

Fig 3. Dependence of the Ratio d/D on the Contact Angle as Given by Equation 10.

$$d/D \cong \text{Sin}\ \theta \qquad (11)$$

The exact and approximate relations are compared in Figure 4.

Substituting the result of equation 11 into equation 8, we find

$$F_a \cong \pi D \gamma_{LV} \text{Sin}^2 \theta \qquad (12)$$

or

$$F_a \cong \pi D \gamma_{LV} (1 - \text{Cos}^2 \theta) \qquad (13)$$

The strength of bubble attachment is thus strongly dependent on contact angle which in turn is determined by the surface energy of both the solid and the medium (equation 5).

To predict values of the contact angle from equation 5, the interfacial tension γ_{LV} between the solid and the medium is needed. Girifalco and Good (6) showed that this parameter can be calculated from the surface energies of the solid and the liquid, γ_{SV} and γ_{LV}, respectively.

$$\gamma_{SL} = \gamma_{SV} + \gamma_{LV} - 2 (\gamma_{SV} \gamma_{LV})^{1/2} \qquad (14)$$

Fowkes (7) observed that, for the interaction of polar materials with nonpolar ones, only the London dispersion component of the intermolecular forces of the polar material was significant. He suggested separating the surface energy of the polar material into dispersion (γ^d) and polar (γ^p) contributions and that these were additive.

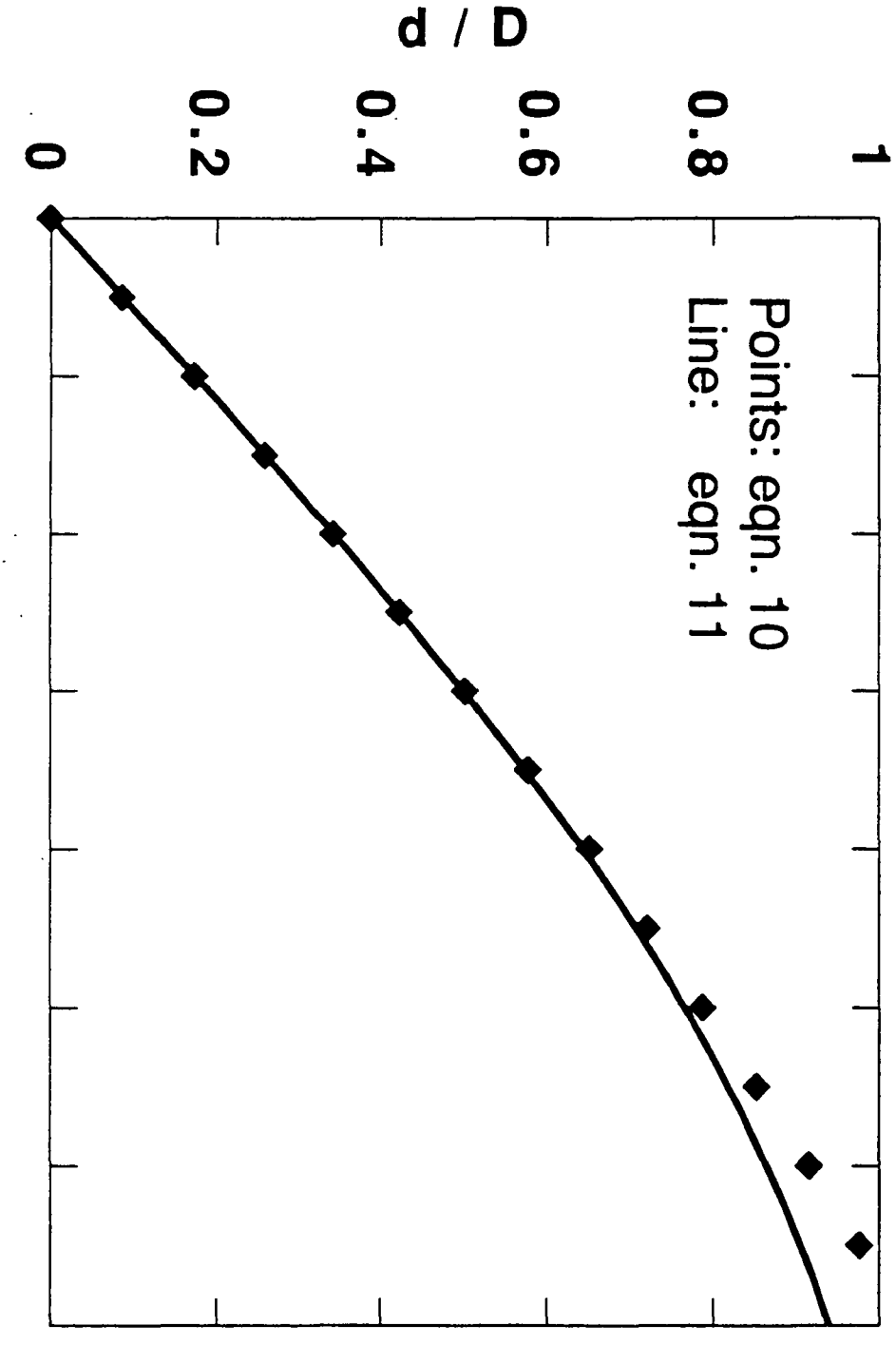

Fig 4. Comparison of the exact (equation 10) and approximate (equation 11) expressions for the ratio d/D.

$$\gamma = \gamma^d + \gamma^p \qquad (15)$$

For the interaction of an aqueous phase, for example, with a hydrophobic solid Fowkes suggests that equation 14 be written as

$$\gamma_{SL} = \gamma_S^d + \gamma_L - 2(\gamma_S^d \gamma_L^d)^{1/2} \qquad (16)$$

Here γ_L represents the combined contributions (equation 15) of the dispersion and polar components of the aqueous phase, γ_L^d is the dispersion component, and γ_S^d is the surface energy of the solid having only a dispersion component. The subscript V indicating the interface with air has been omitted for simplicity. Equation 15 can now be combined with that of Young (equation 5) to give an expression known as the Girifalco-Good-Fowkes-Young (G-G-F-Y) equation (5).

$$\text{Cos } \theta = -1 + 2\left(\gamma_S^d \gamma_L^d\right)^{1/2} / \gamma_L \qquad (17)$$

This equation gives explicitly the dependence of the contact angle on surface energy of the solid γ_S^d and that of the aqueous phase γ_L. The dispersion component of the aqueous phase γ_L^d is expected to be a constant. We will test the validity of equation 17 for flotation systems by independently measuring Cos θ, γ_S^d, and γ_L. These results will then be combined with the concepts behind equation 7 to interpret flotation efficiency data.

EXPERIMENTAL

Four "stickies" materials were chosen for study and are listed in Table 1. Their compositions were determined from FTIR spectra. The surface energy of the stickies was determined by measuring the contact angle of a drop of methylene iodide placed on the solid. The surface tension of methylene iodide is primarily due to dispersion forces with values of γ_L and γ_L^d of 50.8 and 50.4 mN/m (dynes/cm),

respectively. The measured contact angle and these values for γ_L and γ_L^d were substituted into equation 17 which was rearranged to yield γ_S^d. The values listed in Table 1 for HMD, HME, and wax-coated kraft were taken from Project 3428, Report One, Tables V and VI, while that for HMB was previously unreported.

Contact angles of drops of several simulated deinking liquors on the stickies were measured immediately (5 seconds) and as a function of time of contact up to 20 minutes. (The measurements were carried out in a humidified chamber to prevent drop evaporation.) Values of the contact angle between four different liquors and the four stickies measured at 5 seconds are listed in Table 2. (Taken from Report One, Tables IX, X, XI, XIII, and XIV.)

Table 1. Composition of Stickies

Sticky	Surface Energy ergs/cm^2	Composition
Wax-Coated Kraft (WCK)	28.0	paraffin wax
Hot Melt Adhesives		
HMD	27.1	Polyvinyl acetate + Polystyrene + Paraffinic Hydrocarbon (Wax or Polyethylene)
HMB	50.7	Glycerol Ester of polymerized rosin
HME	41.7	Polyethylene base

Table 2. Contact Angles at Five Seconds

Liquor	pH	γ_L, mN/m	θ, deg WKC	HMD	HMB	HME
1	12.4	39.2	76.3	71.3	54.0	58.7
2	12.4	29.9	47.7	43.0	22.0	29.0
4	10.1	39.4	75.0	69.3	54.0	63.0
5	10.1	29.7	47.3	43.7	23.3	28.3

The time variation of the contact angle of deinking liquors 4 and 5 on the hot melt adhesives is presented in Figure 5.

Flotation studies were carried out using a cell developed at the Institute of Paper Chemistry. For the results reported here the critical parameters are listed in Table 3. (Taken from Report One, Table XVIII and Report Two, Table II.)

Table 3. Flotation Parameters

Temperature:	73°F
pH:	10.1 or 12.4
Average Bubble Size:	260 μm (γ_L = 29.7 mN/m)
	350 μm (γ_L = 39.4 mN/m)
Sticky particle Size:	57 - 420 μm
Time of Agitation Prior to Flotation:	1/4 - 60 min.
Time of Flotation:	1 min.

The results for the three (hot melt adhesive) stickies with deinking liquors 1, 4, 5, and 6 and various agitation times are presented in Table 4. (Taken from Report One, Table XVIII. The contact angles at the various agitation times were taken from Report One, Tables X, XIII, XIV, and XV).

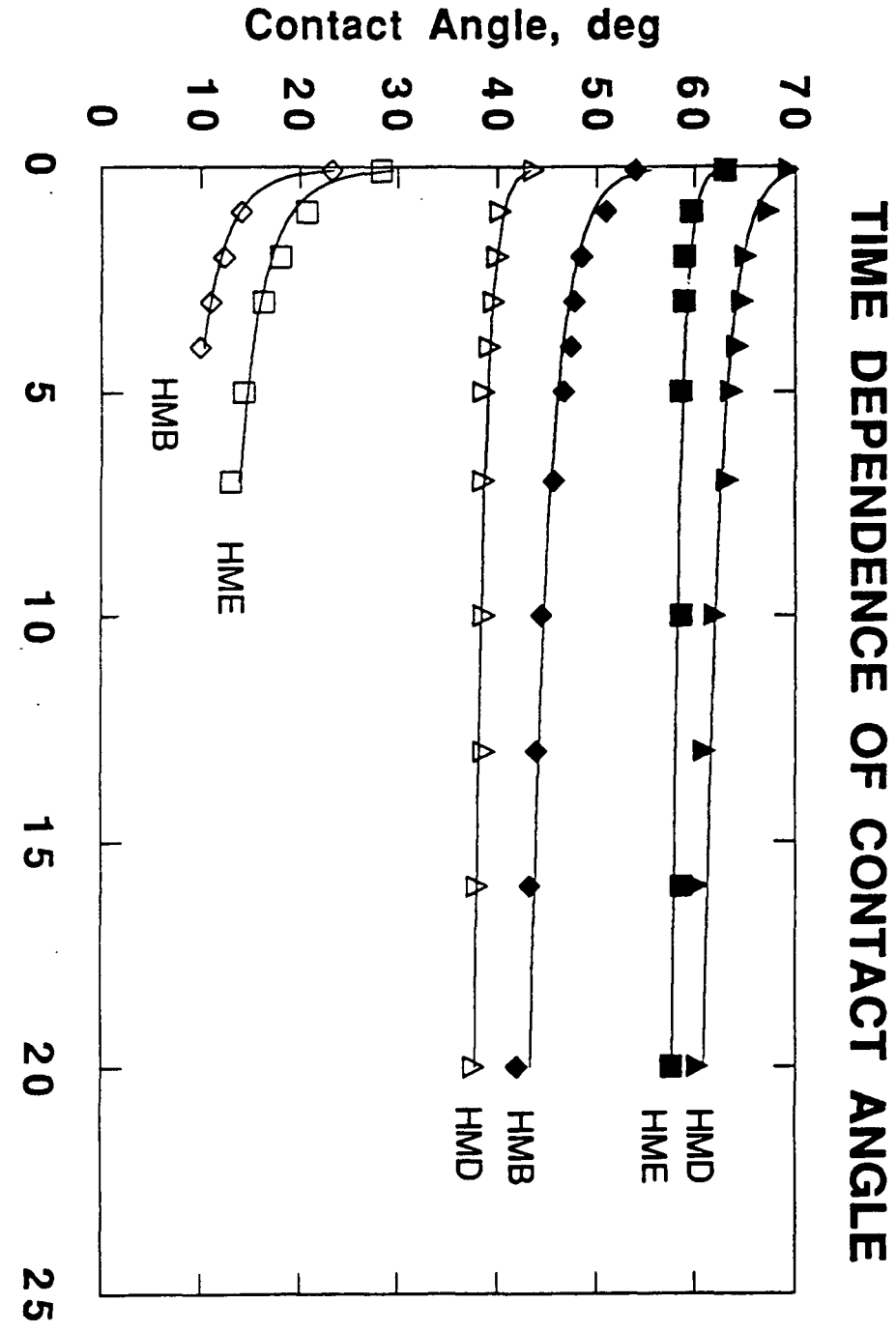

Fig 5. Dependence of the contact angle between various hot melt adhesives and two deinking liquors. Closed symbols: liquor 4, γ_L = 39.4 mN/m; open symbols: liquor 5, γ_L = 29.7 mN/m.

Table 4. Flotation Results

Flotation Test No.	Sticky	Surface Tension, mN/m	Time of Agitation Prior to Flotation, min	Apparent Contact Angle, deg	Sticky Removal %
2	HMD	39.4	6	62.5	93.4
3	HMD	39.4	20	60.0	94.9
4	HMD	29.7	6	38.5	40.8
5	HMD	29.7	20	37.5	67.6
7	HMD	39.4	20	60.0	96.2
8	HMD	29.7	20	37.5	37.8
10	HMB	39.4	17	42.5	96.9
11	HMB	39.4	20	42.0	92.9
12	HMB	29.7	4	10.0	2.7
13	HMB	29.7	4	10.0	3.5
14	HMB	29.7	1/4	~20.0	6.3
15	HMB	39.2	60	~32.0	90.3
16	HMB	39.2	20	~32.0	84.5
17	HME	39.4	20	58.0	98.0
18	HME	39.2	20	47.0	96.3
19	HME	30.1	2	18.0	2.1
20	HME	30.1	1/4	24.0	11.1

DISCUSSION

Validity of the G-G-F-Y Equation

The G-G-F-Y equation is usually used to relate the surface energy interactions between pure liquids and pure solids. To use it in the flotation studies, it is necessary to show that it holds also for aqueous solutions of surfactants.

Of the four stickies considered here the wax-coated kraft has the simplest composition. Its interactions with the liquors should consist of only dispersion forces. Equation 17 was solved for γ_L^d and the measured values of θ (5 sec), γ_L, and γ_S^d for the WCK and the four liquors (From Tables 1 and 2 above) were inserted. The average value for γ_L^d for the four liquors was 21.9 mN/m with a standard deviation of 0.6 mN/m. This value is in excellent agreement with the value found (5) for the dispersion component of water, 22 mN/m, and suggests that the surfactant liquors have dispersion interactions similar to water. Thus, the G-G-F-Y equation holds for the system WCK/deinking liquors with a constant value for γ_L^d of 22 mN/m.

For the hot melt adhesives the situation is more complex. From the compositional and surface energy information in Table 1 it is evident that polar components are present. It would appear that the interaction term in equation 14 should also contain polar contributions rather than just the dispersion contributions shown in equation 16. These contributions would then lead to a modified value for γ_L^d in the G-G-F-Y equation.

The applicability of the G-G-F-Y equation to the hot melt adhesives was tested using the procedure outlined for the WCK and the data in Tables 1 and 2. The values calculated for γ_L^d are given in Table 5. Surprisingly, they do not differ greatly from the value for water. It can be argued that the correct value for γ_S^d to be used in the calculation is not that listed in Table 1 (obtained from interaction with methylene iodide), but should be modified to reflect adsorption of surfactant

Table 5. Calculated Values for γ_L^d

Sticky	Liquor,	γ_L^d, mN/m
HMD	1	24.7
	2	24.7
	4	26.2
	5	24.2
HMB	1	19.1
	2	16.4
	4	19.3
	5	16.0
HME	1	21.3
	2	18.8
	4	19.7
	5	18.7

molecules onto the solid. In the absence of detailed information on this process and in order to follow relative changes we will assume in subsequent calculations using the G-G-F-Y equation that the value for water for γ_L^d is applicable to stickies/deinking liquors systems.

Time Dependence

Stickies in contact with deinking liquors show changes in properties with time. Changes of the contact angle with time are presented in Figure 5. Numerous other examples are given in Reports One and Two of Project 3428. The properties of the deinking liquor would not be expected to change appreciably with time. According to the G-G-F-Y equation changes in the contact angle would then reflect changes in the surface energy of the stickies (and the possible concommitant changes in γ_L^d). The direction of change in all cases is toward smaller contact angles or, equivalently, larger surface energies γ_S^d. To quantify these changes, we have used the time dependent contact angle data along with the appropriate value of γ_L and an assumed constant value of γ_L^d of 22 mN/m to calculate a time dependent value for the sticky's surface energy from the G-G-F-Y equation. The results are shown in Figures 6, 7, and 8 for the three hot melt adhesives.

Although the results are rather different for the three stickies as might be expected from their different compositions, there are some common trends.

a) The surface energy calculated from the contact angle at 5 seconds depends on the relative magnitudes of the surface energies of the liquor and the sticky. This can be seen more clearly in Figure 9 where the 5 sec values are plotted against the (intrinsic) surface energies determined with methylene iodide. The solid line indicates identical values of the two axes. Stickies with (intrinsic) surface energies less than the deinking liquor attain larger values in the presence of the liquor and vice versa. The greater the difference between liquor and sticky surface energy, the greater the change in the latter's properties in the presence of the liquor. A potential

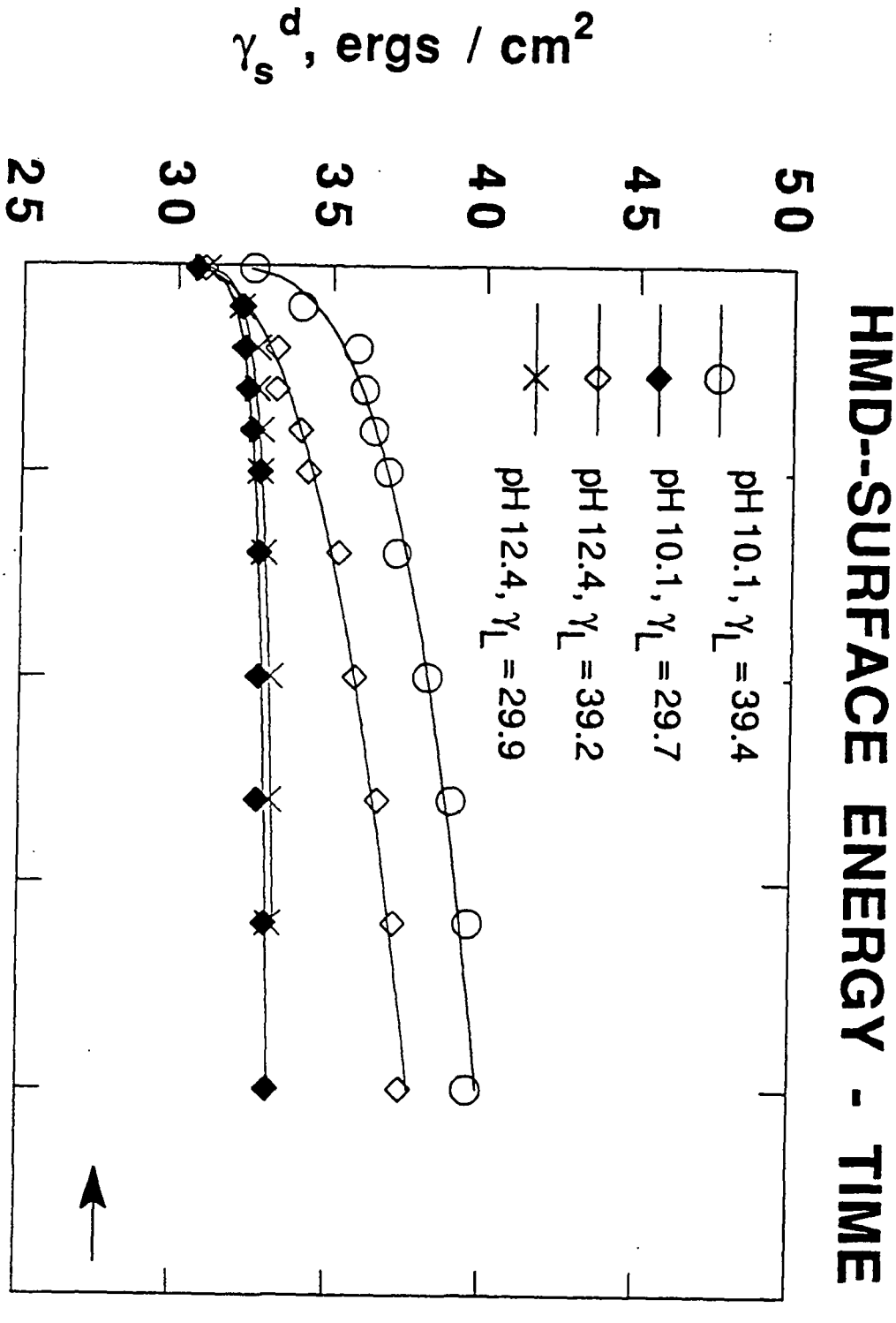

Fig 6. Change of sticky surface energy with time of contact between pulping liquors and hot melt "D" calculated from G-G-F-Y equation. The arrow indicates the value before contact with liquor.

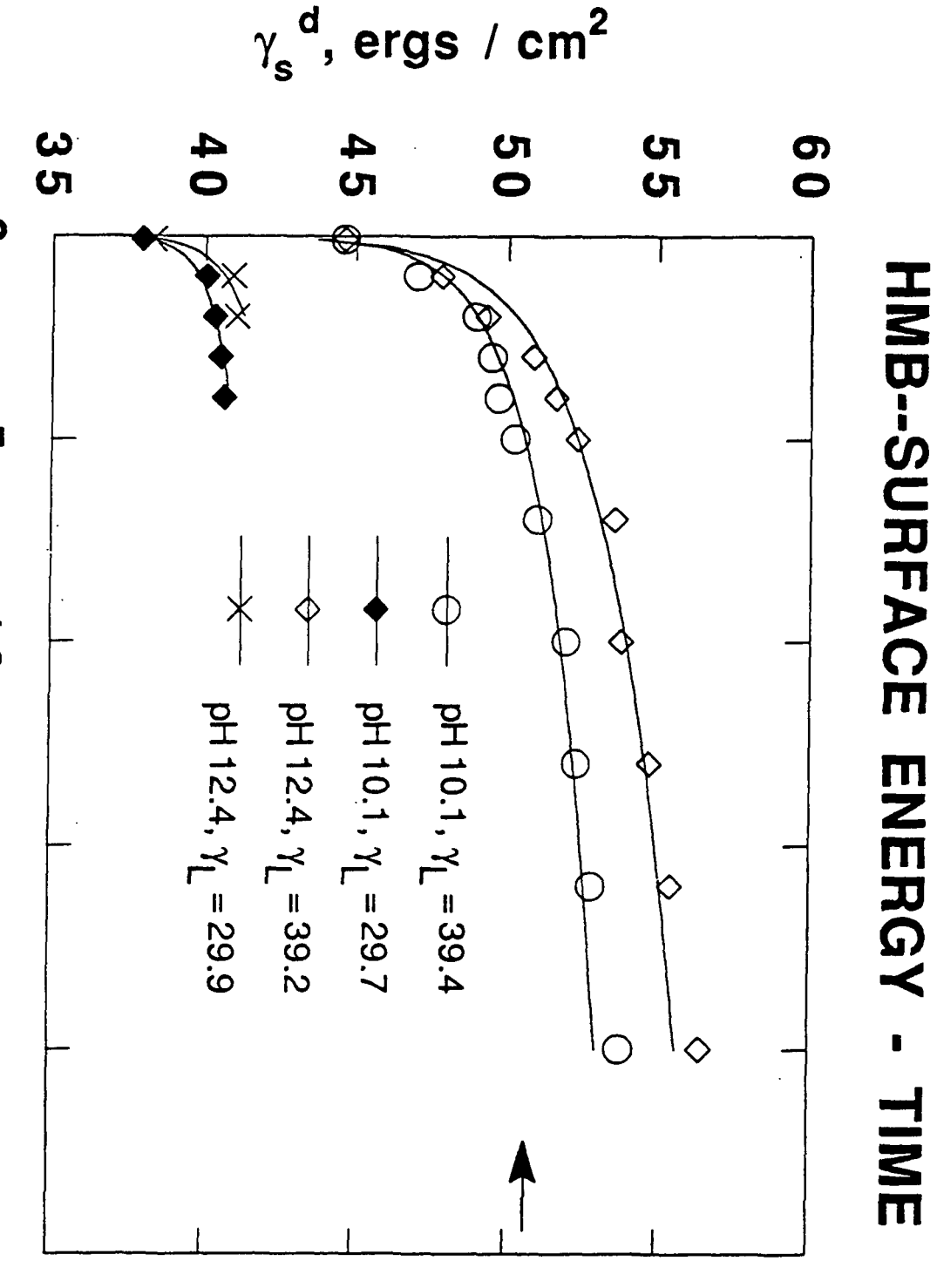

Fig 7. Change of sticky surface energy with time of contact between pulping liquors and hot melt "B" calculated from G-G-F-Y equation. The arrow indicates the value before contact with liquor.

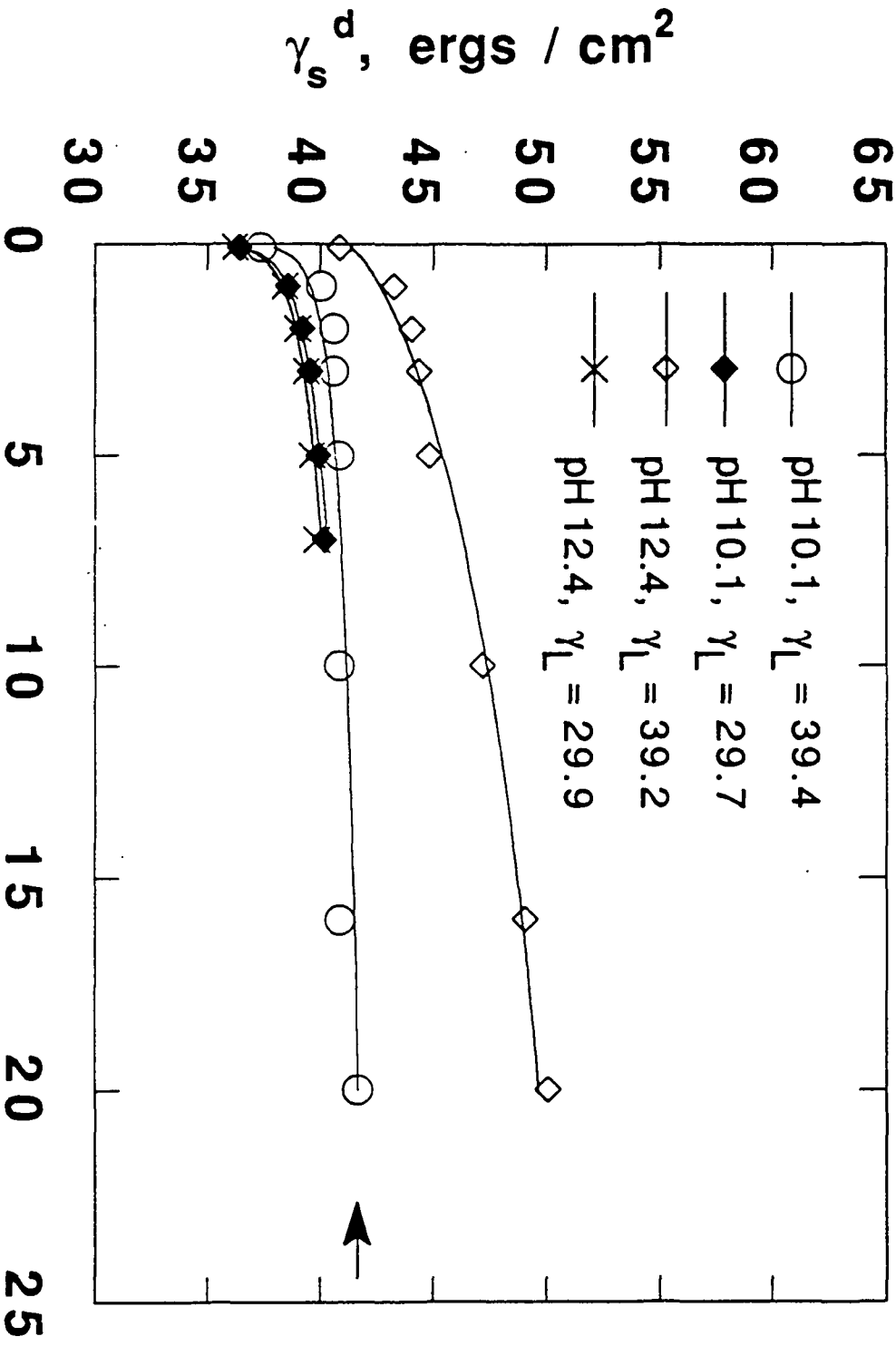

Fig 8. Change of sticky surface energy with time of contact between pulping liquors and hot melt "E" calculated from G-G-F-Y equation. The arrow indicates the valuc before contact with liquor.

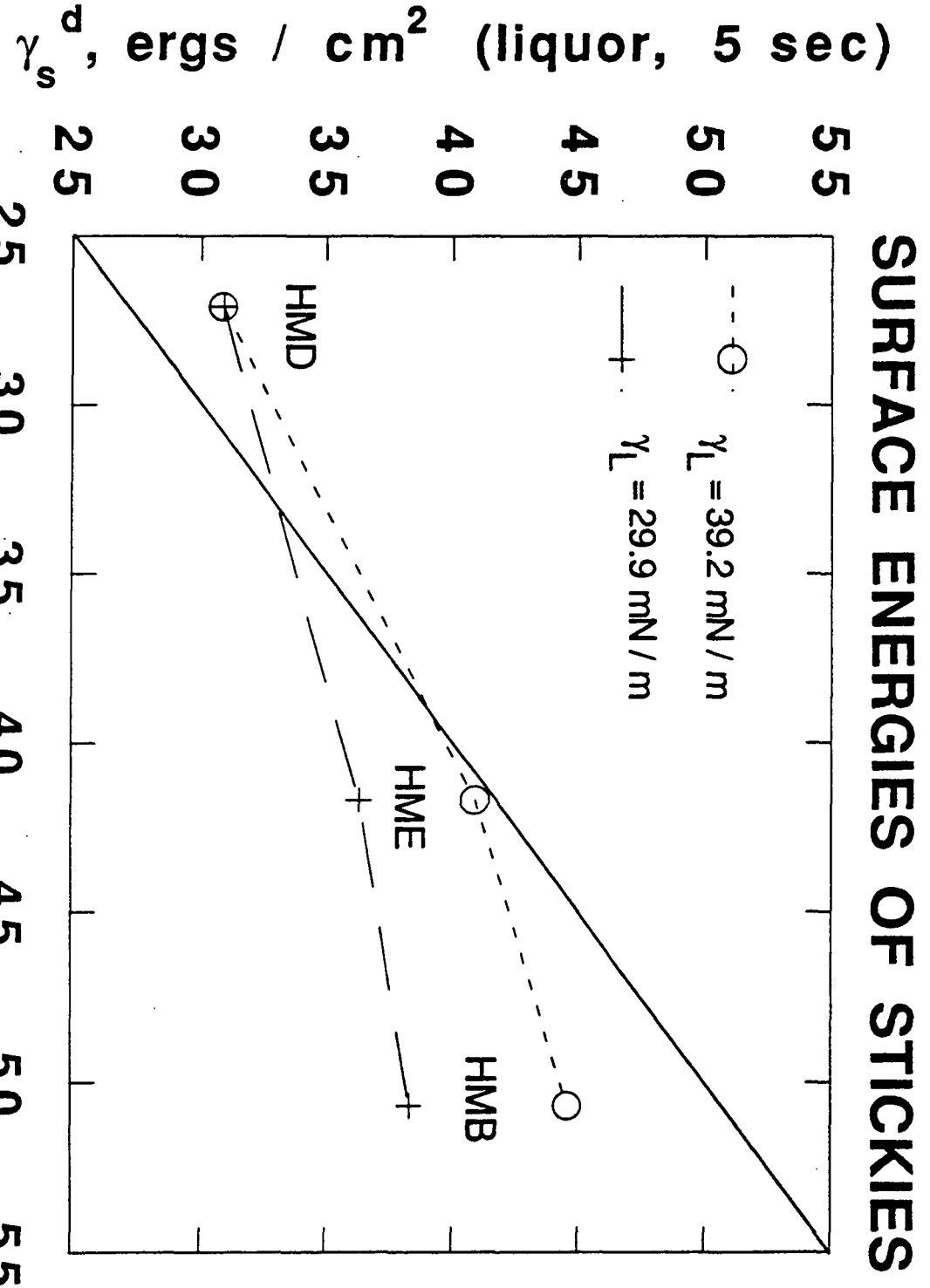

Fig 9. Comparison of surface energy of stickies after 5 seconds of contact with liquors 1 and 2 with that before contact. The solid line indicates identical values for both axes.

explanation is that surfactant molecules adsorb on the sticky's surface in an orientation that tends to minimize the difference between the surface energies of the liquor and the sticky. For a low energy surface (HMD) the polar portion of the surfactant would be oriented toward the liquor, while the reverse would be found for high energy surfaces.

b) In the presence of high surfactant concentration no further changes with time occur after five minutes or less. In contrast at the low surfactant concentration changes continue to 20 minutes or beyond.

c) Effects of pH are evident at low but not at high surfactant concentrations.

There are at least four possible explanations for the change of surface energy with time.

1) Surfactant may adsorb onto the surface of the sticky. The hydrophobic "tails" of the surfactant molecules would tend to adsorb on the sticky surface with the hydrophilic "head" oriented toward the solution (drop of liquor). (However, see the comments under a) above.) This process should be determined by the rate of diffusion of the surfactant molecules and, therefore, should occur on a time scale of the order of seconds or less. The experimental time scales on the order of minutes suggest this explanation is unlikely.

2) Polar species may diffuse from the bulk of the sticky to its surface. Contact with the aqueous solution would be the driving force. Hot melt adhesives are a complex mixture of materials some more polar than others. Even a "simple" material like polyethylene contains antioxidants, residual polymerization catalyst products and perhaps other additives. The diffusion rate of these polar materials will depend upon their molecular weight and upon the segmental mobility of the major components of the sticky. This mobility in turn depends upon the glass transition temperature of these components. The potential contribution of this mechanism to the

observed time dependence would be difficult to estimate without detailed compositional information.

3) Ester groups may hydrolyze. For those stickies comprised of esters (eg. HMB) this would appear to be a likely mechanism. The pH of the deinking liquors studied ranged from 10.0 to 12.4, prime conditions for the hydrolysis of esters. The reaction would produce hydroxyl and carboxylate groups, both more polar than the ester moiety, and would lead to an increase in surface energy. The results shown in Figure 7 (HMB) and additional studies in Report One of Project 3428 at different pH and temperature conditions provide some support for this mechanism. However, hydrolysis at room temperature even at high pH is very slow and probably would not explain the observed effects. In addition, the lack of a pH effect at the high surfactant concentration and the higher surface energy at pH 10.1 for HMD which contains hydrolyzable polyvinyl acetate imply that other mechanisms may be more important.

4) Molecules in the surface layer may reorient. In the last decade it has been shown experimentally that molecules in the surface layer of a solid possess a finite mobility, and their orientation can be influenced by an adjacent liquid phase. This work has been reviewed (8) and an application to flexographic plates has recently been shown (9). Molecules in the solid phase, having both polar and nonpolar groups, tend to orient their nonpolar groups toward an air interface. When this solid is placed in contact with a polar liquid, the molecules reorient to present their polar portions toward the interface. This results in an increase in the surface energy. For polymeric materials the entire chain does not reorient, but only small segments of it do. These might be composed of one to three monomer units or might be side chains. A polymer below its glass transition temperature has sufficient local mobility for this to occur. For example, "secondary transitions" corresponding to reorientation of side chains or portions of side chains can take place well below the glass transition temperature. Typically, the reorientation can be

reversed by replacing the polar liquid by a nonpolar one or by air. Thus molecules or groups in the surface layer of an amorphous solid may have a finite mobility, and their orientation can be influenced by the adjacent phase.

It appears likely that some of the changes seen in Figures 6 - 8 may be a result of this reorientation mechanism. Obviously, the presence of the surfactant in the solution and its orientation (polar head toward or away from the surface) when adsorbed greatly increase the complexity of the system. Without further specific information about surfactant adsorption and hot melt composition and composition homogeneity it is not possible to offer detailed interpretation for the time dependence. It is likely that all four explanations suggested may contribute and that their relative importance depends on the specific sticky material.

Flotation Studies

Flotation tests were carried out on particles of the three hot melt adhesives. A variety of conditions of pH, liquor surface tension, and time of agitation prior to flotation were used. From the data in Table 3 and 4 the force of attachment F_a was calculated from equation 8 using the exact expression (equation 10) for the factor d/D. The percent sticky removed during one minute of flotation is shown plotted against the corresponding force of attachment in Figure 10. Removal efficiency improves with increasing strength of attachment with most of the change occurring over a narrow range of forces. (The curve shown is a least squares fit to the hyperbolic tangent function.)

Although the dependence of removal efficiency on attachment force is believed to be a general relation, the particular "critical" force will be a function of the specific parameters of the flotation system. These parameters would include the ratio of bubble to particle size, mixing conditions in the flotation cell, and the duration of flotation. The sensitivity to these factors needs to be examined in detail.

To gain a better appreciation of the influence of liquor and sticky surface energies on the attachment force, the G-G-F-Y equation can be substituted into equation 13 to give

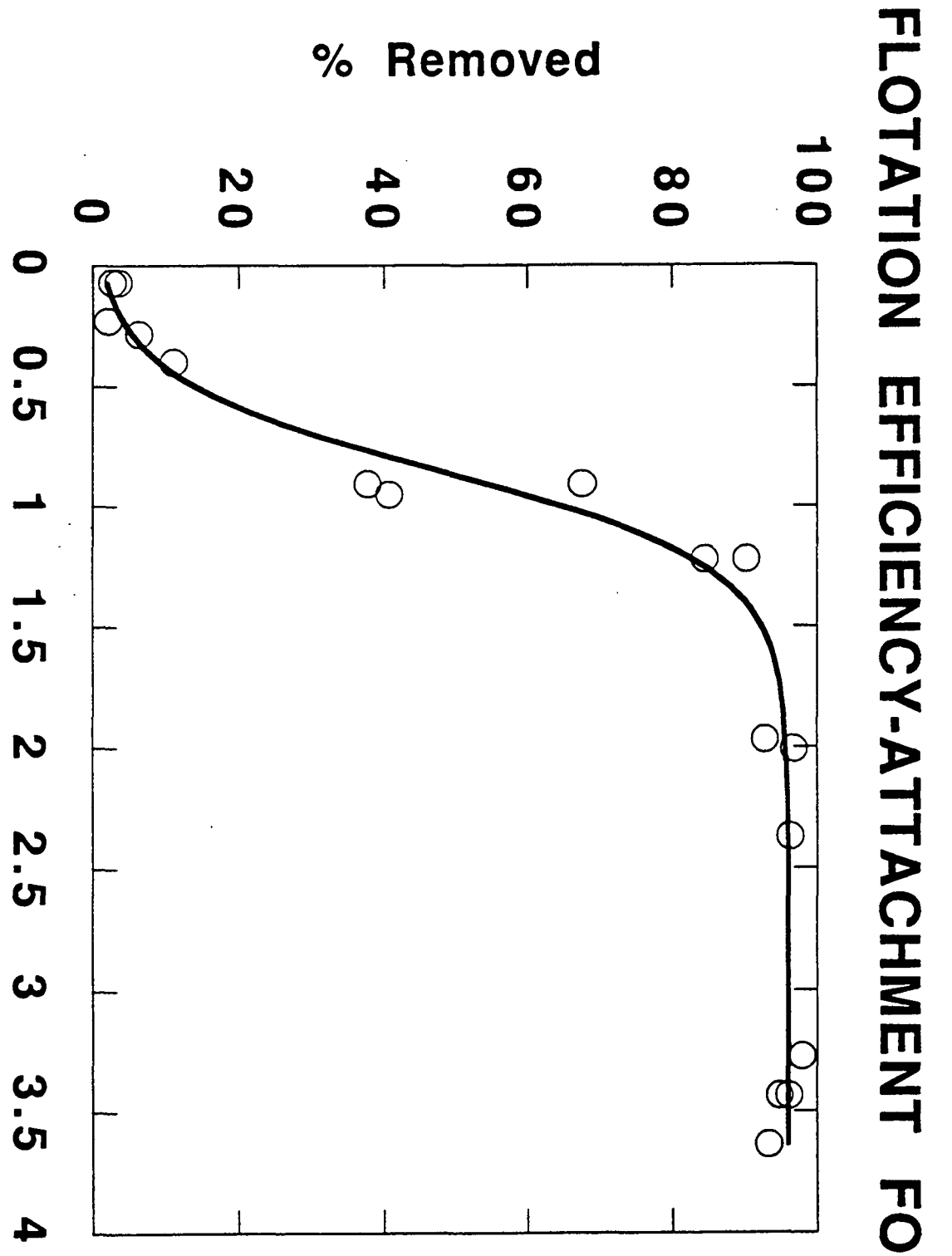

Fig 10. Dependence of stickies removal efficiency by flotation on the force of attachment between air bubble and sticky, the latter calculated from equation 8.

$$F_a \cong 4\pi \gamma_L D (x - x^2) \qquad (18)$$

where

$$x = \left(\gamma_S^d \gamma_L^d\right)^{1/2} / \gamma_L \qquad (19)$$

The ratio $\left(\gamma_S^d\right)^{1/2} / \gamma_L$ is seen to be the critical parameter.

Upon substituting equation 10 into equation 8 and simplifying, the force of attachment can be found as a function of the Cos θ.

$$F_a = 2\pi\gamma_L D \left| \left(1 - \mathrm{Cos}^2\theta\right) / \left(4 + 6\,\mathrm{Cos}\theta - 2\,\mathrm{Cos}^3\theta\right)^{1/3} \right| \qquad (20)$$

Equation 17 can then be used to evaluate this function. A map showing the dependence of the attachment force on the sticky surface energy is shown in Figure 11. The curves represent conditions of constant liquor surface tension at the indicated values obtained from equation 20 and the G-G-F-Y equation. The dashed lines indicate levels of the attachment force required to reach the given recovery efficiencies. These levels were obtained from Figure 10. For a particular sticky with a given surface energy a vertical line can be drawn at that energy to intersect the level of recovery desired. The deinking liquor must then have a surface tension equal to (or greater than) that at the intersection. Intermediate values for γ_L can be interpolated (approximately linearly) between the values for the indicated curves. It is emphasized that these levels (dashed lines) pertain only to the particular flotation conditions used to generate the data in Figure 10. For a different set of operating parameters the attachment force required to achieve a given recovery level would need to be determined experimentally. Once this is done and the level of attachment force is entered on the map in Figure 11, the necessary conditions for liquor surface tension for particular types of stickies can be determined.

The complicating factor in flotation is evident in Figures 6-8, or equivalently, Figure 5. The surface energy increases with time in a manner which depends on the type of sticky, the surfactant concentration, and in some cases the pH. It is

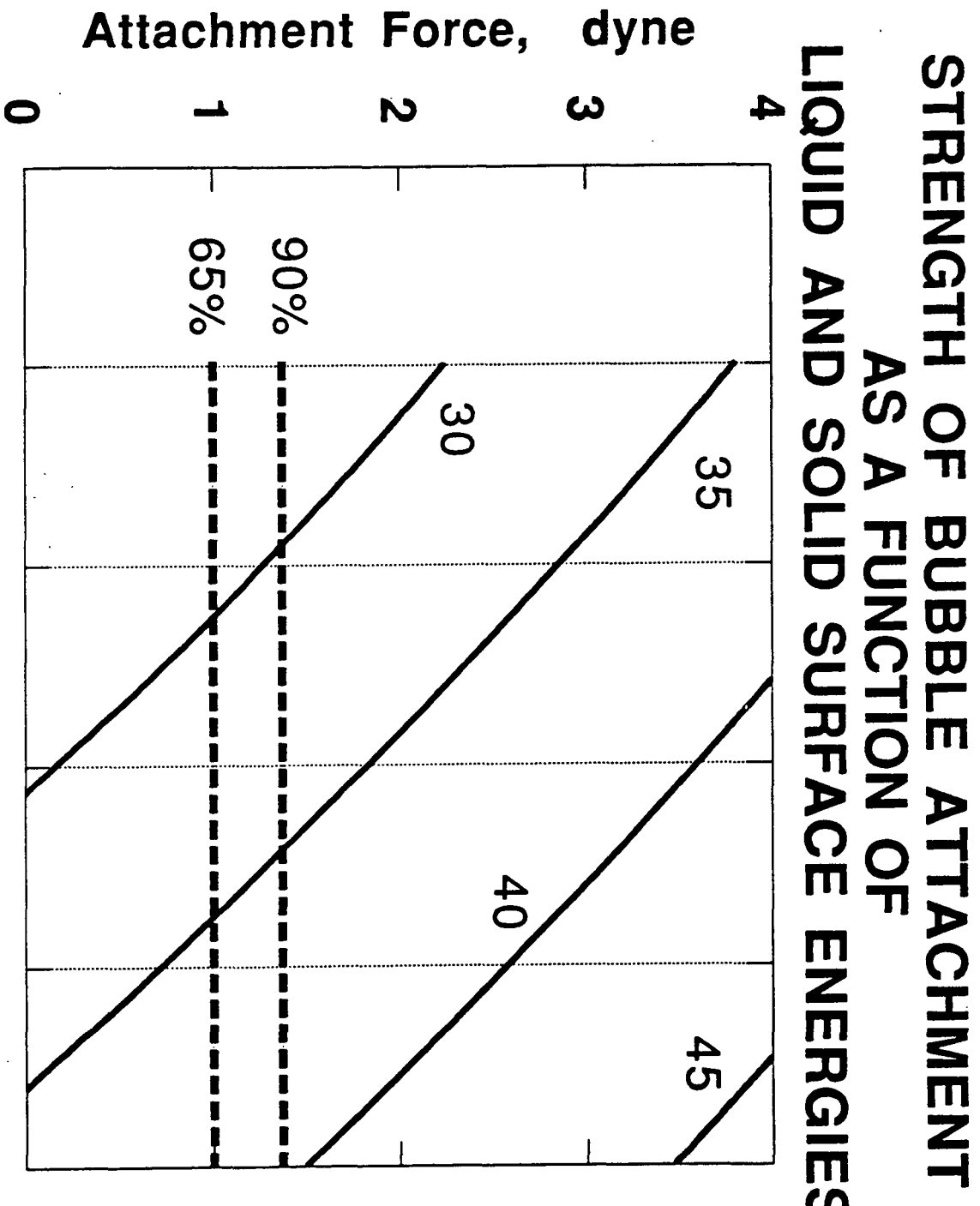

Fig 11. Map of dependence of force of attachment (between air bubble and sticky) and the surface energy of the sticky at several levels of deinking liquor surface tension. Also shown are the levels of attachment force required with the present flotation cell to achieve 65 or 90% removal efficiency.

evident from Figure 11 that to maintain a given recovery efficiency, when the solid surface energy is increasing, requires ever higher values for the liquor surface tension. To minimize fiber and pulp fines flotation, it is desirable to maintain a large difference in surface energy between the stickies and the cellulosic materials. The increase in surface energy of the stickies can potentially be counteracted by the use of a "collector". Such a material might be the combination of oleic acid and calcium ions. The latter would aid the binding of the carboxylate group of the (ionized) oleic acid to negatively-charged sites on the stickies. The orientation of the anchored collector molecules would produce a low energy surface and enhanced stickies separation. It is important that the collector does not also become attached to the cellulosic material thereby lowering the latter's surface energy. Further work will be necessary to define the optimum types of additives to achieve good separation of various classes of stickies.

CONCLUSIONS

1. The G-G-F-Y equation can be used to correlate the experimental data on stickies/deinking liquors systems.

2. The surface energy of the stickies increases with time. The increase depends on the particular sticky material, the surfactant concentration, and the pH.

3. At short times (< 5 sec.) surfactant molecules adsorb on the stickies in an orientation that brings the solid surface energy closer to that of the liquor.

4. The flotation efficiency results can be explained by a theory based on the need for strong air bubble - sticky attachment. It includes the effects of bubble size, liquor surface tension, and the surface energy of the sticky.

FIBER AND SHEET STRENGTH PROPERTIES

Summary

Although many articles appear in the literature which relate the strength of final paper products to the recycle fiber content of these products, there has been no effort to systematically analyze this data. The purpose of such an analysis would be to clearly identify the fiber properties which dominate the observed strength loss. Our approach is to utilize the network theory of paper as embodied in the work of Derek Page et al. The Page equation for tensile strength has been successfully used by Institute of Paper Science and Technology personnel to predict the final properties of paper made from virgin pulp. This work is included with our Process Simulation Program MAPPS.

The approach used by Page stipulates that the tensile strength of paper can be expressed in terms of 1) tensile strength of the fiber, as measured by zero span tensile, 2) the perimeter, coarseness, and length distribution of the fiber, 3) the specific bond strength for fiber-fiber bonds, and 4) the relative bonded area. Several publications in the open literature provide sufficient data to analyze the strength properties of paper in terms of these fiber variables. We have found an ambiguity in the behavior of fiber tensile strength. Some authors report an increase in single fiber tensile strength while others report a decrease. The impact of recycling on coarseness, perimeter, and length is small. We conclude that changes in these properties do not significantly impact on the strength development potential of recycle fibers. The literatures teaches that the recycling of fibers impacts on the compliance of individual fibers to each other. This implies that the relative bonded area of paper made from recycled fibers is lower than from virgin fibers. Our analysis shows this effect. However, our analysis suggests that the contribution is small. We find that recycling lowers specific bond strength by as much as 55%.

Our current work focuses on a study of the principal fiber species found in the United States. We have undertaken a systematic laboratory study to identify the changes in fiber properties brought about by repeated recycling. The direct application of the Page Equation shows that repeated recycle reduces the fiber strength by about 7%. Fiber perimeter is reduced. Fiber coarseness appears to be

slightly reduced by recycle. A surprising result is that all recycle levels lie on the same curve for a plot of the "Page parameter" vs. scattering. This implies that the fiber-fiber bond strength of recycled fiber is equivalent to virgin fiber, and that relative bonded area dominants the observed strength loss in sheets.

INTRODUCTION

The role of recycled chemical fibers will grow rapidly during the decade of the 1990's. Today, the majority of packaging and printing and writing grades consists of virgin fibers. These grades amount to over 60 million tons of paper production each year. The expected increase in recovery of paper products requires a substantial increase in the amount of recycled fibers used in some paper grades. During the past twenty years, numerous studies have been conducted on the papermaking potential of recycled fiber. It has been generally observed that the use of recycled fibers in papermaking results in lower mechanical properties. This apparent deficiency of recycled fiber can be overcome by refining or the addition of a few chemicals to the papermaking process. The papermaking operation most responsible for change in fibers is the drying process. Figure 1 is an example of the tensile strength of linerboard produced from fibers that have undergone repeated drying operations. For the purpose of this paper drying and recycle are synonymous. Figure 1 has been abstracted from the work of McKee. It is clear that repeated drying of fibers produced progressive deterioration of paper tensile strength. From this graph there appears to be a reduced affect of drying reached at recycled levels greater than five. Horn, Klungness, and Bobalek have all conducted experiments similar to McKee's and report similar results. These researchers list the four properties shown in Figure 2 as important to the behavior of recycled fibers.

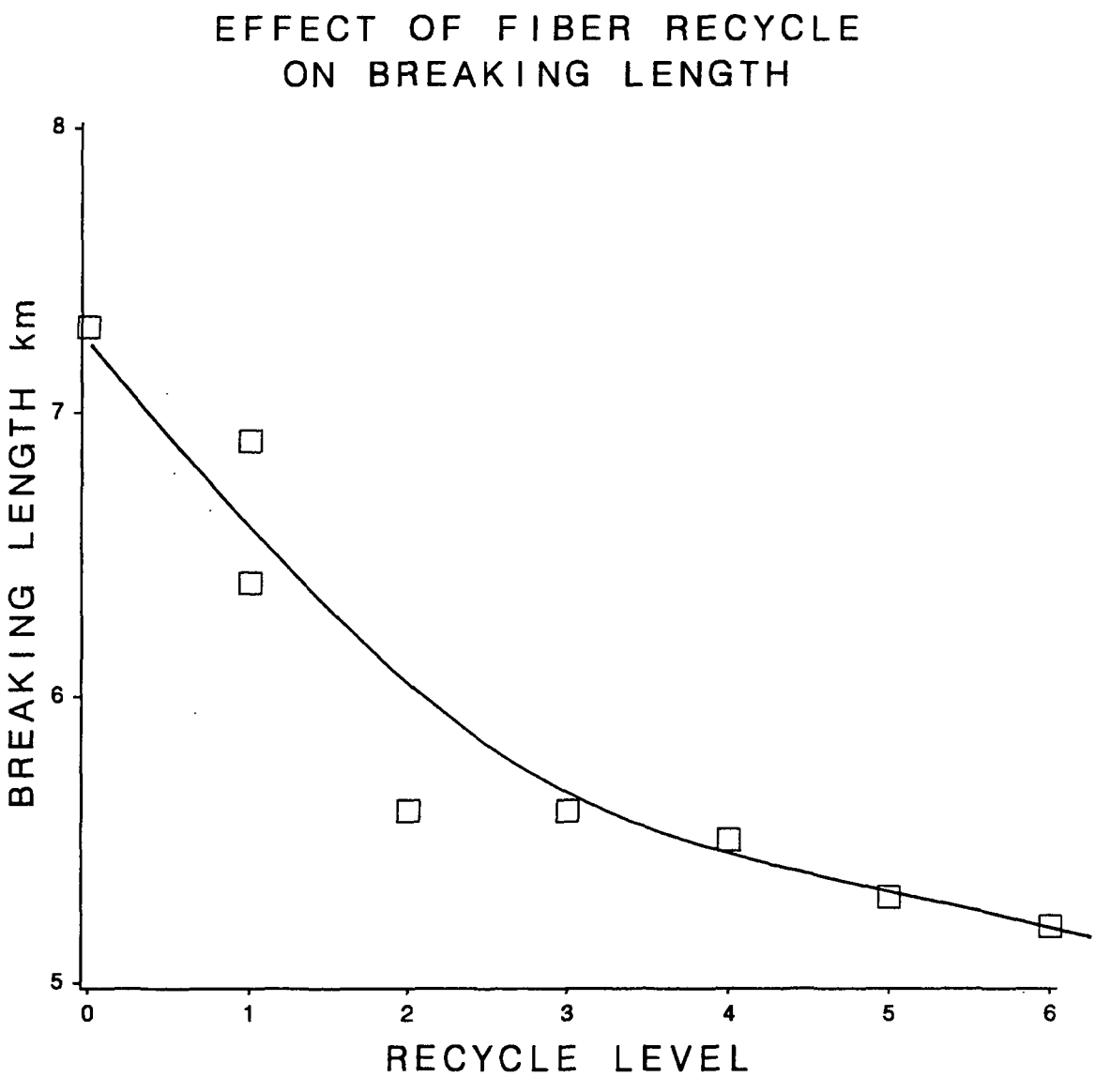
EFFECT OF FIBER RECYCLE
ON BREAKING LENGTH
BREAKING LENGTH km
8
7
6
5
0
1
2
3
4
5
6
RECYCLE LEVEL

Figure 1.

Figure 2. PROPERTIES IMPORTANT TO THE STRENGTH OF PAPER MADE FROM RECYCLED FIBERS

- Fiber Strength
- Fiber Length
- Fiber Swelling/Plasticity
- Fiber Bonding Potential

Fiber strength is generally measured by zero span breaking length of paper sheets. The extent to which the property is impacted by drying is not clear. Horn reported a 33% decrease of fiber strength for a southern unbleached Pine while Bobalek reported an increase of 7% for southern Pine, and an increase of 19% for Eucalyptus. Fiber length of virgin pulp is known to play an important role in the development of paper strength. In the recycled process stiffening of the fibers occurs and subsequent refining of these stiffened fibers causes fiber length to decrease. Fiber-fiber bonding is influenced by two parameters. The first sometimes referred to as fiber swelling or plasticity dictates the conformability of fibers to each other. This conformability determines the relative bonded area. Recycled fibers are known to be less conformable than virgin fibers.

The second important fiber property is the specific bond strength. The mechanics for fiber-fiber bonding involves hydrogen bonding. When fibers dry their hydrogen bonding potential is diminished.

Although all of the literature cited strongly suggests that factors listed in Figure 2 are the principle factors important to development of paper strength, no systematic approach has been suggested to quantify the extent to which recycle impacts on these fibers properties. Only by quantifying these factors will we be able to design economic approaches to regain the observed strength loss. Further, without a systematic approach we are unable to explore the interaction between process variables and fiber properties. It is important that papermakers be able to explain the impact of refining and strength development, through chemical means. A

possible approach is to utilize the network theory of paper. Most representations of this theory are quite complex and generally difficult to apply. However, one particular approach devised by Derek Page et al. offers an empirical methodology for studying the impact of drying on fiber properties.

PAGE EQUATION

Page teaches that the following equation is a satisfactory representation of well bonded sheets. The typical packaging paper and printing/writing paper, are considered to be well bonded sheets. This equation has been used as the basis for the MAPPS computer simulation program. This program predicts the properties of paper based on fiber and process variables. The current validated database for this program is based on virgin fiber properties.

$$\frac{1}{T} = \frac{9}{8Z} + \frac{gC}{P\,L\,b\,RBA} \qquad (1)$$

Where: T = Tensile Breaking Length, km

Z = Zero Span Breaking Length, km

C = Fiber Coarseness, mg/100m

P = Fiber Perimeter, μm

L = Fiber Length, (weight average)

b = Fiber - Fiber Bond Strength, dynes/cm^2

RBA = Relative Bonded Area, %

g = Gravitational Constant

The work presented by Darcy Clark and A. Jones has shown that the best representation of fiber length is the weight average fiber length which is compatible with the measurement of coarseness. RBA can be calculated from the scattering coefficient of the sheets.

$$RBA = \frac{S_0 - S}{S_0} \qquad (2)$$

where: S_0 = the scattering coefficient for an unbonded sheet

S = the scattering coefficient for a paper sheet.

Substituting Equation 2 into Equation 1 and rearranging leads to a relationship between tensile properties of the sheet scattering coefficient:

$$\left[\frac{1}{T} - \frac{9}{8Z}\right]^{-1} = \frac{b}{\gamma} - \frac{b}{\gamma S_0} S \qquad (3)$$

Where

$$\gamma = \frac{gC}{PL}$$

By using the concepts embodied in Equations 1 thru 3 and data provided by McKee, Horn, and Bobalek, one can get a "snap-shot" view of the impact of drying on fiber properties. Table 1 is a summary of results. The results for zero span are not clear. McKee and Horn show decreases while Bobalek shows an increase. In principle, fiber strength should decrease with drying. The results shown in Table 1 suggest that the loss in specific fiber-fiber bond strength is more important than the loss in relative bonded area.

Table 1. PERCENT REDUCTION OF FIBER PARAMETERS DUE TO DRYING

	ZERO SPAN	BONDED AREA	BONDING
IPST			
Southern Pine UB	19	7	53
HORN, FPL			
Southern Pine UB	33		
BOBALEK et al, W. Mich			
Southern Pine	(Increase 7)	0	61
Northern Pine		13	25
Eucalyptus		4	78
Aspen	(Increase 25)	2	22

As part of the newly initiated project of recycled fibers at the Institute of Paper Science and Technology we have decided to develop an information base for the important fiber species found in North American paper products. The data is being generated to utilize the Page equation for analysis.

APPROACH

Virgin kraft pulps are refined in a laboratory valley beater, sheets weighing 42 lb/1000 sq ft are formed on a Formette Dynamique paper machine. These sheets

are pressed and dried under restrained conditions using a pilot scale dryer. The final sheet moisture is controlled to between 4% and 6%.

After drying, these sheets are allowed to condition for at least twenty-four hours and are then reslurried for the next drying treatment. Handsheets are made on a British sheet machine using standard TAPPI techniques. The handsheets are dried with restraint using a steam heated dryer. These handsheets are tested under TAPPI standards conditions.

RESULTS AND DISCUSSION

This part of the recycled project is in its early phases, however, some results are available. Four pulps are being studied. These are bleached and unbleached southern kraft pine and hardwood.

Fiber Strength

Table 2 summarizes the zero span results. The bleached hardwood results show an increase in zero span. This result is similar to that report by Bobalek. The other observations behave as reported by Horn and McKee, i.e., generally decrease in zero span in successive drying steps. The average behavior of these pulps is a decrease in zero span tensile of about 7% after six drying events.

Table 2. THE IMPACT OF REPEATED DRYING ON FIBER STRENGTH MEASURED AS ZERO SPAN BREAKING LENGTH

	Drying Level			
Species	First	Second	Sixth	Ratio Sixth/First
Pine				
Bleached	12.7	12.2	11.6	.91
Unbleached	12.6	12.8	11.7	.93
Hardwood				
Bleached	11.5	12.4	11.8	1.03
Unbleached	12.6	10.0	10.7	.85
			Av. Ratio	.93

Coarseness/Perimeter

Table 3 shows the behavior of fiber coarseness and perimeter. Both of these parameters show a slight decrease at the end of six drying cycles. This is the expected behavior based on fiber wall collapse arguments.

Table 3. THE IMPACT OF REPEATED DRYING ON FIBER COARSENESS AND PERIMETER

	Drying Level			
Species	First	Second	Sixth	Ratio Sixth/First
Coarseness				
Bleached Pine	13.8	13.7	12.9	.93
Perimeter				
Bleached Hardwood	46.6	43.5	42	.90

Fiber Length

Table 4 is a summary of fiber length data. This property has not been impacted by successive drying. However, this is expected since no additional refining has been done on the fibers. A point of a future study is to determine the impact of refining on fiber length.

Table 4. THE IMPACT OF REPEATED DRYING ON FIBER LENGTH

Species	Drying Level First	Second	Sixth	Ratio Sixth/First
Pine				
Unbleached	2.24	2.27	1.95	.87
Hardwood				
Bleached	1.76	1.81	1.80	1.02
Unbleached	2.22	2.19	2.23	1.01

Freeness Change of Recycled Fibers

The most curious observation to date can best be viewed in the context of Figure 3 and Figure 4. These figures show the relationship between tensile strength of the paper sheets and freeness. Figure 3 shows the relationship for pine and behaves as expected. Separate curves are generated for each recycle level. Corresponding points on the "zero" recycle curve move to high freeness on the other curves. The major impact of recycle occurrs at the first recycle level. Figure 4 shows the breaking length freeness relationship for hardwood. In this case the data forms a single curve. The higher recycle levels lie at the high freeness levels. Both the pine and hardwood pulp show a similar behavior of "forgetting" their previous history of refining. The hardwood is extreme in this behavior and appears to have lost all memory of its refining history. Figures 5 and 6 show "Page Plots" for bleached pine and hardwood. The data from each recycle level falls on a common curve in both the pine and hardwoods case. This result implies that recycled fiber has the same fiber-fiber bond strength as virgin fiber. If this observation holds in future

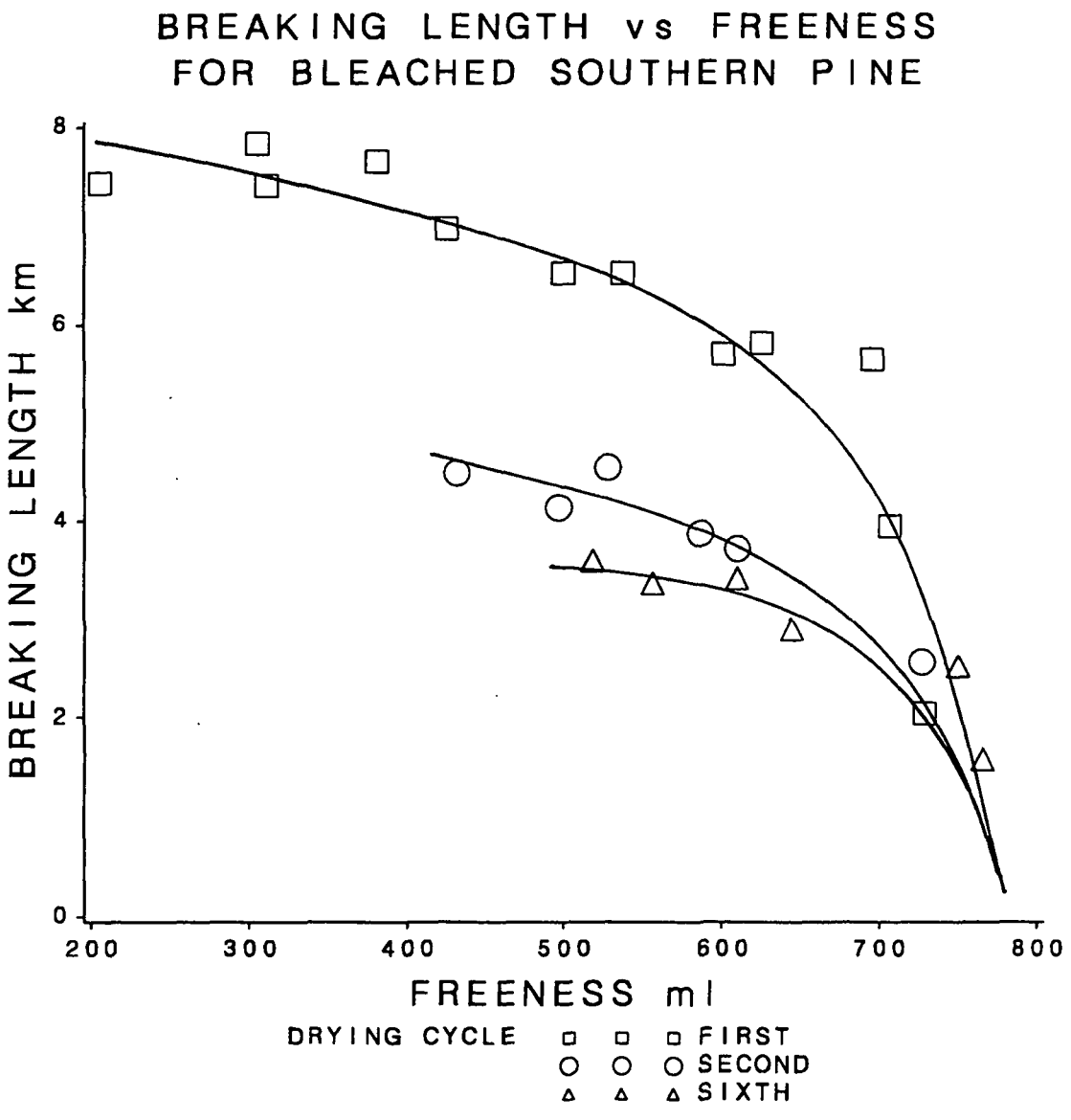
BREAKING LENGTH vs FREENESS
FOR BLEACHED SOUTHERN PINE
BREAKING LENGTH km
0
2
4
6
8
200
300
400
500
600
700
800
FREENESS ml
DRYING CYCLE
FIRST
SECOND
SIXTH

Figure 3.

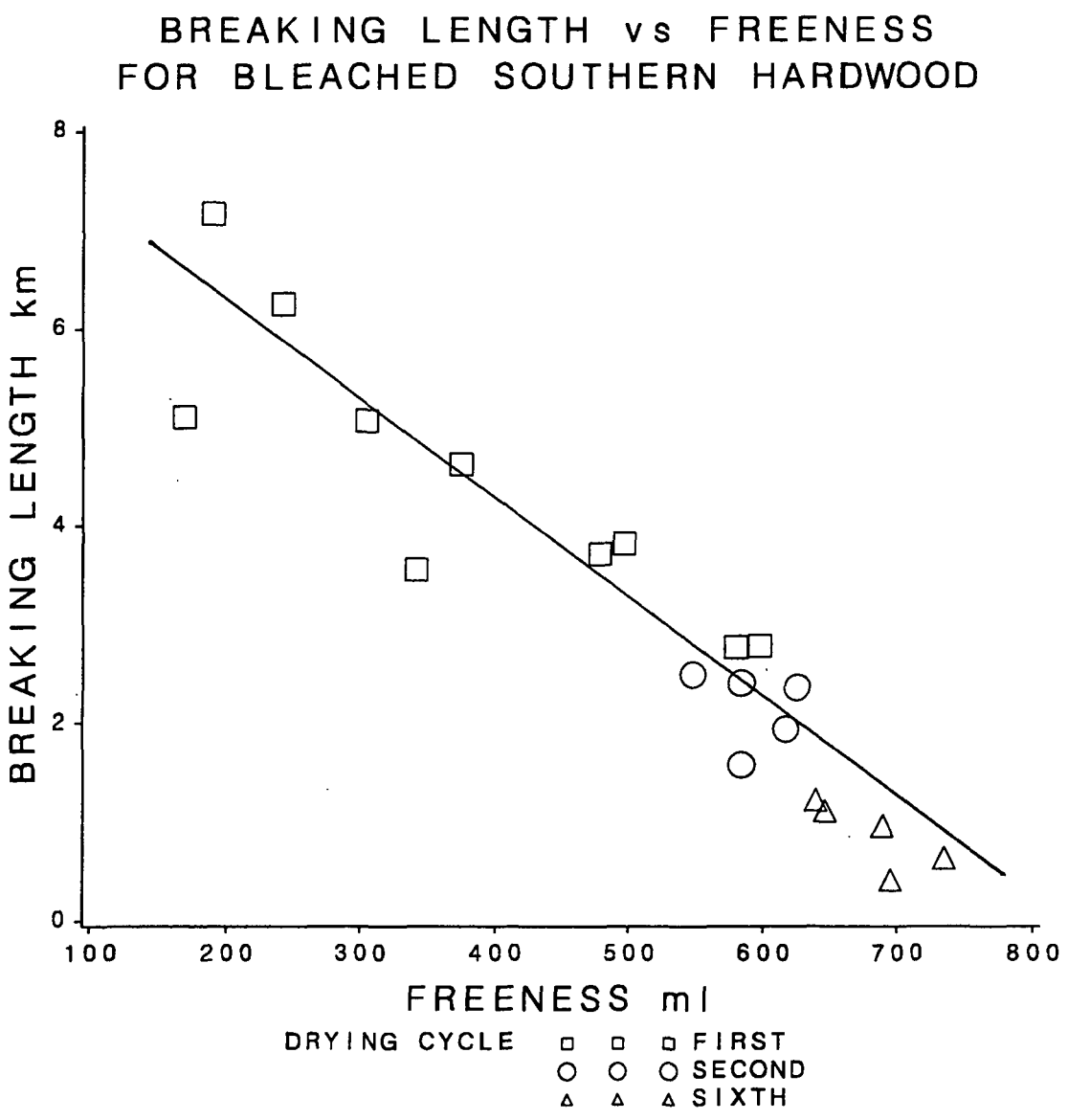
BREAKING LENGTH vs FREENESS
FOR BLEACHED SOUTHERN HARDWOOD
BREAKING LENGTH km
0
2
4
6
8
100
200
300
400
500
600
700
800
FREENESS ml
DRYING CYCLE
FIRST
SECOND
SIXTH

Figure 4.

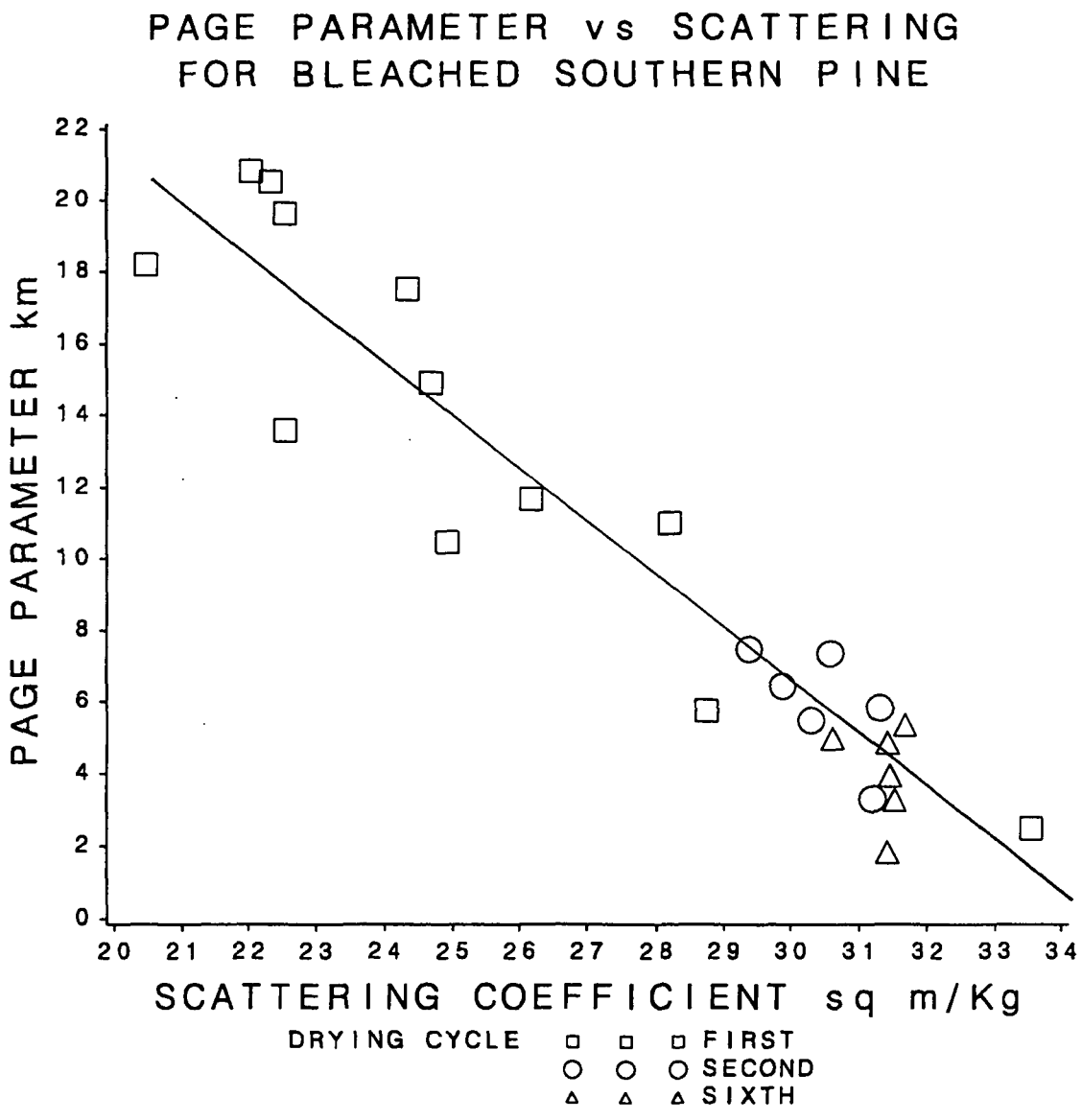
PAGE PARAMETER vs SCATTERING
FOR BLEACHED SOUTHERN PINE
PAGE PARAMETER km
0
2
4
6
8
10
12
14
16
18
20
22
20 21 22 23 24 25 26 27 28 29 30 31 32 33 34
SCATTERING COEFFICIENT sq m/Kg
DRYING CYCLE
FIRST
SECOND
SIXTH

Figure 5.

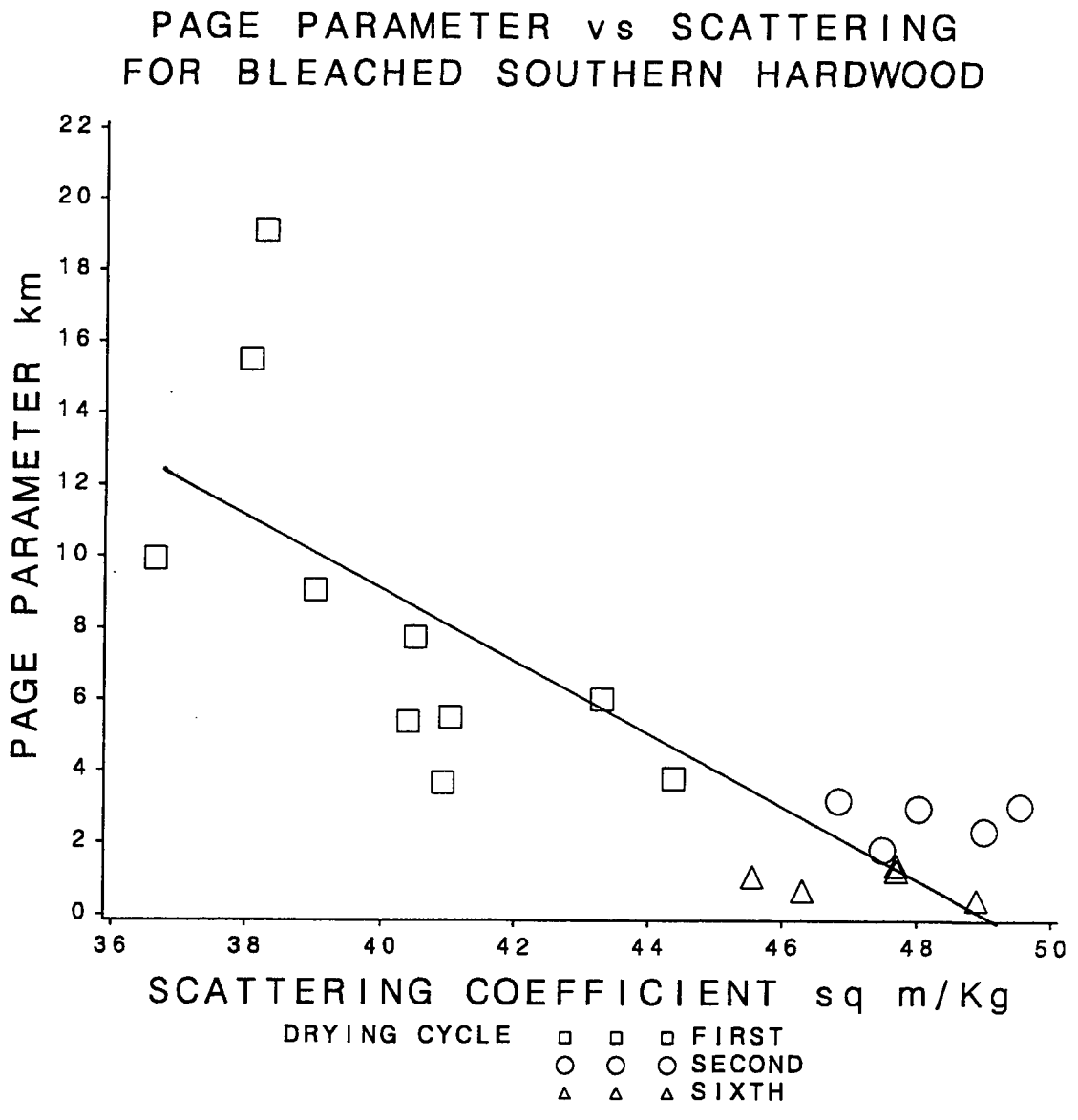
PAGE PARAMETER vs SCATTERING
FOR BLEACHED SOUTHERN HARDWOOD
PAGE PARAMETER km
0
2
4
6
8
10
12
14
16
18
20
22
36
38
40
42
44
46
48
50
SCATTERING COEFFICIENT sq m/Kg
DRYING CYCLE
FIRST
SECOND
SIXTH

Figure 6.

work then the implication is that loss of bond strength observed in recycled sheets is the sole result of poor development of bonded area.

The implications of these results may be stated as follows. If a recycled fiber receives no refining treatment, then it behaves the same as a virgin pulp with the same fiber-fiber bond strength, and same unbonded scattering coefficient. This implies that the weakness of the recycled paper sheet, made in this study, is due largely to the inability of the fibers to develop bonded area, and partly due to changes in zero span, perimeter, and coarseness.

CONCLUSIONS AND FUTURE WORK

Our results to date lead us to the following conclusions:

1. The recycling of pulp fibers leads to a reduction to zero span tensile perimeter and coarseness. This observation is consistent with past observations and is explained by the various theories of fiber wall collapse.

2. The specific fiber-fiber bond strength is unaffected by drying. The reader should remember this applies only to a fiber which has not received subsequent refining. This result suggests that the loss in total board strength is due to a significant reduction in bonded area.

Future work includes a study of the impact of refining on fiber properties. The impact of recycled fibers on properties important to paper machine productivity will also be measured. These factors include drainage resistance and pressing response.

LITERATURE CITED

1. Hultman, J.D., Becher, J.J., Swanson, J.W., and Bowers, D.F., Removal of "Sticky" Contaminants from Recycled Fiber, Progress Report One, Project 3428, Appleton, WI, The Institute of Paper Chemistry, June 18, 1980.

2. Hultman, J. D., Becher, J.J. Davis, E. J., and Doshi, M.R., Removal of "Sticky" Contaminants from Recycled Fiber, Progress Report Two, Project 3428, Appleton, WI, The Institute of Paper Chemistry, May 6, 1981.

3. McCool, M. A., and Silveri, L., Tappi J. 70 (11), 75 (1987).

4. Leja J., "Surface Chemistry of Flotation", Plenum Press, New York, 1982.

5. Adamson, A.W., "Physical Chemistry of Surfaces," Wiley - Interscience, New York, 4th Ed., 1982.

6. Girifalco, L.A., and Good, R.J., J. Phys. Chem. 61, 904 (1957).

7. Fowkes, F.M., J. Phys. Chem., 67, 2538 (1963).

8. Morra, M., Occhiello, E., and Garbassi, F., Adv. Coll. Interf. Sci., 32, 79 (1990).

9. Valenzuela, D.P., and Zettlemoyer, A.C., paper presented at 200th National ACS meeting, Washington, D.C., August 28, 1990.